# INFORMATION TO USERS

# NOTE TO USERS

This reproduction is the best copy available.

UMI®

AN INVESTIGATION OF THE MECHANISMS OF HIGH INTENSITY

FOCUSED ULTRASOUND INDUCED PLATELET ACTIVITY

Sandra Louise Poliachik

A dissertation submitted in partial fulfillment of the requirements for the degree of

Doctor of Philosophy

University of Washington
2001

Department of Bioengineering

UMI Number: 3036519

# UMI®

In presenting this dissertation in partial fulfillment of the requirements for the Doctoral degree at the University of Washington, I agree that the Library shall make its copies freely available for inspection. I further agree that extensive copying of the dissertation is allowable only for scholarly purposes, consistent with "fair use" as prescribed in the U.S. Copyright Law. Requests for copying or reproduction of this dissertation may be referred to Bell and Howell Information and Learning, 300 North Zeeb Road, Ann Arbor, MI 48106-1346, to whom the author has granted "the right to reproduce and sell (a) copies of the manuscript in microform and/or (b) printed copies of the manuscript made from microform."

Signature _____

Date: _____ 19 September 2001 _____

University of Washington

Graduate School

This is to certify that I have examined this copy of a doctoral dissertation by

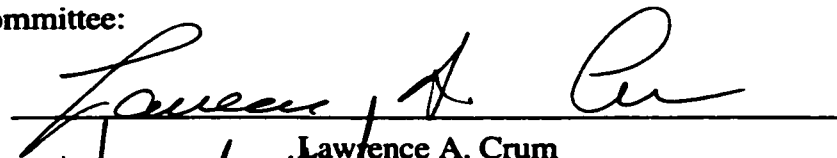Sandra Louise Poliachik

and have found that it is complete and satisfactory in all respects,

and that any and all revisions required by the final

examining committee have been made.

Chair of Supervisory Committee:
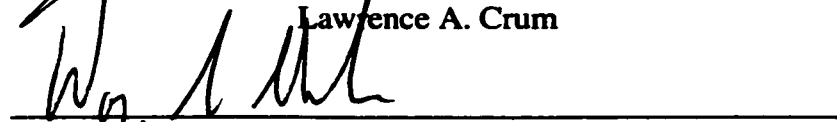
_____
Lawrence A. Crum
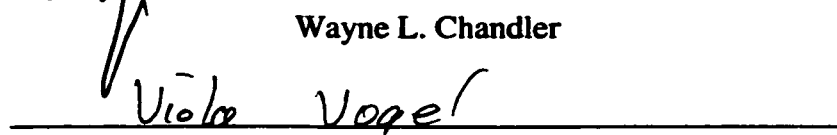
Reading Committee:
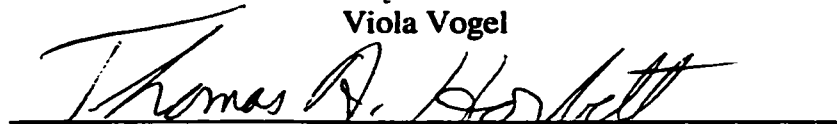
_____
Lawrence A. Crum
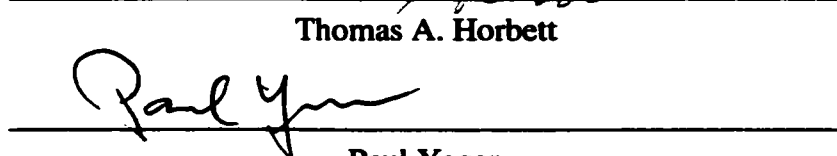
_____
Wayne L. Chandler

_____
Viola Vogel

_____
Thomas A. Horbett

_____
Paul Yager

Date: _____19 September 2001_____

University of Washington

Abstract

# AN INVESTIGATION OF THE MECHANISMS OF HIGH INTENSITY FOCUSED ULTRASOUND INDUCED PLATELET ACTIVITY

Sandra Louise Poliachik

Chairperson of Supervisory Committee: Professor Lawrence A. Crum

Department of Bioengineering

The goal of the acoustic hemostasis project is to locate a hemorrhage using diagnostic ultrasound and halt the bleeding using high intensity focused ultrasound (HIFU). To enhance the imaging of blood, the use of ultrasound contrast agents (UCA; gas filled microbubbles that increase the echogenicity of fluids), has been proposed as a means to locate internal bleeding (Schmiedl et al., 1999). This study investigates the mechanisms of HIFU-induced bioeffects in blood which may lead to primary, or platelet-related, hemostasis.

Using platelet rich plasma (PRP), we investigated the effect of 1.1-MHz continuous wave (CW) HIFU on platelet activation, aggregation and adhesion to a collagen-coated surface. Flow cytometry, laser aggregometry, and environmental scanning electron microscopy (ESEM) were used to quantify platelet activation and aggregation, and to observe adhesion to a collagen-coated surface.

To investigate the role of cavitation as a mechanism for platelet aggregation, a 5-MHz passive cavitation detector was used during aggregation trials to monitor cavitation activity, which was then quantified to provide a relative measure of the

amount of cavitation that occurred in each aggregation trial. The effects of HIFU induced cavitation on platelet aggregation in PRP were investigated by enhancing cavitation activity through use of UCA, and by limiting cavitation activity through use of an overpressure system. Platelet aggregation was measured in PRP with laser aggregometry, and in whole blood using an impedance measurement technique. Doppler ultrasound and high speed camera observations were used to measure bulk streaming velocities, providing an estimate of shear stresses due to bulk flow.

Our results show that in PRP, increased cavitation activity lowers the intensity threshold to produce platelet aggregation and decreased cavitation activity in the overpressure system raises the intensity threshold for platelet aggregation. Resulting platelet aggregation in whole blood is less than in samples of PRP for comparable cavitation doses. Shear stresses due to bulk flow are insufficient to stimulate platelet aggregation.

It was determined that HIFU can activate platelets, stimulate them to aggregate and promote their adherence to a collagen-coated surface. In principle, HIFU can stimulate primary, or platelet-related, hemostasis. This study explores the HIFU exposure mechanisms responsible for inducing platelet activity *in vitro*.

# TABLE OF CONTENTS

iii

# LIST OF FIGURES

.

# LIST OF TABLES

## Acknowledgements

I would like to thank all the people who helped me to focus and complete this degree, including all the folks at CIMU, family and friends, Supervisory Committee members and the Bioengineering Department.

## Dedication

To my parents, who always believed I could do anything I set my mind to.

# 1.0 INTRODUCTION

High intensity focused ultrasound (HIFU) has been used successfully to produce acoustic hemostasis, with the primary mechanism suspected to be thermal effects. The purpose of this research is to investigate a more subtle effect -- the stimulation of the body's natural coagulation system; more specifically the ability of HIFU to promote primary hemostasis (that part of the coagulation process which involves platelets).

The body's normal response to vessel injury is to cause vasoconstriction, thereby reducing blood flow to the injured area, followed by platelet aggregation and thrombus formation. Platelets form the initial hemostatic plug after an injury occurs. The platelets may be activated by contacting exposed collagen in the wound, shear, or released contents of other platelets.

Use of HIFU is linked to cavitation, the expansion and compression of gas bubbles caused by the applied acoustic field, bulk fluid streaming and thermal effects. These acoustic mechanisms are investigated in this study to determine which is the most likely to cause platelet activity as a result of HIFU exposure.

## 1.1 Previous Studies of the Effects of Ultrasound Exposures on Blood

The ability to perform acoustic hemostasis using high-intensity focused ultrasound (HIFU) has been investigated by a number of researchers (Delon-Martin et al. 1995; Hynynen et al. 1996a, 1996b; Martin et al. 1999; Vaezy et al. 1997, 1998, 1999ab). The goal of non-invasive acoustic hemostasis is to locate the hemorrhage using diagnostic ultrasound and then to use HIFU to induce hemostasis. Continuous wave (CW) ultrasound at spatial average intensities of 500 to 3100 W/cm$^2$ at center frequencies of 2.0, 3.3 and 3.5-MHz has been used successfully to halt bleeding in

exposed rabbit liver (Vaezy et al. 1997) and in punctured blood vessels (Vaezy et al. 1998) for exposure times of less than two minutes. In the acoustic hemostasis studies performed by Vaezy et al. (1997, 1998, 1999ab), the dominant mechanism appears to be a temperature rise sufficient to cauterize the tissue at the bleeding site. Acoustic cavitation, the expansion and compression of gas bubbles caused by the applied acoustic field, was not monitored during these HIFU exposures. Delon-Martin et al. (1995) attributed the formation of venous thromboses in normal blood vessels to thermal damage of the vessel. Using a passive cavitation detector, they did not detect any cavitation activity during 7.31-MHz CW HIFU exposures at spatial average temporal peak intensities of 167 $W/cm^2$. Hynynen et al. (1996b) suggested that a mechanical/thermal stimulus ceased blood flow in a healthy vessel after application of HIFU. They purposely applied CW HIFU above the cavitation threshold (peak intensity 6500 $W/cm^2$), verified by strong subharmonic noise in the spectrum of acoustic emissions monitored by a passive cavitation hydrophone, in order to constrict the vessel. Without the cooling blood flow, sonications at lower intensities (peak intensity 2800 $W/cm^2$) were used to produce thermal coagulation of the vessel. Our studies concentrate on the stimulation of platelet related hemostasis under controlled temperatures such that non-thermal effects of HIFU can be evaluated. Our research studies the application of HIFU and if it can be utilized as a means to stimulate the natural hemostatic system without causing thermal effects and detrimental bioeffects.

Ultrasound contrast agents (UCA), gas filled microbubbles that increase the echogenicity of fluids, are frequently added to blood to enhance ultrasonic images. Schmiedel et al. (1999) have been studying the use of exogenous UCA to help

visualize hemorrhage. The acoustic generation of microbubble boluses has also been suggested as a means to locate hemorrhage (Ivey et al. 1995). However, the interaction of ultrasound with microbubbles can produce potentially harmful biological effects (Azadniv et al. 1996; Brayman et al. 1995, 1996, 1999a; Brayman and Miller 1997a, 1999b; Dalecki et al. 1997; Everbach et al. 1997; Miller et al. 1997; Miller and Gies 1998; Poliachik et al. 1999). Therefore, if microbubbles are to be used to locate hemorrhage, then the effects of HIFU exposure of UCA with blood and tissues should be investigated.

Prior studies have investigated the effect of ultrasound exposure on platelets. At spatial average therapeutic intensities (0 - 5 W/cm$^2$), unfocused ultrasound can decrease the recalcification time (time required to form a clot after addition of sufficient calcium ions to a sample) (Williams et al. 1976a), increase the release of the platelet specific protein B-thromboglobulin (Williams et al. 1978), and change platelet morphology and function *in vitro* (Williams et al. 1976b). Using light transmittance aggregometry, platelet aggregation was shown to occur at therapeutic intensities for 5 minutes CW ultrasound exposures by Chater et al. (1977). Platelet calcium concentration increased and platelet aggregation was stimulated by 16 W/cm$^2$ ultrasound applied through a wire guide *in vitro* (Samal 2000). In the Chater et al. study, platelet aggregation was more likely to occur at lower ultrasound frequencies, with most aggregation occurring for spatial average intensities above 3.75 W/cm$^2$ at 0.75-MHz, more so than at 1.5 or 3.0-MHz. Although cavitation was not measured, Chater et al. suggested the mechanism that induced aggregation was cavitation.

Miller et al. (1979) suspected cavitation as a mechanism for platelet activity and thus designed an experiment that would produce stable cavitation. 2.1-MHz

ultrasound exposure of gas-filled micropores in a membrane immersed in platelet rich plasma (PRP) at spatial peak 16 - 32 mW/cm$^2$ caused platelets to aggregate around the pores. Miller attributed this to the intensification of the acoustic field near the pore, thus attracting platelets with radiation force. Acoustic microstreaming around the bubble at the pore produced velocity gradients near the platelet membrane surface. Platelets are sensitive to shear and may become activated by shear values as low as 50 dynes/cm$^2$ (Colman 1994). Shear was not quantified in the Miller study.

Zarod et al. (1977) used therapeutic ultrasound meter intensities of 1 W/cm$^2$ to create platelet aggregates in the microcirculation of subcutaneous tissues of guinea pig ear at frequencies of 3.0-MHz for CW exposures and 0.75-MHz for pulsed exposures. Frizzell et al. (1986) created ultrasonic streaming at the tip of a micropipette tip inserted into mouse mesenteric arteries and veins, which led to intravascular thrombus formation. A study by Everbach et al. (1998) investigated the effect of inertial (i.e. violent collapse) acoustic cavitation on platelets. In these studies, platelets were exposed to 1.1-MHz pulsed (0.08 - 3.2% duty cycle at 20-Hz pulse repetition frequency) ultrasound at intensities of 730 W/cm$^2$ spatial peak pulse average intensity. UCA were added in some cases and the resulting amount of inertial cavitation increased such that platelet destruction increased from virtually zero with no UCA to 75% destruction with UCA. In light of these results, both cavitation and shearing seem to be viable mechanisms to explain platelet activity induced by ultrasound.

Many studies have been completed investigating the effect of ultrasound on blood samples containing UCA (Azadniv et al. 1996; Brayman et al. 1995, 1996, 1999a; Brayman and Miller 1997a, 1999b; Dalecki et al. 1997; Everbach et al. 1997;

Miller et al. 1997; Miller and Gies 1998; Poliachik et al. 1999). In general, most of these studies used diluted blood with large UCA concentrations, and low intensity or plane wave (non-focused) ultrasound. For example, pulsed 1.1-MHz, 8.5 W/cm$^2$ spatial peak temporal average system with 35 $\mu$L UCA/mL 1% hematocrit blood caused nine times more damage than in 1% hematocrit blood without UCA (Brayman et al. 1995). A few studies have determined the effect of ultrasound on whole blood with UCA added (Brayman et al. 1996, 1997b; Brayman and Miller 1999b; Miller et al. 1997; Poliachik et al. 1999). In these studies, whole blood alone is not damaged much beyond sham level when no UCA are included in the sample. Inclusion of UCA, however, increases the amount of damage drastically, depending on the ultrasound exposure conditions and amount of UCA used. 1.07-MHz center frequency pulsed ultrasound exposures of spatial peak temporal peak 1100 W/cm$^2$ produced 85% hemolysis using 1 s pulses on samples of human whole blood that contained 36 $\mu$L UCA/mL blood (Brayman et al. 1996). Hemolysis in whole blood containing 36 $\mu$L UCA/mL blood was also found to increase with pressure, and at high pressures was strongly dependent on frequency (Brayman et al. 1997). Pulsed ultrasound of 2.25-MHz center frequency at an acoustic pressure amplitude of 1.6 MPa (approximately 85 W/cm$^2$) in combination with 50% UCA in whole canine blood produced 6% hemolysis (Miller et al. 1997). 1.1-MHz center frequency CW HIFU exposures at spatial average 2000 W/cm$^2$ with a maximum of 4.2 $\mu$L UCA/mL blood produced 45% hemolysis for a 1 s exposure (Poliachik et al. 1999). Miller and Gies (1998) studied different UCAs and determined that perfluorocarbon based UCA cause more damage than air based UCA under otherwise comparable exposure conditions.

Studies of the effect of ultrasound on whole blood alone determined that 782-kHz CW ultrasound exposures at intensities up to spatial peak temporal average 15 W/cm$^2$ for 5 minutes were insufficient to cause damage (Ellwart et al. 1988). Less than 5% hemolysis was achieved in 1.7-MHz CW ultrasound 16 minute exposures for spatial peak intensities of 1 - 36 mW/cm$^2$ (Miller et al. 1988a). Hemolysis equivalent to sham exposures resulted from 1.1-MHz HIFU 1s exposures of whole blood at intensities up to 2360 W/cm$^2$ (Poliachik et al. 1999).

A method of measuring platelet aggregation in whole blood was developed by Cardinal and Flower (1980) and is in common clinical use (Series 500 Whole Blood Aggregometer, Chrono-log Corp., Havertown PA). The advantage of using whole blood samples to measure platelet activity is ease of sample preparation and increased efficiency. The whole blood aggregation method produces results comparable to the laser light transmittance method used by researchers Chater et al. (1977) and Samal et al. (2000). We use *in vitro* experiments to investigate HIFU induced platelet aggregation in samples of whole blood and whole blood with UCA.

The application of an overpressure to samples has been used as a means to reduce the number of cavitation nuclei in a sample (Bailey 2001, Delius 1997, Lokhandwalla 2001, Williams 1999). In these experiments, samples to be exposed were placed in overpressure chambers built of plastic and/or metal depending on pressures used. In a study on cell suspensions, shock-wave lithotripsy exposures of erythrocytes (diluted to 10g/L) and mouse leukemia cells at overpressures up to 4atm (400 kPa), Delius et al. (1997) found that as overpressure increased, hemolysis decreased. With maximum peak rarefactional pressures of 10.4 MPa, the interaction of the shock wave with bubbles in the samples was decreased as overpressure

increased. In a study by Williams et al. (1999), high overpressures (80 - 120 atm) for erythrocyte concentrations of 3.1% still resulted in some cell damage, though about four times less than samples at atmospheric pressure, suggesting non-cavitational mechanisms such as shear or bulk fluid streaming may cause some cell damage at high overpressures. In a similar study, erythrocytes at 120 atm (12 MPa, which is greater than the shock wave rarefactional pressure) also produced cell damage that was attributed to shear, and cell deformation (Lokhandwalla et al. 2001). We use overpressure to reduce the likelihood of cavitation, but not eliminate it completely, for samples of PRP in laser aggregometry.

Our studies measure platelet aggregation in PRP under three conditions: 1) HIFU exposure of PRP; 2) HIFU exposure of PRP + UCA; and 3) HIFU exposure of PRP subjected to 7 atm (700 kPa) overpressure. These experiments are used to investigate platelet aggregation in conditions of normal, enhanced and limited cavitation, respectively. Experiments using the whole blood impedance method of determining aggregation are performed on samples of whole blood and whole blood with UCA to test HIFU effectiveness in forming platelet aggregates in whole blood, to simulate more closely *in vivo* conditions.

## *1.2 Mechanisms of Ultrasound Bioeffects*

### *1.2.1 Cavitation*

Cavitation can be divided into two types: inertial and stable cavitation. Inertial cavitation, the violent collapse of a bubble, can destroy cells within the vicinity of the event (Leighton 1994). During stable cavitation, bubbles undergo radial oscillation in response to the compression and rarefaction pressures of the impinging acoustic waves. These bubble oscillations may persist for hundreds to

millions of acoustic cycles. Bubbles undergoing stable cavitation produce a flow pattern within a very thin boundary layer about their surface, termed acoustic microstreaming. The shear stress generated within the microstreaming boundary layer of a bubble on a surface may lyse cells in suspension, cause cell death in plant tissue and may produce other effects as well (Miller 1988b).

Vibrating bubbles may produce two effects: radiation forces and acoustic microstreaming. The radiation forces produce particle migration near a vibrating bubble, even at low amplitude, such that cells and other biological particles brought into the vicinity of the bubble are subject to mechanical stresses that exist near the surface of the bubble. Acoustic microstreaming produces circulatory flow in the surrounding medium as depicted in Figure 1, producing viscous shear stresses that may damage cells (Nyborg and Miller 1982). In experiments to test the ability of acoustically stimulated bubbles to disrupt cells, researchers have used fixed bubbles on a surface to permit observation of microstreaming (Miller and Thomas 1990, Miller 1988b, Nyborg and Miller 1982, Rooney 1970, 1972), although viscous interactions with the sound wave scattered from the bubble and rigid surface may effect microstreaming (Elder 1959). Calculations by Rooney (1970) determined that 20-kHz exposure of a fixed 130 $\mu$m diameter bubble in diluted blood samples may produce velocity gradients leading to viscous shear stresses on the order of 3000 dyne/cm$^2$ at the threshold for hemoglobin release. Large microstreaming speeds, and thus greater viscous shear stresses, should be possible at higher frequencies, yet the damping constant will also increase with frequency such that larger incident fields would be necessary to create higher streaming speeds (Elder 1959).
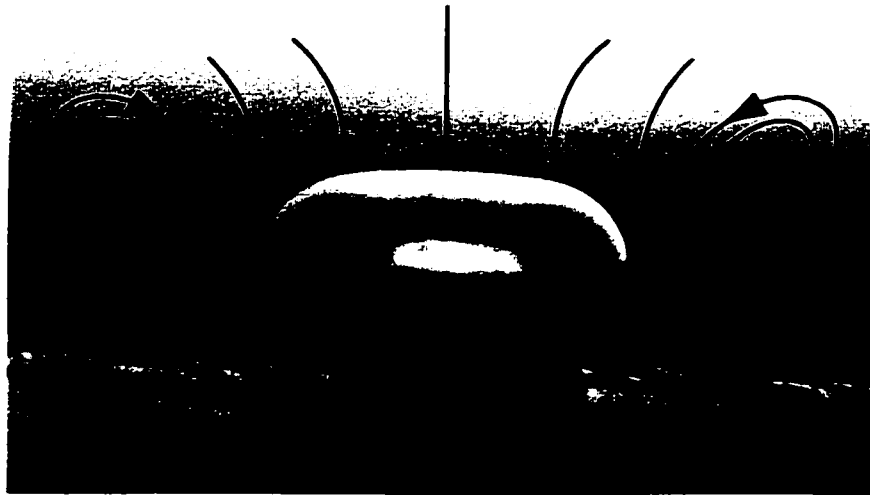
Figure 1: Microstreaming produces circulatory flow around a pulsating bubble, as depicted by arrows. (based on Elder, 1959, and photograph by Crum in Leighton 1994)

During stable cavitation, bubbles may tend to grow due to rectified diffusion, a phenomenon that occurs due to the changing surface area of a bubble and the gas concentration gradient in and around the bubble. Rectified diffusion is explained by two effects: the area effect and the shell effect. Pressure differences drive the area effect, in which gas tends to diffuse out of the bubble when the bubble has a radius less than equilibrium radius, and gas will diffuse into the bubble when its radius is greater than the equilibrium radius. The shell effect occurs because the layers, or shells, of liquid that surround the bubble react to its changing size. As the bubble expands, the thickness of the liquid shells contract. The dissolved gas concentration is less than the equilibrium concentration next to the bubble, but the shell is thinner and the gradient across the shell is higher, so the rate of diffusion of gas into the bubble is high. As the bubble contracts, the liquid shells increase in thickness. The concentration of gas near the bubble wall is higher than when the bubble is expanded,

yet the increased shell thickness creates a gas concentration gradient that is less than when the bubble is expanded, leading to a lower rate of gas diffusion into the bubble. The end result is that on expansion, a large gradient drives gas a short distance through a large surface area, while on compression a lesser gradient drives gas a longer distance through a smaller surface area (Leighton 1994).

If a bubble grows beyond the limit $R_{max}/R_o$ (maximum bubble radius/equilibrium bubble radius) (Flynn et al. 1975), it will tend to implode violently, a process called inertial cavitation. The violent collapse of a bubble can lead to the production of high-velocity liquid jets, strong shear forces, shock waves, sonochemicals and free radical species that can damage cells (Leighton 1994; Miller and Thomas 1993; Miller et al. 1996).

### 1.2.2 Bulk Streaming

Bulk streaming within a sample of blood or PRP can occur as a result of a combination of acoustic streaming and radiation pressure. Acoustic streaming occurs in a homogenous medium as a result of momentum absorption that creates flow in the direction of the sound field. If an impedance discontinuity exists in the medium, as in inhomogeneous blood or PRP, momentum transfer due to scattering can generate a force on the medium, known as radiation pressure. Whole blood contains larger cells and a greater concentration of cells than PRP and thus will likely have different streaming reactions to HIFU. Addition of UCA may greatly increase streaming, especially as bubbles grow due to rectified diffusion, thereby creating a larger surface for the force to act upon. This bulk flow may be enough to shear platelets and activate them.

*1.2.3  Thermal Effects*

Thermal effects can also cause platelet activity.  If the temperature of a platelet rises to a point where the platelet membrane becomes disorganized, platelet contents may leak out and cause activation of other platelets.  Previous studies used temperature controlled tanks to avoid thermal effects (Chater et al. 1977; Everbach et al. 1998), or did not consider temperature rise to be a mechanism of platelet activity.

The following experiments are performed on samples of PRP and whole blood.  Differences in cell concentrations may effect the ability of HIFU to produce bioeffects in the sample.  The platelet concentration in PRP used in these experiments is roughly $2 \times 10^5$ platelets/$\mu$L, while whole blood contains roughly $5 \times 10^6$ erythrocytes/$\mu$L plus $2 - 3 \times 10^5$ platelets/$\mu$L (Williams et al. 1995).  Previous studies have determined that cavitation is more likely to occur in low hematocrit samples, while the high hematocrit samples seem to shield or damp bubbles as a result of radiation force that attracts cells to the bubbles (Ellwart et al. 1988).  The ability of HIFU to produce platelet activity may be influenced by the cell concentrations in samples.

*1.3 Overview of Platelets in the Hemostatic System*

If a vessel is damaged, subendothelial proteins such as collagen are exposed.  The hemostatic process starts when platelets come into contact with collagen.  Platelets adhere to the exposed collagen in the damaged vessel, become activated, spread out and release their contents, thereby recruiting other platelets which leads to the formation of a primary hemostatic plug.  Platelet adherence and activation in turn leads to activation of the coagulation system resulting in formation of fibrin that stabilizes the hemostatic plug.  These studies investigate the ability of HIFU to

stimulate the primary hemostatic plug consisting of platelets and do not look further into the coagulation process.

The human hemostatic system reacts to vascular injury by first constricting the vessel, and then sealing the damaged area of the vessel wall. Normally, endothelial cells inhibit platelet aggregation and blood coagulation, promote fibrinolysis and act as a barrier between blood and the underlying subendothelial cells that may activate platelets. Upon injury, a vessel will constrict to divert flow from the damaged area. Blood that does come into contact with the damaged vessel wall is exposed to the subendothelial cells that stimulate formation of the hemostatic plug. The sequence for this process is first to produce platelet adhesion and aggregation, known as primary hemostasis, followed by blood coagulation. The platelet plug that is formed in primary hemostasis is a fragile, but necessary, step in the hemostatic process. Platelets within the plug provide necessary components that stimulate and support the steps of the coagulation cascade. Blood coagulation then occurs to create a more stable fibrin plug, followed by clot dissolution, collagen deposition and fibrous tissue formation that leads to final wound healing.

Platelets are fragments of a larger cell, the megakarocyte, and range in diameter from 2 - 4 $\mu$m (Thomas 1978). They contain granules, but no nucleus, and vary in shape from round to elongated cigar-shaped forms. Cell concentration is about 2 - 3 x$10^5$ platelets per $\mu$L blood, compared with 5x$10^6$ erythrocytes per $\mu$L blood (Williams 1995). A platelet has an active cytoskeleton and many receptors on its surface. Upon activation, which may be stimulated by exposure to components such as epinephrine, collagen, adenosine diphosphate (ADP), thrombin, platelet activating factor (PAF), or exposure to adequate shear forces, the platelets are capable

of activating other platelets nearby (see Figure 2). Platelets bind to collagen through von Willebrand factor (vWf) as well as having a specific collagen receptor on their surface. Binding to collagen activates platelets. Platelet activation changes the conformation of the GPIIb-IIIa receptor on the platelet surface causing it to bind fibrinogen and other ligands. Binding of two activated platelets to a single fibrinogen molecule causes the platelets to stick together, or aggregate. The conformation change of the GPIIb-IIIa receptor caused by activation is necessary for platelet aggregation, thus, resting platelets will not aggregate, and fibrinogen will not activate a platelet (Colman 1994).

In a damaged vessel, the collagen beneath the layer of endothelial cells is exposed. Platelets stick to the exposed collagen and become activated, spread out and release their contents, thereby recruiting other platelets. If the damaged vessel is an artery, flow velocities are approximately 10 to 20 cm/s (Colman 1994), large enough to apply a removal force to the adhered platelets. The protein vWf acts as a tether to help platelets adhere in an arterial system. The vWf is activated by shear and converts from a globular protein to a long, sticky chain that attaches to platelets and a component of the extracellular collagen. The higher the shear, the more effective the vWf becomes, thus enabling platelets to adhere to a wound even in the high flow conditions found in arteries.

The flow in a venous system is much slower than arterial flow; i.e., on the order of 0 - 5 cm/s (Colman 1994). vWf does not tend to activate in low flow situations where platelets can adhere to wounds adequately without the extra "glue". Since flow carries the platelets and proteins to the wound, platelet aggregates in low flow system form more slowly than in high flow systems (Colman 1994).
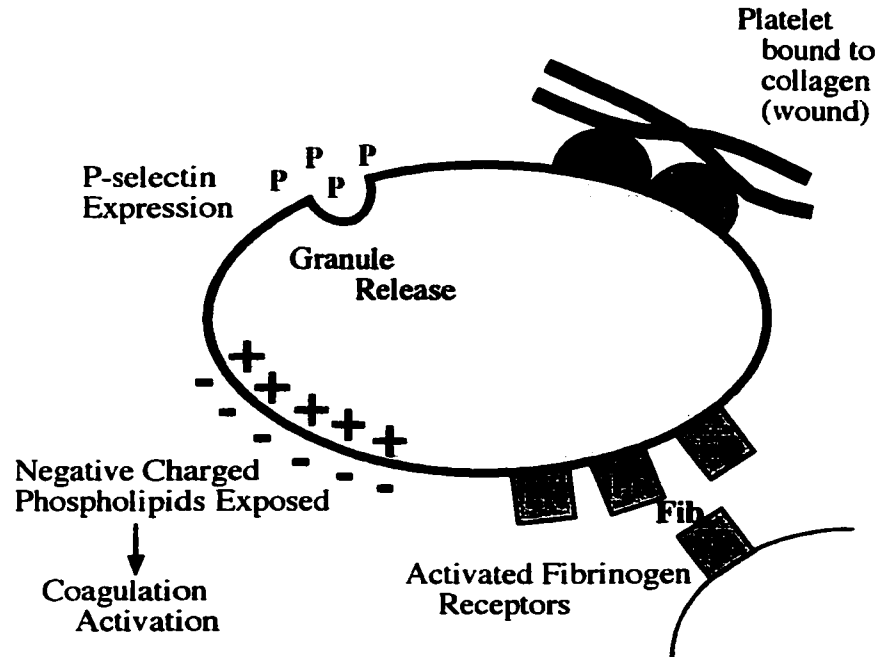
Figure 2: Platelet Function. Platelets can be activated by a number of processes, such as exposure to collagen, ADP and other factors. Platelet activation may be measured by platelet aggregometry (indicating fibrinogen activation), and flow cytometry (indicating expression of the protein P-selectin, activated fibrinogen receptors, and negative phospholipid exposure). Some steps in the coagulation cascade require negative phospholipids to proceed.

## *1.4 HIFU Investigation of Platelet Activity*

The research pursued in the following studies investigates the mechanisms responsible for platelet activity resulting from HIFU exposure. Cavitation, bulk acoustic streaming and thermal mechanisms are considered, and platelet activation, adhesion to a collagen-coated surface and aggregation are observed and quantified.

# 2.0 OBJECTIVES FOR HIFU-INDUCED PLATELET ACTIVITY STUDY

## 2.1 Study Plan

Previous studies have shown that ultrasound can produce bioeffects in blood, including hemolysis and stimulation of platelet aggregation. We hypothesize that HIFU stimulates platelet activation, aggregation and adhesion to a collagen-coated surface through a combination of effects: cavitation ruptures platelets, releasing their contents into plasma, in turn activating other platelets in the vicinity. This leads to increased binding to neighboring platelets (aggregation) and adhesion to exposed collagen. These cavitation induced effects are enhanced by HIFU induced bulk fluid flow which mixes the released activation factors and platelets, increases platelet-platelet and platelet-collagen interactions to enhance binding, and increases shearing. The critical step is cavitation, which leads to the rupture of platelets and release of their contents, while bulk fluid flow alone is insufficient to cause platelet activation and aggregation. Based on this hypothesis, we further hypothesize that increasing cavitation will lead to increased platelet activation and aggregation, while suppression of cavitation will decrease platelet activation and aggregation. We evaluate platelet activation, adhesion and aggregation in samples of PRP and whole blood with and without UCA to determine exposure conditions necessary for HIFU stimulation of platelet activity.

In considering acoustic mechanisms, we hypothesize that HIFU causes cavitation and acoustic streaming in samples of PRP, which can lead to ripping or shearing of platelets. Inertial cavitation, the violent collapse of a bubble, can rip platelets apart, thus releasing platelet contents that can activate other platelets. Microstreaming can occur near the surface of bubbles undergoing stable cavitation,

and a platelet that is in the vicinity can be sheared or ripped apart by the microstreaming. Acoustic streaming and radiation pressure can produce flow in the sample chamber that may be of sufficient magnitude to shear platelets, thereby activating them. In an attempt to determine the mechanisms responsible for HIFU stimulation of platelets, we control variables which effect the amount of cavitation, such as pressure and the number of cavitation nuclei available (UCA increases number of cavitation nuclei, addition of overpressure reduces number of cavitation nuclei), and the amount of shear (acoustic streaming in chamber) occurring in PRP samples. A Doppler method is used to measure the velocity of particles in the aggregation sample chamber configurations to estimate the amount of shear present. Inertial cavitation is measured using a passive cavitation detector during HIFU exposures of PRP.

The ability to absorb energy and the number of cells within a sample of whole blood are sufficiently greater than in PRP that the HIFU-induced cavitation and shearing effects will be reduced and will be less effective at producing platelet aggregation. To investigate the response in whole blood, we apply HIFU to samples of whole blood, with and without UCA, and measure the amount of platelet aggregation that occurs for a range of exposure intensities and compare to platelet aggregation results from the PRP studies.

## 2.2 Specific Aims

A summary of the hypothesis and specific aims guiding this research is included below.

<u>Hypothesis</u>:  Application of HIFU to platelet rich plasma can shear and/or rip the platelets, thus causing platelet activation, aggregation, and adhesion to a collagen-coated surface.  UCA can enhance the effects of HIFU on platelets.

<u>Specific Aim 1</u>:  Demonstrate that the application of HIFU to PRP samples can cause platelet activation, aggregation and adhesion to a collagen-coated surface for a range of CW exposure times and intensities.  Show that addition of UCA to PRP samples causes a greater extent of platelet aggregation at lower intensities than in samples without UCA.

<u>Hypothesis</u>:  HIFU causes cavitation and bulk acoustic streaming in samples of PRP, which can lead to ripping or shearing of platelets.  Inertial cavitation, the violent collapse of a bubble, can rip platelets apart, thus releasing platelet contents that can activate other platelets.  Microstreaming can occur near the surface of bubbles undergoing stable cavitation, and a platelet that is in the vicinity can be sheared or ripped apart by the microstreaming.  Acoustic streaming and radiation pressure can produce bulk flow in the sample chamber that may be of sufficient magnitude to shear platelets, thereby activating them.

<u>Specific Aim 2</u>:  Demonstrate that the stimulation of platelet aggregation is primarily a function of cavitation and not HIFU intensity or bulk acoustic streaming.  Show that UCA-enhanced cavitation stimulates platelet aggregation at lower HIFU intensities and that cavitation suppressed by overpressure decreases aggregation, even at higher intensities.  Measure inertial cavitation during HIFU exposures of PRP.  Use Doppler

ultrasound to measure velocity of particles in sample chambers and estimate amount of shear due to bulk flow.

Hypothesis: The conditions within a sample of whole blood (number of cells, ability to absorb energy) are sufficiently different from PRP that the cavitation and shearing effects generated by HIFU, with and without UCA, will be less effective at producing platelet aggregation due to suppression of cavitation by erythrocytes.

Specific Aim 3: Demonstrate that application of HIFU to samples of whole blood with and without UCA will produce less aggregation than in samples of PRP. Show that HIFU intensities required to produce the cavitation that stimulates aggregation are higher in whole blood than in PRP.

# 3.0 GENERAL MATERIALS AND METHODS FOR HIFU EXPOSURES

## 3.1 Human Subjects

Studies on human subjects were carried out according to the principles of the Declaration of Helsinki. Informed consent was obtained from all participants and the study was approved by the University of Washington Human Subjects Review Committee.

## 3.2 Blood Samples

Immediately before experiments were started, human blood was drawn from one of three healthy donors and 4.5 mL whole blood was anticoagulated with 0.5 mL of 0.105 M sodium citrate. Blood handling was minimized and blood was typically used within two hours of being drawn, while no experiment lasted longer than four hours. Whole blood or platelet rich plasma (PRP) was used for the experiments. PRP was prepared by centrifuging whole blood at 800 rpm for 10 minutes and removing the PRP supernatant from the tube. The remaining blood was then centrifuged at 2500 rpm for 10 minutes to remove the platelets and other cellular components from the plasma. The resulting platelet poor plasma (PPP) was used to calibrate the aggregometer and to dilute the PRP to provide approximately $2 \times 10^5$ platelets per microliter plasma based on automated cell counting. At least three 1.3 mL samples of PRP or blood were used for each exposure condition.

Whole blood samples were used directly from collection tubes. If bubbles existed in collection tubes, the blood was placed in a 50 mL polypropylene tube (Becton-Dickinson, Franklin Lakes NJ) under vacuum for 15 minutes to remove gas from the blood. Hemolysis resulting from this procedure was negligible.

The UCA used in the PRP experiments was Albunex® (Mallinckrodt Medical, Inc., St. Louis MO), consisting of air-filled, albumin covered microbubbles, or in whole blood experiments Optison® (Mallinckrodt, Inc., St. Louis MO), consisting of octafluoropropane-filled, albumin covered microbubbles. The Albunex® and Optison® were stored at 3°C prior to the experiment. The initial microbubble concentration in Albunex is 3.0 - 5.0 x $10^8$ microbubbles/mL, with a mean diameter of 3.0 to 5.0 $\mu$m. In Optison®, the initial microbubble concentration is 5.0 - 8.0 x $10^8$ microbubbles/mL, with a mean diameter of 2.0 - 4.5 $\mu$m. When UCA was used, a fresh container was removed from the refrigerator and gently rolled to distribute the bubbles evenly within the vial. The UCA was premixed into a portion of degassed phosphate buffered saline (PBS) and the mixture was then reverse pipetted into sample chambers containing PRP or whole blood. Reverse pipetting was accomplished by drawing the PBS and UCA mixture into a pipette tip, marked to indicate the specific volume to be used in the trial. The pipette tip was then placed in the sample and some of the sample was drawn into the tip before the entire contents of the pipette tip were gently expelled into the sample, whereupon two more courses of gently withdrawing and expelling sample were completed. The sample was then placed into the HIFU tank for exposure. UCA was added no more than 10 minutes prior to ultrasound exposure. A concentration of 1.0 $\mu$L UCA per mL PRP and 0.1 $\mu$L UCA per mL whole blood was used. The concentration of UCA was chosen such that a bioeffect was produced, but not such a great effect as to destroy all the cells in the sample. Since the octafluoropropane gas in Optison does not dissolve in blood as readily as air, the lower dose of Optison was used.

## 3.3 Ultrasound Exposure Experimental Setup

All ultrasound exposures occurred in a 16.5 cm L x 12.5 cm W x 12.5 cm H acrylic tank (Sonic Concepts, Woodinville, WA) containing degassed phosphate buffered saline (PBS). PBS was used in the tank to prevent cell damage in samples in the event that a leak occurred in the sample chamber. The PBS was degassed just prior to the experiment, using a hydrophobic polypropylene filter (Spectrum Microgon, Laguna Hills CA). A vacuum pump (KNF Neuberger Inc., Trenton NJ) was used to apply a vacuum of 28 in Hg on the interior of the polypropylene filter fibers while the PBS was pumped around the outer surface of the filter. Using degassed PBS during experiments reduced the amount of cavitation nuclei present in the tank and improved the propagation of ultrasound energy to the sample chamber. The beginning tank temperature was 30 ± 1.0°C during the trials.

Figure 3 shows the experimental arrangement. To reduce reflections, an acoustic absorber with a textured surface, made of Sylgard (Dow Corning), nickel powder (Cerac, Inc., Milwaukee WI) and microballoons (The PQ Corporation, Valley Forge PA), was placed in the tank opposite the insonating 1.1-MHz transducer. The passive cavitation detector (PCD), a 5-MHz focused hydrophone (Sonic Concepts, Woodinville, WA) with a bandwidth of 2-MHz, was positioned in the wall of the tank, 90° from the insonating transducer. The tank was constructed specifically to allow transducer mounting in the sidewalls, which permitted both the HIFU transducer and the hydrophone to be aligned confocally within the tank.

The spherically curved single-element 1.1-MHz HIFU transducer (Sonic Concepts, Woodinville, WA) had an aperture of 69.9 mm, with a radius of curvature of 62.6 mm. The transducer was mounted in one end of the acrylic tank. The

cylindrical sample chamber was mounted vertically from a rack over the tank and centered on the geometric focus of the source. The sample chamber was also held in a positioning block in the bottom of the tank to maintain the focal region of the transducer within the chamber cavity in the presence of streaming forces. For control samples in aggregation experiments, a magnetic stir bar was placed in the sample chamber, with the stir plate (Scinics Co., Ltd., Tokyo, Japan) situated beneath the HIFU tank. Rectangular sample chambers used in adhesion studies were positioned within the tank using a 3-axis motion stage (Techno Isel, New Hyde Park, NY). The sample chambers were placed in the tank so that the HIFU geometric focus was
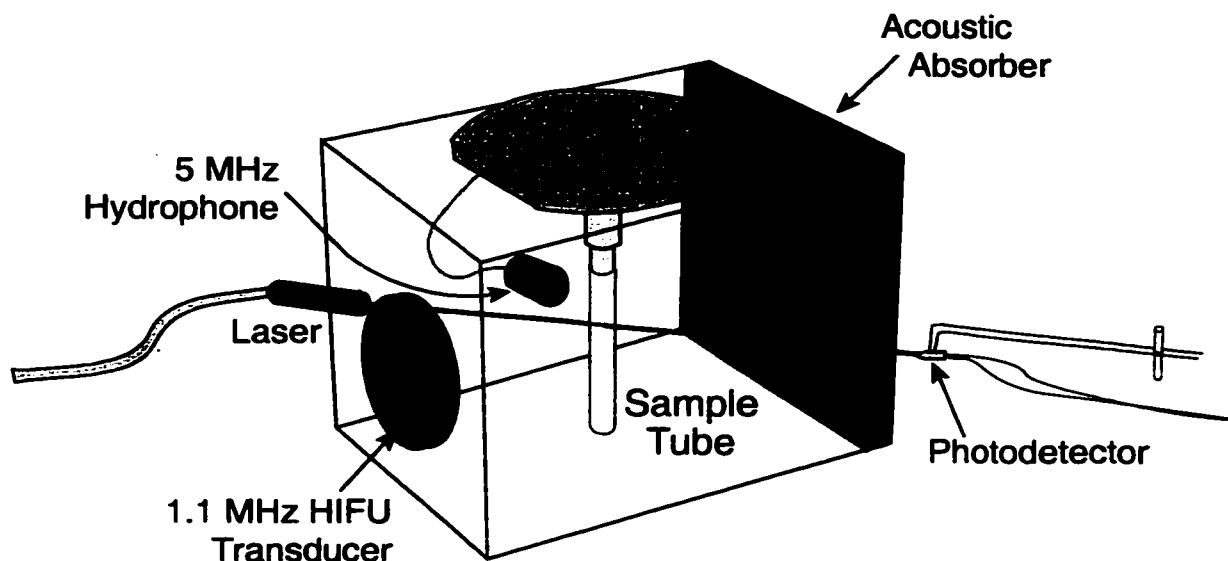
Figure 3: Experimental arrangement for high-intensity focused ultrasound exposures. A 5-MHz hydrophone acts as a passive cavitation detector and is aligned confocally with the 1.1-MHz HIFU transducer. An acoustically transparent sample chamber is stationed so that the focus of the 1.1-MHz transducer is located within the sample volume. For aggregation studies, a laser is aimed through the sample chamber and a photosensor detects the amount of light transmitted through the sample. The photosensor output is connected to an oscilloscope.

located in the center of the rectangular sample chamber. Also pictured in Figure 3 is the laser system used in platelet aggregation studies (described later).

The transducer was energized by a function generator (HP33120A, Hewlett Packard, Palo Alto CA) applied to a power amplifier (AP-400B, ENI, Rochester NY) and matching network (Sonic Concepts, Woodinville WA). The function generator was used to obtain the 1.1-MHz frequency and the voltage of the input signal. The matching network altered the electrical signal to provide a minimal impedance mismatch to the transducer.

In aggregation trials, PRP samples were exposed to CW HIFU for 500 s, whole blood was exposed for 400 s, adhesion study samples were exposed for 120 s, and activation samples were exposed from 1 s to 100 s. CW ultrasound was used in the studies in order to produce the streaming in the sample chambers that was necessary to mix the samples so that platelets could interact and simulate blood flow in a vessel. Intensities up to 4860 W/cm$^2$ were used during the experiments.

### 3.4  HIFU Calibration

The low intensity spatial distribution of pressure of the 1.1-MHz transducer was measured by Sonic Concepts (Woodinville WA) using a calibrated Dapco needle hydrophone (Dapco Industries, Ridgefield CT) with a 0.64 mm active diameter. From the transverse and axial beam plots, an oblong focal zone of 1.5 mm by 8.2 mm is defined by the full width at half maximum (FWHM) pressure points, as shown in Figures 4 and 5. We spatially average acoustic intensity over the transverse focal area to obtain our reported values of intensity.

The low intensity beam profile was scaled to higher intensity by calibration measurements performed using a radiation force balance (IEEE Std 790-1989) with

Figure 4: Transverse beamplot at 1.38-MHz for HIFU tansducer showing full width at half maximum pressure points. (Sonic Concepts, Woodinville WA)

24

Figure 5: Axial beamplot at 1.38-MHz for HIFU transducer showing full width at half maximum pressure points. (Sonic Concepts, Woodinville WA)

an absorbing target as in Poliachik et al. (1999). The radiation force balance measurements provide a measure of total acoustic power radiated into the water as a function of applied voltage (which is proportional to pressure at the transducer face). The result is a smooth parabolic relationship between the acoustic power and the applied voltage, suggesting a linear system. The radiation force balance measurements, however, are taken near the transducer face and do not include any non-linear propagation effects occurring between the face and the focal region. An anti-streaming membrane is used near the face of the absorbing target to reduce the effects of bulk streaming force when performing calibrations.

Comparison measurements were acquired with a calibrated 0.6 mm diameter polyvinylidene fluoride (PVDF) needle hydrophone (NTR Systems, Inc., Seattle WA) using a tank with a 3-axis motion stage (Techno Isel, New Hyde Park, NY) which allowed positioning of the hydrophone at the focus of the 1.1-MHz HIFU transducer. An oscilloscope (LeCroy LT344, Chestnut Ridge NY) displayed the resulting hydrophone output. The voltage from the matching network into the transducer was measured for each calibration voltage level and used as the standard by which exposure levels were evaluated to eliminate any variability introduced by the function generator or amplifier. At higher pressures, non-linearity increased in the system, thus producing a signal in which the positive pressure was greater than the negative pressure. Table 1 lists equivalent measured spatial average intensities and measured pressures for the HIFU transducer.

In summary, absolute focal zone intensities and pressure amplitudes were determined using the beam profiles, radiation force balance measurements and

calibrated hydrophone measurements. All acoustic exposure values are presented as spatial average intensity, in $W/cm^2$, for a given insonation time.

The 5-MHz hydrophone was mapped at low power by Sonic Concepts (Woodinville WA) using a Dapco needle hydrophone, as was accomplished with the 1.1-MHz HIFU transducer. When placed in the specially constructed HIFU tank, the focus of the 5-MHz hydrophone aligns with the focus of the 1.1-MHz HIFU transducer.

Table 1: Equivalent measured pressures and measured intensities for 1.1-MHz HIFU transducer

| Acoustic Intensity $(W/cm^2)$ | Positive Acoustic Pressure (MPa) | Negative Acoustic Pressure (MPa) |
|---|---|---|
| 500 | 2.7 | 2.2 |
| 1000 | 3.9 | 2.9 |
| 1500 | 4.7 | 3.4 |

## 3.5 Cavitation Data Collection

During ultrasound exposure, data from the hydrophone was collected using an oscilloscope (LeCroy 9301A, Chestnut Ridge NY) and a LabVIEW program (See Appendix B). The signal from the 5-MHz hydrophone was routed through a peak detector circuit (PKD01, Analog Devices, Cambridge MA; see Appendix C, Figure C.1) and then into the oscilloscope to capture hydrophone data for the entire exposure time of 400 or 500 s at the maximum available sample rate of 500 samples/second. The LabVIEW program triggered the transducer and oscilloscope and saved the data to disk on a pentium computer (Gateway, North Sioux City SD).

Cavitation data collected from the hydrophone during the exposures were analyzed with a LabVIEW program (see Appendix B) that calculated the integral of the demodulated data that were above a specified noise level for each trial. Figure 6 shows a segment of hydrophone data with the shaded area indicating the integral. Because this data is from the peak detector, the program calculates an area under the curve that is approximately 20% larger than the area that would be calculated for raw data. Given the low sample rate and peak detected data, the calculated area under the curve provides only an estimate of the amount of cavitation occurring during a trial. We term this quantity the relative cavitation dose (RCD), which supplies information on the amount and duration of cavitation that occurs during sample exposure to HIFU. CW exposures of long duration are limited by a sampling rate that is insufficient to properly analyze the data to give an exact measure of the amount of cavitation that occurred in a sample. Since all samples were compared with a similar method, the relative amount of cavitation is an adequate measure of cavitation activity occurring in a sample during the CW HIFU exposure.

## 3.6 Sample Chambers

Two types of sample chambers were used in the experiments. Cylindrical sample chambers for the whole blood or PRP specimens in activation and aggregation studies consisted of a reusable delrin plug, acoustically transparent 0.03 mm thick biocompatible polyester tubing (Advanced Polymers, Salem NH), and a reusable delrin tube through which the sample chamber could be filled, as shown in Figure 7. A delrin sample chamber carrier then attached to the sample chamber, allowing the chamber to be suspended in the HIFU tank. The length of the polyester tubing was 18 mm, with a diameter of 8.6 mm, which provided an exposure volume of 1 mL.
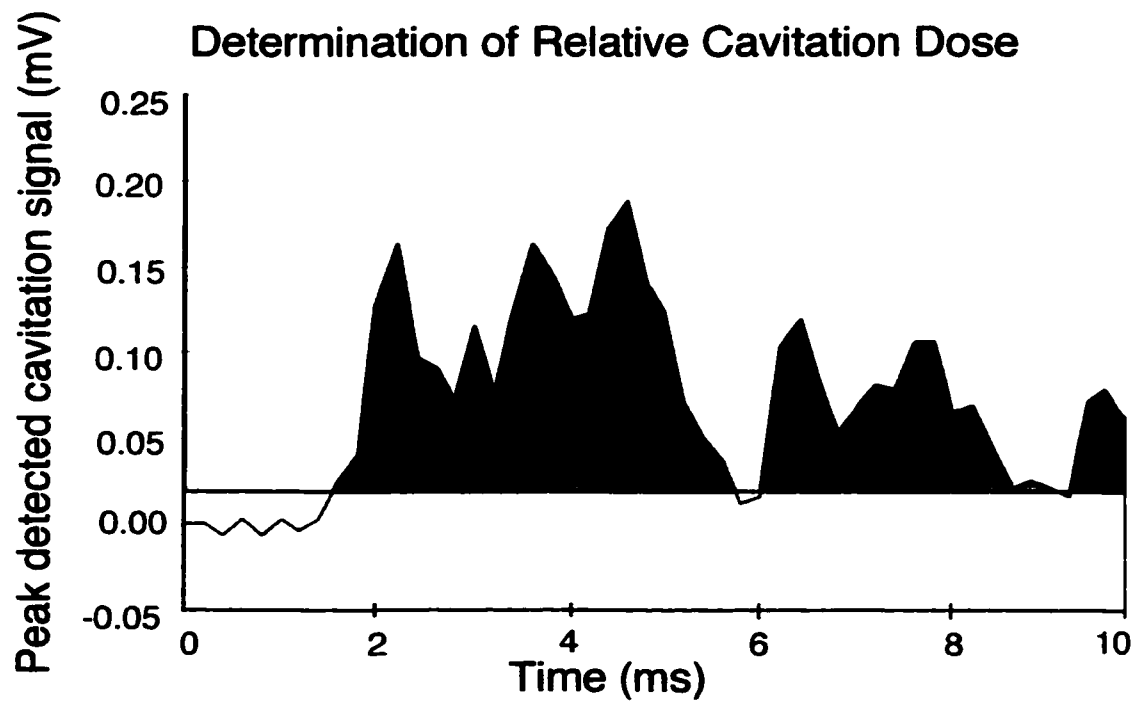
Figure 6: Segment of cavitation data from 5-MHz hydrophone, as routed through the peak detector. To determine relative cavitation dose, the integral of the data was determined above a noise baseline for each trial.

The top surface of the sample was exposed to air, so a sample size of 1.3 mL was used to move the air interface away from the transducer focus. Immediate application of high intensities had a tendency to pit and scar the acoustically transparent sample chambers at the beam focus, thereby causing partial reflections of the ultrasound energy. In order to avoid damage to the sample chamber when the power was initially activated, a LabVIEW program (National Instruments Corporation, Austin TX; Appendix B) was written to increase the voltage applied to the transducer over 5 to 10s.

For platelet adhesion studies, the sample chambers consisted of a 1 cm square polystyrene cuvet (VWR, San Francisco CA) cut to 3 cm length with the collagen-

delrin sample
chamber
carrier

delrin tube

biocompatible
polyester tubing
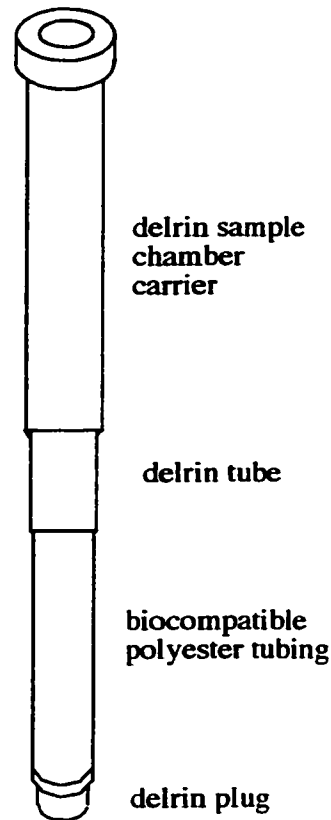
delrin plug

Figure 7: Cylindrical sample chamber used in platelet activation and aggregation trials, consisting of a delrin plug, tube and carrier with an acoustically transparent biocompatible tubing component at the exposure site.

coated glass slide affixed to one end, as in Figure 8. The sample chamber was positioned with the long axis parallel to the axis of the 1.1-MHz transducer as depicted in Figure 9. Glass slides were coated with collagen by adding 10 $\mu$L of a Type I collagen containing solution (No. 385 collagen, Chrono-PAR, Chrono-Log, Haverton PA), and then dried at room temperature for 12 hours. The collagen-coated glass slide was affixed with silicone adhesive on one end of the rectangular chamber while parafilm (American National Can, Neenah WI) was sealed over the opposite end (the transducer-facing end) after sample loading.
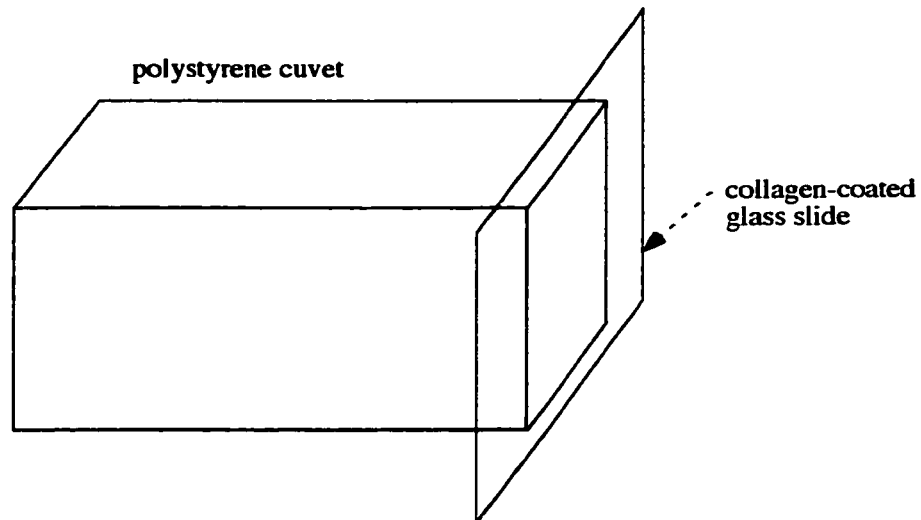
Figure 8: Rectangular sample chamber used in platelet adhesion trials. A collagen-coated glass slide is affixed to the end of a polystyrene cuvet. Parafilm is used to cover the open end once a sample is loaded.
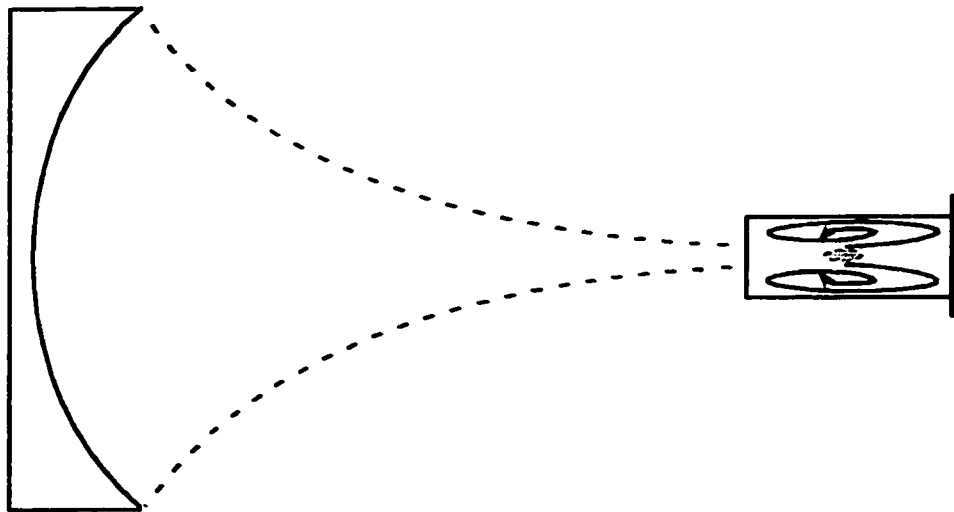


Figure 9. Schematic of the orientation of the rectangular sample chamber relative to the 1.1-MHz HIFU transducer. The focus is positioned in the center of the sample chamber and the flow pattern induced during HIFU exposures is shown.

### 3.7 Statistics

Data are presented as means ± standard error of the means (SEM), unless otherwise noted. The probability of significant differences in aggregation and RCD at different intensities and RCDs were determined through analysis of variance (ANOVA) using a *post hoc* analysis with the Tukey Honest Significant Difference Test. A P value of 0.05 or less was considered significant. Statistica/Mac™ software (StatSoft™, Tulsa OK) was used for all statistical calculations.

### 3.8 Error Analysis

A source of error that is difficult to avoid for *in vitro* experiments is the introduction of cavitation nuclei into samples of PRP or whole blood. Although blood handling was minimized during experiments, the existence of bubbles in blood draw tubes or scratches in the reusable blood sample chambers can harbor sufficient cavitation nuclei to produce cavitation. An attempt was made to remove bubbles introduced during blood draw by placing the blood under vacuum for 20 minutes. However, this introduced another step in blood handling that may just as easily contribute to addition of more cavitation nuclei during the pipetting and transferring process. Scratches in the reusable sample tube parts can be kept to a minimum by careful assembly and disassembly of chambers. The polyester heat shrink tubing portion of the sample chambers is also capable of introducing cavitation nuclei if it is scratched or bent. Careful handling of the tubing is required during tube assembly to avoid such problems.

The PCD responds to signals reflected from the contents of the sample chamber. These signals represent the occurrence of cavitation, but may also be the result of particles moving within the sample chamber. Work by Calabrese (1996)

evaluated cavitation data using a derivative method in an effort to remove signals of moving particles from cavitation events. Comparison studies by Poliachik et al. (1999) showed that cavitation "events" determined using the derivative method were sufficiently similar to cavitation dose to warrant the use of either method to quantify cavitation, thus showing that scattering from particle motion is minimal.

Another cavitation measuring issue is one of sample rate. For long CW exposures such as the experiments described in this work, collecting sufficient data to produce fast Fourier transforms (FFTs) of data is difficult. The method of peak detecting allows for compression of data, yet much information is lost in the process. A 20-kHz decay time in the peak detector (Appendix C) causes this loss of data, but also allows data to be compressed. FFTs are no longer possible and the amount of cavitation calculated by taking the integral above a baseline is an overestimate of the true cavitation activity. A system with 10-MHz sampling rate and a 5 Gbyte memory, or real-time data analysis would be necessary to collect sufficient cavitation data to produce FFTs.

If the PBS in the HIFU tank is inadequately degassed, bubbles in the fluid can act to shield the cavitation signal travelling to the PCD. Proper degassing of the fluid in the HIFU tank is essential for not only PCD function, but also to prevent HIFU energy from being shielded from entering the sample chamber. Also, scarred or pitted chambers reflect ultrasound energy, resulting in underexposed samples.

## 4.0 HIFU-INDUCED THERMAL EFFECTS

Heating of the sample due to absorption of HIFU energy has the potential to provide stimulus for platelet activity through thermal effects. Temperature is monitored in whole blood samples and in the HIFU tank during HIFU exposures. Calculations of heating due to absorption provide information on temperature rise at the HIFU focus.

### 4.1 Materials and Methods

The temperature within the HIFU tank was measured using a 0.005 cm diameter Type K thermocouple (Omega Engineering, Inc., Stamford CT) connected to a 52 K/J thermometer (Fluke Corporation, Everett WA). The starting temperature of the tank was 30 ± 1.0°C. If a temperature rise occurred during HIFU exposure, cool degassed PBS was pumped into the tank after each exposure until the temperature was 30 ± 1.0°C. Temperature in the rectangular sample chambers used in adhesion studies was measured with a 0.013 cm diameter Type K thermocouple. Pulsing schemes were employed (500 cycle bursts at 1500-Hz pulse repetition frequency) to maintain stirring in the chamber while the sample temperature remained below 42°C during adhesion experiments, which used sample chambers that trapped heat more effectively than the cylindrical sample chambers. This particular temperature control scheme was used because the response time of automatic temperature control was not adequate. The average temperature in the tank during the PRP experiments was 33.8 ± 4.0°C.

During whole blood aggregation experiments, temperature was measured in the sample chamber, 5 mm above the impedance sensor, using a 0.005 cm diameter Type K thermocouple that was connected to a data acquisition unit (HP39470A, Agilent, Loveland CO). A second thermocouple, also connected to the data

acquisition unit, was placed in the HIFU tank to track PBS temperatures. Sample rate for temperature data was 1 sample/s per channel.

In whole blood experiments, PBS pumped through a circuit of cooling coils served to cool the tank during HIFU exposures. Average tank temperature during HIFU exposures was 34.4 ± 2°C. Temperatures within the sample chamber tended to increase during the first 50 s of exposure and then stabilize, as shown in Figure 10.
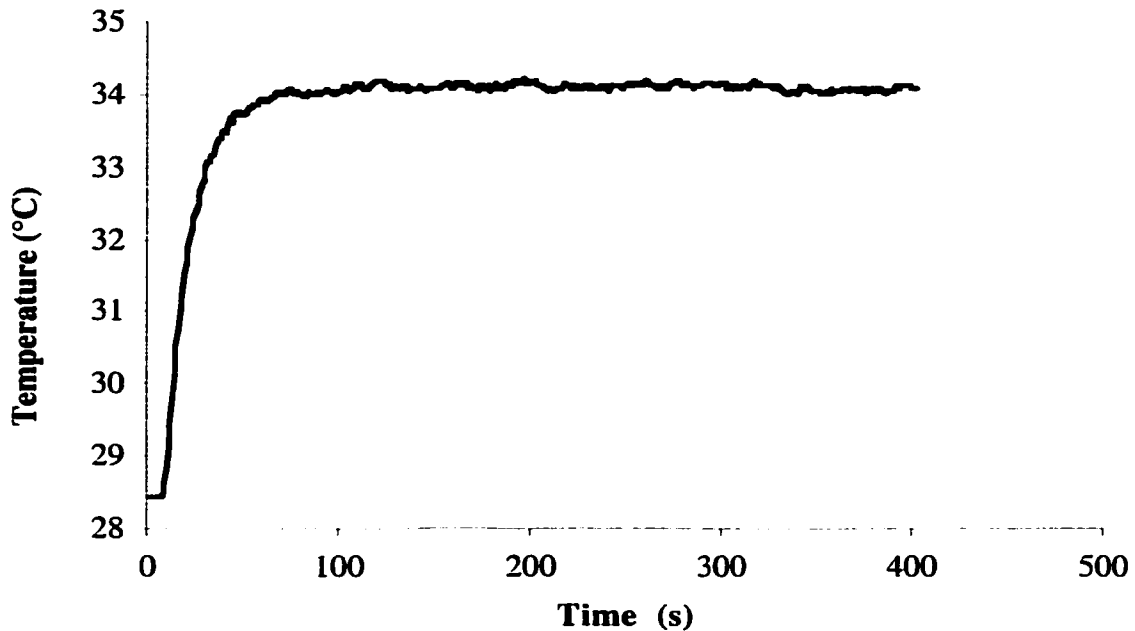


Figure 10: Example of temperature rise in sample chamber during HIFU exposure in whole blood aggregation experiments. Typically, the temperature increases over the first 50 s of HIFU exposure, and then stabilizes. This sample was exposed to a HIFU intensity of 1915 W/cm$^2$.

The voltage from the impedance circuit used to measure aggregation in whole blood increased linearly with temperature, as presented in Figure 11. Temperatures measured within the sample tube during HIFU exposures were used in a series of MatLab programs to adjust impedance circuit voltages to compensate for temperature changes within the sample (see Appendix A).
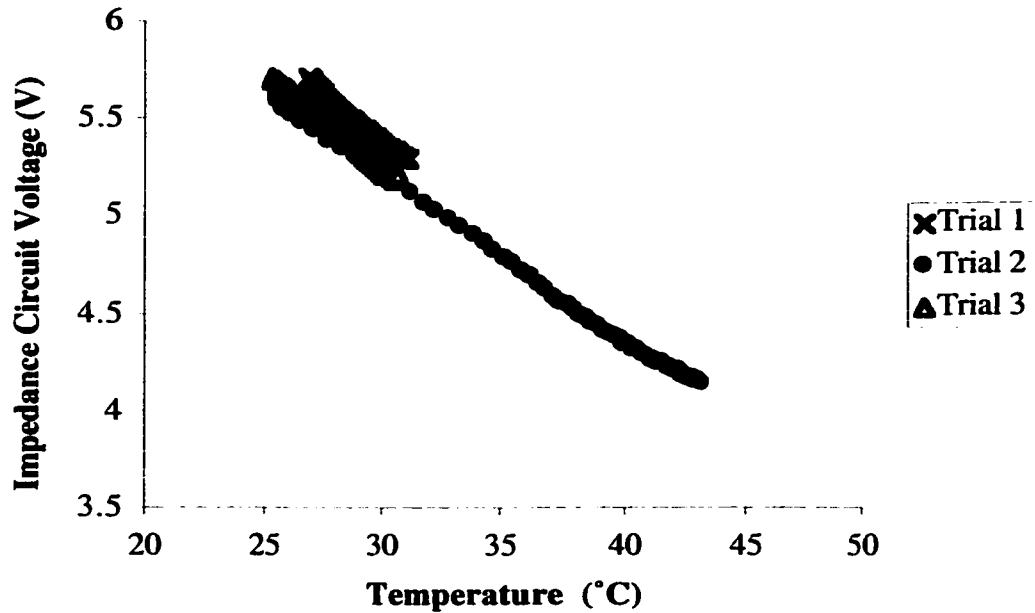
Figure 11: Example of the voltage from the impedance circuit within a sample of whole blood when subjected to controlled temperature rise. The voltage changes linearly with temperature, regardless of the range of temperature increase.

## 4.2 Absorption Calculations

The temperature change in a sample due to absorption can be calculated from:

$$\Delta T = (\alpha_a * 2000 * I * \Delta t) / (\rho * c_t)$$

where $\Delta T$ is the temperature change in the exposure volume (°C), $\alpha_a$ is the absorption coefficient dependent on exposure frequency (Np/cm), I is HIFU intensity (W/cm$^2$), $\Delta t$ is exposure time (s), $\rho$ is sample density (kg/m$^3$), and $c_t$ isthe specific heat of the sample (J/g*°C) (Damianou et al. 1997). Sample attenuation, $\alpha$, is composed of the absorption coefficient, $\alpha_a$, and the scattering coefficient, $\alpha_s$. The attenuation in whole blood at 1.2-MHz is $\alpha = 0.009$ Np/cm (Goss et al. 1978), and the scattering coefficient is $\alpha_s = 0.0002$ Np/cm (Duck 1990). The absorption coefficient is then $\alpha_a = \alpha - \alpha_s = 0.0088$ Np/cm.

For a range of intensities from 1000 to 3000 W/cm$^2$, with $\rho$ = 1060 kg/m$^3$

(Duck 1990), $c_t$ = 3.72 J/g*°C (Duck 1990) and time in the HIFU focus of $\Delta t$ = 100

ms, temperature elevation of a volume of whole blood in the HIFU focus is shown in

Table 2. The exposure time is based on the velocity measurements made in Chapter

8.0, indicating how long a cell would be in the HIFU focus and exposed to HIFU

energy. A velocity of 8 cm/s within the focus of length 8.2 mm gives an exposure

time of 103 ms.

Table 2: Whole blood sample heating due to HIFU exposure

| Intensity (W/cm$^2$) | $\Delta T$ (°C) |
| --- | --- |
| 1000 | 0.45 |
| 1500 | 0.67 |
| 2000 | 0.89 |
| 2500 | 1.12 |
| 3000 | 1.34 |

*4.3 Error Analysis*

Temperature measurements in sample chambers were made with thermocouples placed above the HIFU focus in order to avoid absorption artifacts. The temperatures measured within samples, therefore, do not reflect the largest temperature reached at the HIFU focus. However, mixing in the chamber is sufficiently strong to cause cells to be in the high temperature region for only 30 to 200 ms, depending on HIFU intensity.

*4.4 Summary and Discussion*

From absorption calculations, cells are subject to a temperature rise on the order of 1 °C while they are in the HIFU focus. The HIFU focal volume comprises

2% of the sample volume and consistent stirring occurs within the sample during HIFU exposure. Assuming complete mixing, a temperature rise of 1 °C would occur in the sample chamber every 5 s, which matches closely the data presented in Figure 10. As the temperature of the sample increases, the tank cooling system removes heat from the sample resulting in the steady state temperature seen in Figure 10 after 50 s. During exposures, HIFU energy is also converted to heat in the acoustic absorber located in the HIFU tank opposite the transducer. The tank cooling system serves to cool the sample chamber as well as the water near the absorber. Since thermal effects are dose dependent, a 100 ms exposure to a 1 °C temperature rise, or a 500 s exposure to a 5 °C temperature rise, is insufficient to promote platelet activity.

## 5.0 EFFECT OF HIFU EXPOSURE ON PLATELET ACTIVATION

When a platelet is activated, granules are released and the protein P-selectin is expressed on the surface of the platelet. Also, the platelet membrane inverts such that anionic phospholipids are exposed. These anionic phospholipids are essential for activation of the coagulation cascade. An activated platelet will change the conformation of the GPIIb-IIIa receptors such that fibrinogen can bind to it. These changes can be measured using flow cytometry. Samples of whole blood were exposed to HIFU intensities of 1530 W/cm$^2$ CW for 1 s or 380 W/cm$^2$ for 100 s. PRP samples were exposed to HIFU CW intensities ranging up to 2200 W/cm$^2$ for 100 s.

### 5.1 Materials and Methods

After ultrasound exposure, PRP or whole blood samples in activation studies were placed into polypropylene microcentrifuge tubes (CMS, Inc., Federal Way WA) and analyzed in a flow cytometer within 30 minutes (see Appendix D). As described in Tait et al. (1999), fluorescently labeled antibodies for the P-selectin protein (phycoerythrin-anti-CD62P, Becton-Dickinson, Franklin Lakes NJ), the activation-dependent epitope of GPIIb-IIIa (FITC-PAC1, Becton-Dickinson, Franklin Lakes NJ) and labeled annexin V for anionic phospholipids (Wood et al. 1996) was added to PRP samples that had been exposed or sham exposed to HIFU. Samples were then analyzed in a flow cytometer (XL-MCL, Beckman Coulter, Fullerton CA). The intensity of fluorescence per platelet was measured for a platelet count of 5000. The background fluorescence of platelets was determined by adding fluorescently labeled non-specific IgG. Platelets with fluorescence above the background level were defined as activated platelets. The percentage of activated platelets was determined before and after exposure to HIFU.
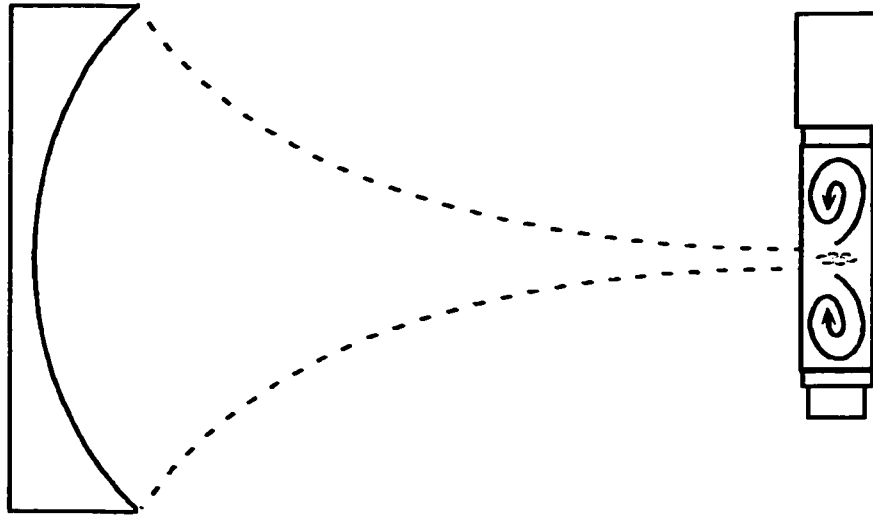
Figure 12: Schematic of flow patterns in the cylindrical sample chamber induced during CW HIFU exposures. The 1.1-MHz HIFU transducer focus is positioned in the center of the sample chamber. The general flow pattern is shown in the cylindrical sample chamber used in activation and aggregation studies.

## 5.2 Results

Activation studies were completed on samples of whole blood and PRP. Whole blood samples in cylindrical sample chambers were exposed to two HIFU conditions: 1530 W/cm$^2$ CW for 1 s or 380 W/cm$^2$ for 100 s. Exposure of the sample to HIFU resulted in stirring of the platelets within the chamber due to acoustic streaming and radiation pressure, as depicted in Figure 12. Based on the size of the HIFU focus and a 1 mL sample exposure volume, only about 2% of the sample was within the beam focus during exposure, but vigorous HIFU-induced stirring within the sample chamber allowed an estimated 85% of the sample to be exposed to HIFU

(based on high speed camera observations). An example of whole blood activation results is illustrated in Figures 13 and 14. In Figure 13 the x-axis displays PAC-1, representing activated fibrinogen receptors, while the y-axis displays CD62, representing P-selectin expression. The control sample contained a few platelets that were activated in both PAC-1 and CD62, as seen by the marks in quadrant 2, while most platelets remained in areas indicating low activation in quadrants 1, 3, and 4. The sample exposed to HIFU at 1530 W/cm$^2$ for 1 s, however, shows that a majority of the platelets contain activated PAC-1 and CD62 markers, as seen by the marks in quadrant 2 of the second plot.

In Figure 14, the x-axis scale provides a measure of Annexin V markers while the y-axis is unused. In the control sample, very few platelets show Annexin V binding, while the sample that was exposed to 380 W/cm$^2$ HIFU for 100 s shows a 35% increase in the number of active Annexin V markers.

Activation studies were also performed on PRP samples in cylindrical sample chambers that were exposed to HIFU CW intensities ranging up to 2200 W/cm$^2$ for 100 s. An example of results from a single sample set for exposure of PRP to HIFU showed a trend of intensity dependent increase in platelet activation markers present on the platelet surface (Figure 15). Without HIFU exposure, 4.8% of platelets expressed P-selectin on their surface while 0.5% bound Annexin V. After 100s of 2200 W/cm$^2$ HIFU exposure 8.8% of platelets were expressing P-selectin, and 3.1% bound Annexin V, indicating that HIFU had stimulated both granule release and anionic phospholipid exposure.

The intent of the platelet activation studies is to show that HIFU does stimulate platelet activation as exposure conditions are varied, including HIFU

**Control**



Activated Fibrinogen Receptors -->

**HIFU, 755 W/cm² for 1 sec**
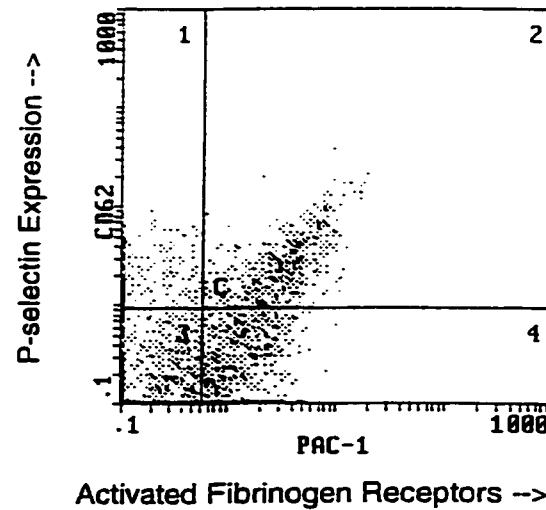


Activated Fibrinogen Receptors -->
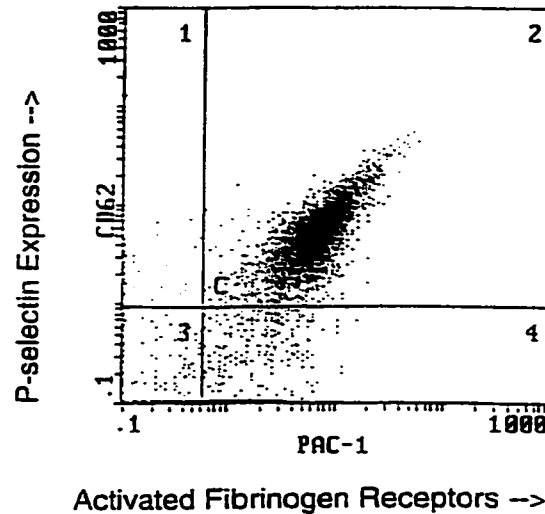
Figure 13:  Platelet activation measured by flow cytometry.  The x-axis indicates increasing activation of fibrinogen receptors (PAC-1), and the y-axis indicates increasing P-selectin expression (CD62).  In the control sample (upper plot) unexposed whole blood had minimal activation, as seen by the sparse number of dots in sector 2.  In whole blood exposed to HIFU at 1530 W/cm² for 1 s (lower plot), most of the platelets activated, as seen by the great number of dots located in sector 2.  P-selectin signals platelet activation and fibrinogen receptor activation allows platelet aggregation.

**Control**
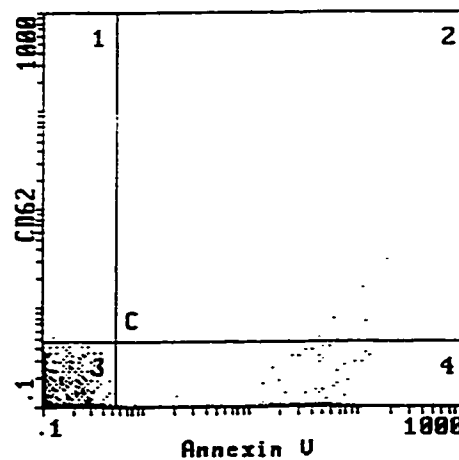


Increasing Negative Phospholipid -->

**HIFU, 380 W/cm2 for 100 sec**
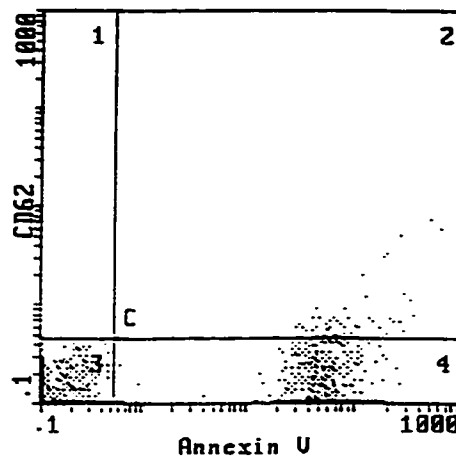


Increasing Negative Phospholipid -->

Figure 14: Platelet activation steps necessary for coagulation to proceed, measured by flow cytometry. The x-axis indicated increasing amount of exposed negative phospholipid (Annexin V). The y-axis is not used. In the control sample (upper plot), very few dots show negative phospholipid exposed, as seen along the x-axis. In whole blood exposed to HIFU at 380 W/cm$^2$ for 100 s (lower plot), many platelets show negative phospholipids exposed. Negative phospholipid is a necessary component in the coagulation cascade leading to fibrin clot formation.
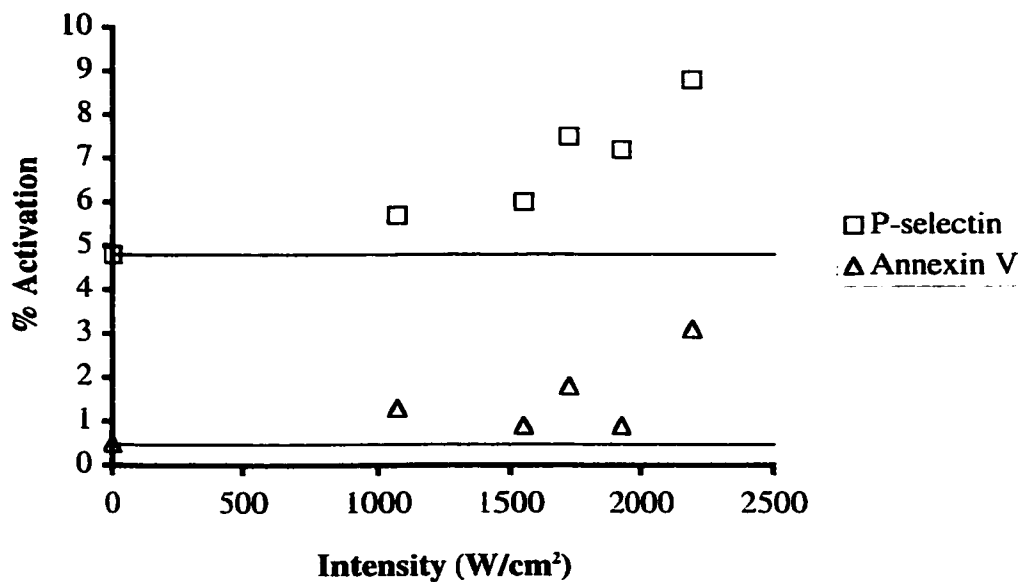
Figure 15: Platelet activation response to HIFU intensities in samples of PRP. Flow cytometry was used to measure expression of P-selectin (□) and anionic phospholipids, as marked with Annexin V (Δ). Baseline values of Annexin V and P-selectin are noted by horizontal lines. For the single sample set shown, a trend of platelet activation increasing as intensity increases is apparent.

intensity and exposure time. In samples of whole blood, P-selectin expression increases with intensity for exposure times up to 10 s. Negative phospholipid display, however, requires longer HIFU exposure times to produce an increase in display. PRP studies demonstrate a general trend towards platelet activation increase with intensity. Due to the cost effectiveness of the platelet aggregation studies, quantification of platelet activity was accomplished in aggregation studies instead of activation studies.

## 5.3 Error Analysis

Samples used in activation studies are ideally exposed within an hour of blood draw to maintain maximum platelet function. HIFU exposures of samples for

activation studies typically are analyzed within 60 minutes. Because each sample is placed in the HIFU tank and exposed separately, a time delay from the first sample through the last may introduce some amount of error in measuring platelet activation.

A limit on the duration of HIFU exposures is placed on activation samples. If platelets are exposed for longer than 100 s, platelets tend to aggregate, thus covering receptors used in activation assays. At high intensities, some aggregation may take place before the 100 s time limit, thus producing activation results that may be too low, inaccurately representing the amount of activation in a sample.

## 5.4 Summary and Discussion

HIFU exposure of whole blood samples led to activation of platelet protein P-selectin, receptor GPIIb-IIIa and some negative phospholipid display. The exposure time required to activate these components varied, with P-selectin and GPIIb-IIIa responding quickly at higher intensities, while the display of negative phospholipid occurred after longer, lower intensity exposures. Since the negative phospholipid is a component in the coagulation cascade, this result sets parameters for identifying which HIFU exposure conditions will best form a hemostatic plug.

PRP exposed to HIFU intensities of 1050 to 2200 W/cm$^2$ expressed P-selectin and anionic phospholipids, with expression increasing with acoustic intensity. Thus, HIFU can stimulate the platelet release reaction and platelet membrane reorganization. Anionic phospholipid exposure is a requirement for activation of the coagulation cascade. Part of the hemostatic effect attributed to HIFU may be due to platelet activation and acceleration of coagulation.

Exposure conditions in platelet activation studies are limited due to the receptors or proteins that are marked with the fluorescently tagged antibodies. If

HIFU exposure is allowed to proceed long enough to induce platelet aggregation, the antibodies cannot attach to their intended targets because the platelets will stick to each other first. This limits HIFU exposures to low intensities for long durations or high intensities for short durations.

.

# 6.0 EFFECT OF HIFU EXPOSURE ON PLATELET ADHESION TO A COLLAGEN-COATED SURFACE

Platelets bind to collagen through vWf and through a specific collagen receptor. This leads to platelet activation and recruitment of additional platelets. After HIFU exposure of samples of PRP in collagen-coated chambers, platelet adhesion to collagen can be observed using optical or scanning electron microscopes.

## 6.1 Materials and Methods

PRP samples for adhesion studies were gently pipetted into the rectangular exposure chambers that contained a collagen-coated surface on one end. While carefully excluding air bubbles, parafilm was used to cover the open end of the chamber, which was also the end that faced the 1.1-MHz transducer. Exposure times were 120 s CW for all trials, at intensities of up to 2120 W/cm$^2$. When pulsed ultrasound was used to prevent sample heating, 500 cycles at 1500-Hz pulse repetition frequency was used, maintaining the total exposure time (HIFU on-time) was at 120 s. Some control chambers did not contain collagen-coated surfaces but contained plain glass slides instead, to determine if platelets adhere to plain glass.

After HIFU exposure, the collagen-coated glass slide was removed from the cuvet and the slide was gently rinsed with PBS. The collagen-coated surface was then stained with Wright's stain, which served to fix and stain the platelets. Environmental Scanning Electron Microscopy (ESEM) was performed using an ESEM (FEI Company, Hillsboro OR) that operated in a vacuum of 5-15 Torr. (See Appendix E) The samples analyzed with ESEM were used as a qualitative evaluation of platelet adhesion. Due to the inconsistent, or "patchy", nature of platelets adhering to the collagen-coated surface as a result of variations in collagen-coating and stirring

in the sample chamber during HIFU exposure, quantitative analysis was not deemed appropriate.

### 6.2 Results

While platelet activation and aggregation are important steps in platelet related hemostasis, the platelet clump must adhere to a surface in order to provide a solid base upon which a full thrombus may grow. In the body, platelets adhere to subendothelial proteins such as collagen. To demonstrate that HIFU exposure can stimulate platelets to adhere to collagen, we simulated a wound by using collagen-coated surfaces that were exposed to PRP (sham) and PRP plus HIFU. Figure 16 shows environmental scanning electron microscope (ESEM) images of a control showing a collagen-coated surface in which no HIFU or PRP was applied, a sham collagen-coated surface that had been exposed to PRP for 5 minutes, and a sample with platelets attached to a collagen-coated surface resulting from 2 minutes of HIFU exposure of a PRP sample at 1000 W/cm$^2$. Visible in each figure are collagen strands, while the HIFU exposed sample also contains clumps of platelets attached to the collagen strands. Similarly, HIFU exposures from 14 total trials at 960 to 2120 W/cm$^2$ for 2 minutes caused platelets to adhere to collagen (not shown). Exposures of PRP to diagnostic ultrasound (2 W/cm$^2$) for 8 minutes in collagen-coated chambers or of PRP in chambers containing plain glass slides did not produce adhesion (not shown).

### 6.3 Error Analysis

Several sources of error existed in the platelet adhesion studies. The sample chamber (polystyrene) tended to absorb the acoustic energy and heat the sample. Although a pulsing scheme of HIFU exposure was used to maintain temperature in

the chamber, the temperature rise may have effected some platelets. Also, the ultrasound tended to become more focused as it passed through the parafilm cover over the open end of the chamber. Instead of producing attenuation, the parafilm



Figure 16: Adhesion of platelets to a collagen-coated surface. This figure displays environmental scanning electron microscope images of: a) control collagen-coated surface in which no HIFU or PRP was applied; b) sham collagen-coated surface in which PRP was allowed to contact the surface for 5 minutes without HIFU exposure; and c) a collagen-coated surface that was exposed to PRP and 2 minutes of 1.1-MHz HIFU at 1000 W/cm$^2$. A few platelets can be seen on the sham collagen-coated surface (b), but several platelets and platelet clumps are attached to the collagen strands in the HIFU exposed sample (c).

slightly increased the intensity at the focus, thus making intensity reporting for adhesion studies slightly inaccurate.

Collagen-coated surfaces used in the adhesion studies were constructed of glass slides upon which collagen was dried. The glass slide tends to reflect ultrasound energy back into the chamber, at times creating a standing wave in the chamber. Also, the method of drying a drop of collagen-containing solution onto a slide may lead to an inconsistent and non-uniform surface of collagen-coating. This non-uniformity may be to blame for the "patchy" nature of platelet adhesion to the

collagen-coated surface. Upon inspection by optical microscope, groups of adhered platelets appeared scattered in clusters throughout the slide. This inconsistent platelet adhesion may also be due to the non-uniform flow field or sound field that existed in the sample chamber, or vibration of the glass slide.

## 6.4 Summary and Discussion

Platelet adhesion trials demonstrated that HIFU exposure of PRP near a collagen-coated surface for intensities between 960 and 2120 W/cm$^2$ for 2 minutes can cause platelets to adhere to the collagen, whereas shams do not show platelet adhesion. This result indicates that HIFU may prove to be an effective means to speed up platelet plug formation in low flow systems without causing collateral damage to surrounding tissues as might be the case with HIFU cauterization.

Platelet adhesion trials showed that HIFU exposure of PRP near a collagen-coated surface at 1000 W/cm$^2$ can cause platelets to adhere to the collagen, whereas intensities used in diagnostic exposures (2 W/cm$^2$) or controls do not show platelet adhesion. This result indicates that HIFU may prove to be an effective means to speed up platelet plug formation in low flow systems, which is important because if HIFU can stimulate platelet aggregation, the aggregate should ideally adhere to a wound and not flow through the circulatory system.

## 7.0 EFFECT OF HIFU EXPOSURE ON PLATELET AGGREGATION AND ASSOCIATED CAVITATION

Platelet aggregation occurs when platelets are activated and the conformation of the GPIIb-IIIa receptors changes such that fibrinogen and other ligands can bind to them. A single fibrinogen molecule can bind to GPIIb-IIIa receptors on different platelets, thus causing platelet aggregation. Laser aggregometry was used to measure HIFU induced platelet aggregation in samples of PRP and impedance aggregometry was used to measure HIFU induced platelet aggregation in samples of whole blood. Cavitation was monitored and quantified for each HIFU exposure.

### 7.1 Materials and Methods

For PRP samples, aggregation was measured within the cylindrical sample chambers with a laser and a photodetector system. A 670 nm laser (Quarton Inc., Taipei Hsien, Taiwan) was mounted outside the acrylic tank and positioned to locate the beam within the sample chamber with the emerging beam striking the OP803SL photosensor (Newark Electronics, Kirkland WA) as in Figure 3. The signal from the photodetector was amplified using the circuit presented in Appendix C, Figure C.2 and was recorded on a LeCroy oscilloscope along with cavitation data from the 5-MHz hydrophone. All ultrasound exposures for PRP aggregation studies were monitored with a CCD camera (Sony Electronics, Inc., Park Ridge NJ) and the output recorded using a VCR (Samsung Electronics Co., Ltd., Seoul, Korea). The amount of aggregation was determined by comparing the final photosensor voltage for each exposed sample to the amount of light transmitted through a sample of PPP (assumed to be 100% aggregation). CW HIFU intensities up to 2265 W/cm$^2$ were used in 500 s exposures of PRP.

In order to investigate the ability of a limited amount of HIFU induced cavitation to aggregate platelets, PRP in the cylindrical sample chambers was exposed to CW HIFU for 10 s and then stirred for 490 s with a magnetic stir bar. Intensities of up to 4860 W/cm$^2$ were used. Photosensor and cavitation data were collected for the combined 10 s HIFU exposure and 490 s stirring time. A control sample that was stirred for 500 s but not exposed to HIFU was used for comparison.

Experiments to limit cavitation were completed through the use of an overpressure chamber, similar to that used by Bailey et al. (2001). The entire tank was not pressurized because the 1.1-HMz HIFU transducer is air-backed and cannot withstand pressurization. Figure 17 shows a schematic of the overpressure chamber located in the HIFU tank. A polyethylene terephthalate (PETE) bottle was attached to a flange (Appendix F, Figure F.9). Fittings on the flange allowed pressurization of the fluid-filled bottle through use of a handpump (Ralston Instruments, Chagrin Falls OH). Pressures of 7 atm (700 kPa) were used for all overpressure experiments. A blood carrier mount consisting of a 0.625-18UNF-2A threaded screw fitted with an o-ring seal was used to introduce the samples into the overpressure chamber. A transition piece that fit over the cylindrical sample chamber was threaded such that it would mate with the blood carrier mount. The higher pressure provided by the overpressure chamber will tend to decrease the occurrence of cavitation by decreasing the size that cavitation nuclei can reach because the maximum rarefaction pressure will be reduced.

Sample chambers used in the overpressure studies were the same as those used in previously described aggregation studies, consisting of the acoustically transparent polyester tubing, delrin plug and tube. An additional PVC center plug

(Appendix F, Figure F.4) with a tolerance fit was used to block the tube once the sample had been introduced, in order to eliminate air from the chamber. Special filling tubes (Appendix F; Figure F.10) were added to the PVC center plug to allow for total filling of all existing spaces within the sample chamber resulting in elimination of air from the sample tube.
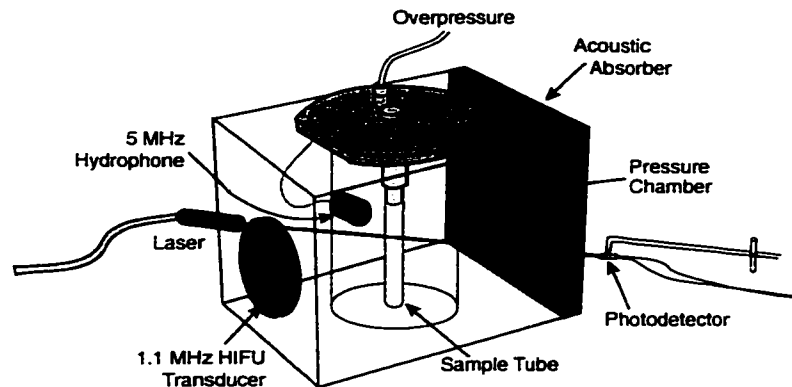


Figure 17: Experimental setup for HIFU overpressure aggregation exposures. The setup is the same as seen in Figure 3, with the exception of the addition of an overpressure chamber, which allows the sample to be pressurized without pressurizing the HIFU transducer or the PCD. An overpressure of 7 atm was used in all experiments.

Sample chamber filling proceeded as follows. After the sample chamber was carefully filled with sample, the PVC center plug was inserted into the delrin tube. The sample was drawn into an insulin needle and then gently expelled into a filling tube until sample appeared in the opposite filling tube, indicating that the sample chamber was filled and all air was excluded from the chamber. A PVC cap (Appendix F, Figure F.5) was then placed over the chamber filling tubes, whereupon the transition piece (Appendix F, Figure F.3) was attached to the chamber and connected to the blood carrier mount (Appendix F, Figure F.8). The entire assembly was then inserted into the overpressure chamber, which was filled with degassed

PBS, and the blood carrier mount was tightened into place. The handpump was then used to increase the pressure in the chamber to 7 atm. CW HIFU exposures up to 3350 W/cm² were used for overpressure samples. If the temperature in the overpressure chamber increased beyond 32°C, the PBS was drained and refilled with room temperature PBS.

Platelet aggregation in whole blood was measured using an impedance sensor (Chrono-Log, Havertown PA), in a method developed by Cardinal (1980). In this method, an electrode assembly is inserted into a sample of PRP or whole blood, as shown in Figure 18. A 4V peak to peak 15-kHz sinusoidal voltage is applied to the electrodes and a monolayer of platelets forms on the electrodes during a 2 minute acclimation period. In the absence of any aggregation stimulus, no other platelet accretion occurs and the conduction between the electrodes is unaffected. If platelets adhere to the electrodes, the conduction between the electrodes is impaired resulting in a change in the impedance of the electrode assembly, which is converted to a voltage output by the impedance aggregometer circuit shown in Appendix C, Figure C.3.

In order to calibrate aggregation measuring methods, collagen or adenosine diphosphate (ADP) were used to stimulate platelet aggregation. A cylindrical sample chamber was filled with a PRP sample and a magnetic stirbar was used to stir the calibration sample. A dose of 6 $\mu$g collagen (Chrono-log Corp., Havertown PA) or 7 $\mu$L of 10 $\mu$M ADP (Chrono-log Corp., Havertown PA) was used to stimulate aggregation. These trials were used to calibrate impedance as compared to laser aggregometry

impedance
sensor

electrode wires

cylindrical
sample
chamber
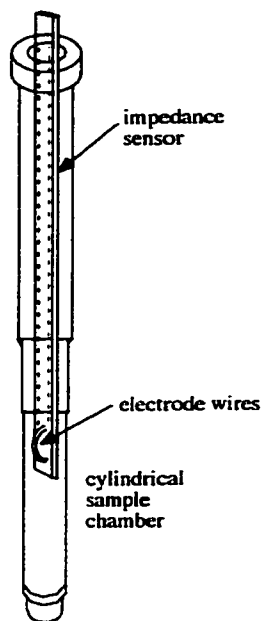
Figure 18: Schematic of impedance sensor located in cylindrical sample chamber. During HIFU exposures, the sensor was inserted in whole blood samples such that the electrode wires were completely submerged in the sample, yet the sensor was located above the HIFU focus. During experiments, a thermocouple was attached to the impedance sensor, just above the electrode.

## 7.2 Spectroscopy to Measure Hemolysis

After HIFU exposure of some of the whole blood trials, spectroscopic analysis of the plasma hemoglobin content was applied to determine the amount of erythrocyte damage that occurred. A spectrophotometer measuring absorbance of 541 nm light (Shimadzu Scientific Instruments, Inc., Columbia MD) was used in the analysis. Samples were centrifuged at 20,000 rpm for 2 minutes after HIFU exposure. The supernatant was removed and stored in an epindorf tube until analysis. A control sample (not exposed to HIFU) was analyzed as a 0% hemolysis point and a 100% hemolysis sample was prepared by adding 1 mL deionized water to an unexposed 1 mL whole blood sample. All samples were diluted equally with Drabkins reagent

placing all hemoglobin in the same conformation to allow for more consistent absorbance measurements.

### 7.3 Platelet Secretion of Activating Agents

Platelets can be activated by ADP, which is exclusively an intracellular substance appearing only after cell lysis or by dense granule secretion in platelets. The concentration of ADP in dense granules is 650 mM, and in platelets is 15 mM. The volume of a platelet is $8 \times 10^{-15}$ L/platelet, and the concentration of platelets in whole blood is $3 \times 10^{11}$ platelets/L (Colman 1994). The volume of whole blood made up by platelets is then 0.24% volume. If all platelets in a sample of whole blood were to release the contained ADP, the total release of ADP would be $15 \times 10^{-3}$ mol/L * 0.0024 volume fraction platelets = 36 $\mu$M ADP.

Platelets require a stimulus of 2 5 $\mu$M ADP to aggregate (Colman 1994), so destruction of 6 - 14% of platelets in a sample would be enough to initiate aggregation. In a previous study using the same experimental setup as used herein, 1 s HIFU exposures of whole blood containing 4.2 $\mu$L UCA/mL sample caused 45% hemolysis at 2000 W/cm$^2$ (Poliachik et al. 1999). The UCA concentration used in the current platelet studies is 1 $\mu$L UCA/mL sample. For the longer exposure times used in the platelet aggregation studies, it is reasonable to assume that at least 10% of the platelets are being lysed and releasing sufficient ADP into the sample to stimulate platelet activity.

### 7.4 Results

Aggregation studies consist of HIFU exposures completed on two types of samples: PRP and whole blood. The PRP samples are composed of: 1) PRP alone; 2)

PRP with UCA; 3) PRP in an overpressure chamber. The whole blood samples are both with and without UCA.

### 7.4.1 Platelet Aggregation and Cavitation in Platelet Rich Plasma

Since HIFU exposures of 100 s successfully produced platelet activation, and platelet aggregation cannot occur without platelet activation, aggregation was used to quantify the effect of HIFU exposure on platelet activity. Exposure of PRP to HIFU results in platelet aggregation when exposure conditions are suitable. Figure 19 shows the time course of visual changes and platelet aggregation in the PRP during exposure to HIFU. Prior to HIFU exposure, the PRP is cloudy due to the suspended platelets (19a). After initiating HIFU exposure, the platelets begin streaming around the HIFU focus as in Figure 12. The first evidence of platelet activation on video microscopy is the appearance of microscopic aggregates in the sample that appear prior to any changes in laser aggregometry. When the aggregometry begins to show a change from baseline, visible clumps of platelets are seen streaming within the sample chamber (19b). As aggregation continues, the platelet clumps become larger and the background plasma becomes clear (19c). A sample is considered to be fully aggregated when the photodetector voltage matches the voltage measured when a sample of PPP is placed in the sample chamber. Full aggregation was not measured in any sample, possibly due to excessive cavitation that may rip platelets apart such that they are no longer capable of aggregation, yet still scatter light from the laser. Quantification of platelet destruction resulting from HIFU exposure was not attempted because platelet counts are not possible once the platelets aggregate.

The three types of PRP samples were exposed to a range of HIFU intensities,

depending on the sample. Different intensity ranges were used for different sample

conditions to ensure platelet reaction to HIFU without destroying the platelets. Table
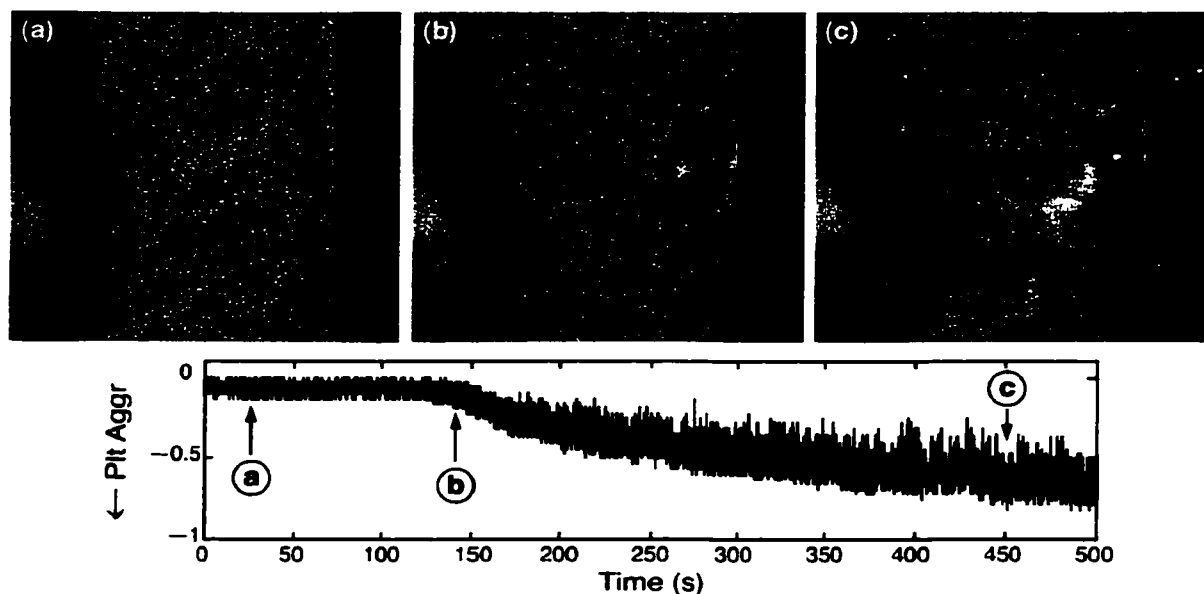


Figure 19: Video frames showing progression of aggregation. Frame a) depicts platelet rich plasma which is cloudy and thus does not transmit light, as shown on the associated aggregation curve by arrow (a). Frame b) depicts small aggregates formed in the sample chamber, allowing some light transmittance as shown by the decreasing voltage noted by arrow (b) on the aggregation curve. Frame c) depicts nearly full aggregation and greater light transmittance, as shown by arrow (c) on the aggregation curve. The red spot on the chamber is the location of laser beam.

2 presents the exposure conditions used for each type of sample. Exposure durations were all 500 s.

Some examples of platelet laser aggregometry traces are shown in Figure 20, comparing aggregation traces of different types of PRP samples. In the aggregation curves, as platelet aggregation increases photodetector voltage decreases. In the ADP control, a PRP sample + 7 μL of 10 μM ADP stirred with a bar magnet results in the

aggregation curve in trace 20a, which is typical of an aggregation curve measured in clinical work. In the trial depicted by trace 20b, PRP was exposed to 2020 W/cm$^2$ HIFU. Note that aggregation does not appear on the trace until approximately 130 s.

Table 3: HIFU exposure conditions for PRP aggregometry samples

| Sample | Intensity (W/cm$^2$) | Maximum Negative Pressure (MPa) |
|---|---|---|
| PRP | 1020 - 2265 | 2.9 - 4.1 |
| PRP + UCA | 545 - 1550 | 2.2 - 3.5 |
| PRP @ 7 atm overpressure | 1135 - 3350 | 3.0 - 4.9 |

The trial shown in trace 20c represents PRP + 0.1% UCA exposed to HIFU at 1355 W/cm$^2$. With UCA added to the sample, aggregation occurs more quickly (50 s) and at a lower intensity than the sample without UCA. The trial shown in 20d represents a sample of PRP subjected to 7 atm overpressure exposed to HIFU at 2265 W/cm$^2$. In the pressurized sample, aggregation takes much longer to occur (420 s) and requires a much higher intensity than samples without overpressure.

Figure 21 shows representative aggregation curves (top portion) collected during trials along with associated cavitation data (bottom portion) for the three types of PRP samples. Column A represents data from aggregation trials of PRP samples containing 0.1% UCA (1.3 mL PRP + 1.3 $\mu$L UCA), in which cavitation is expected during HIFU exposures. The top set of data in Column A represent a HIFU exposure at an intensity of 545 W/cm$^2$, resulting in an RCD of 4 and no measurable aggregation. The bottom set of data in Column A show data from a 1470 W/cm$^2$ HIFU exposure, resulting in an RCD of 1225 and aggregation of 66%. For samples containing UCA, when cavitation occurs, it begins with HIFU exposure, stays strong

for more than a minute and then gradually reduces. Associated aggregation begins within 50 s of the onset of cavitation.
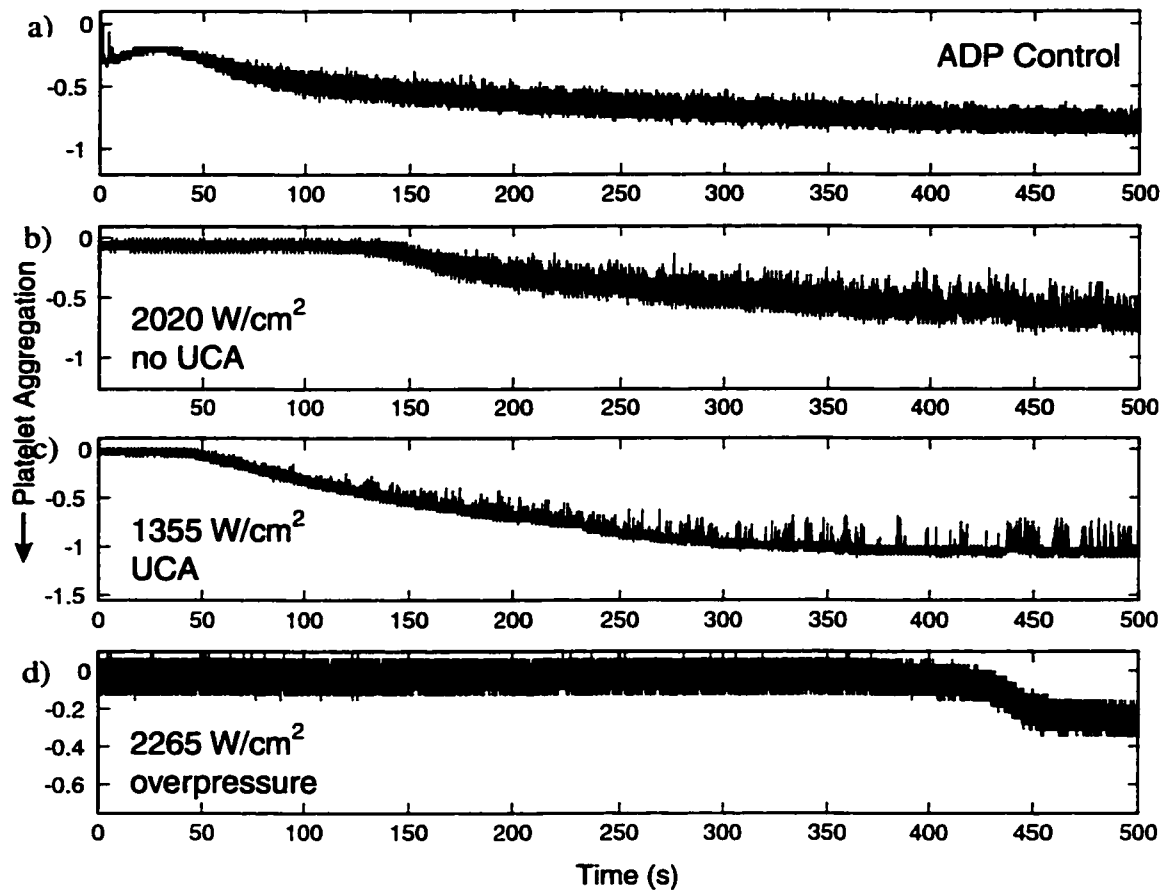


Figure 20: Platelet aggregation traces measured by platelet aggregometry. In a) the ADP control, a PRP sample + 7 $\mu$L of 10 $\mu$M ADP was stirred with a bar magnet. The trace is typical of an aggregation curve measured in clinical work. In b) PRP was exposed to 2020 W/cm$^2$ HIFU. Aggregation did not appear on the trace until approximately 130 s had passed. In c) PRP + 0.1% UCA by volume exposed to HIFU at 1355 W/cm$^2$. Aggregation occurred more quickly (50 s) and at lower intensity than the sample without UCA. In d) PRP subjected to 7 atm overpressure is exposed to HIFU at 2265 W/cm$^2$. Aggregation occurred well into the exposure (420 s) and required a higher intensity than samples at atmospheric pressure.

Figure 21: Paired passive cavitation data and aggregation data. These images depict platelet aggregation data paired with its associated data from the passive cavitation detector. Three sample conditions are depicted: Column A) 1 mL PRP + 1 $\mu$L UCA at 1 atm; column B) 1 mL PRP at 1 atm and Column C) 1 mL PRP at 7 atm overpressure. The first row shows results of samples exposed near the platelet aggregation intensity threshold, where little cavitation or platelet aggregation occurs. The bottom row shows results of samples exposed above the intensity threshold for each sample condition. In these results, the different patterns of cavitational activity that occur in each sample condition is evident. In samples containing UCA at 1 atm, cavitation occurs mainly at the beginning of HIFU exposure. In PRP at 1 atm, cavitation is sporadic, while in the overpressure sample cavitation does not occur for some time, and then when it does, platelet aggregation follows almost immediately.
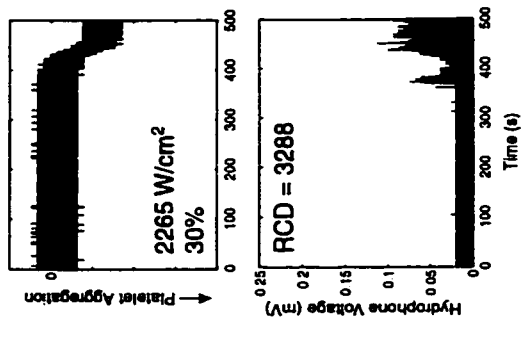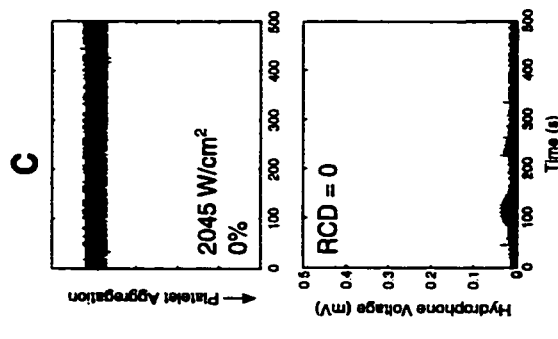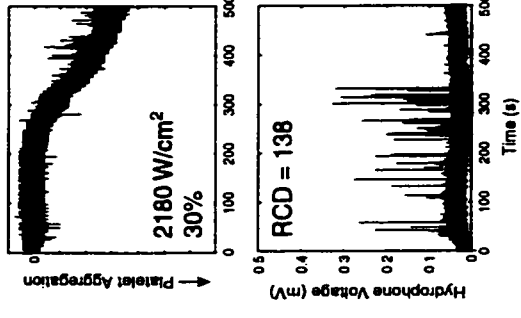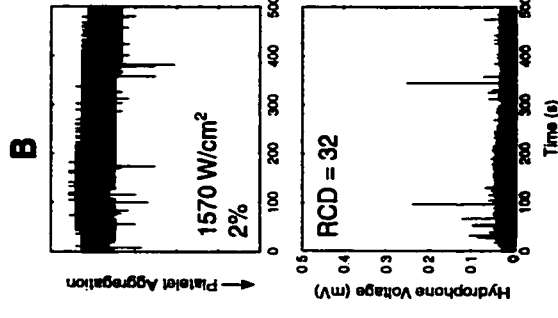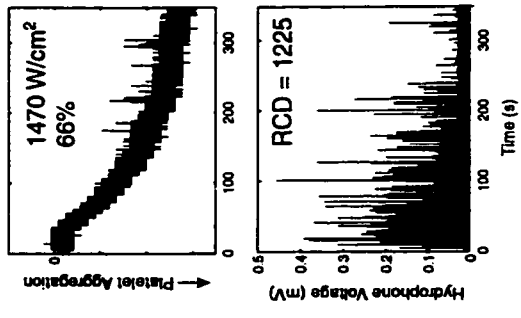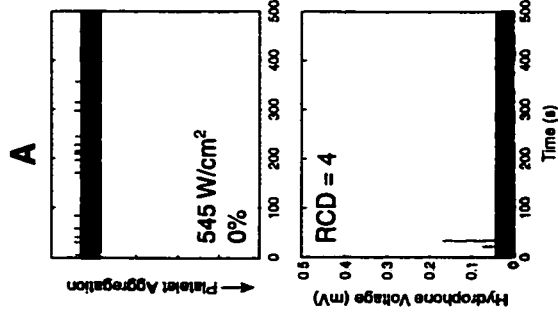
Column B in Figure 21 contains data from aggregation trials in which PRP samples alone were used. The top dataset represents a HIFU exposure at an intensity of 1570 W/cm$^2$, resulting in an RCD of 32 and aggregation of 2%. The bottom dataset represent an exposure of 2180 W/cm$^2$, resulting in an RCD of 138 and associated aggregation of 30%. Samples of PRP alone produce less cavitation than samples containing UCA. The cavitation events tend to be randomly spread throughout the exposure duration, and are of lesser magnitude than UCA enhanced cavitation. Associated aggregation takes several minutes to occur and is not as extensive as aggregation in samples containing UCA.

Column C in Figure 21 represents data from PRP samples with an applied overpressure of 7atm. The top dataset contains data from a 2045 W/cm$^2$ HIFU exposure, resulting in an RCD of 0 and no measurable aggregation. The bottom dataset shows results of a 2265 W/cm$^2$ HIFU exposure, with an RCD of 3288 and associated aggregation of 30%. In the overpressure samples, cavitation did not readily occur and when it did, it was extreme. Aggregation did not start in any overpressure sample until cavitation was detected, and was not as extensive as aggregation in samples with UCA.

Using various intensities, aggregation of platelets and associated cavitation were measured during each trial for all three types of PRP samples. Figure 22 shows cavitation measured as a function of HIFU intensity for samples of PRP, PRP with UCA and PRP at 7 atm overpressure. The top plot represents data from aggregation trials for samples of PRP + UCA showing that cavitation is detected at intensities as low as 500 W/cm$^2$, and generally increases with intensity. A significant increase in RCD occurs above 1500 W/cm$^2$. The center plot presents data from aggregation trials

for samples of PRP. Cavitation was detected in samples exposed to HIFU intensities above 1000 W/cm$^2$, but no significant increase in RCD was measured over the range of intensities used. In the bottom plot, an overpressure of 7atm applied to PRP samples during HIFU exposures generated the cavitation data shown, with cavitation detected in samples exposed at 2000 W/cm$^2$ or higher, yet with no significant increase in RCD between intensities.

Figure 23 shows percent platelet aggregation as a function of HIFU intensity for the three PRP sample types. For samples with UCA, a significant difference in aggregation occurs between intensities of 1165 and 1375 W/cm$^2$, but no significant threshold is apparent in samples of PRP alone or PRP subject to overpressure. An apparent intensity threshold below which aggregation does not occur exists for each sample type. PRP containing UCA samples begin aggregation at approximately 750 W/cm$^2$ and above, while PRP samples require an intensity of at least 1750 W/cm$^2$. Overpressure samples did not begin to aggregate until intensities reached 2000 W/cm$^2$ or above. Some samples in overpressure trials were discarded because so much cell damage occurred that no platelet aggregation was possible.

Comparisons were also made between RCD and platelet aggregation as shown in Figure 24 for the three PRP sample types. For samples containing UCA, no significant increase is apparent between cavitation activity levels and platelet aggregation, though above an RCD of 20, platelet aggregation generally occurs. Samples of PRP alone show a significant increase in platelet aggregation at an RCD of 135 or higher. In samples of PRP subject to 7 atm overpressure, significant increases in platelet aggregation occur between RCD of 5 and 80, as well as between 80 and 12000. Aggregation correlated better with cavitation than with intensity for

Figure 22: Cavitation data and HIFU intensity. These data demonstrate the amount of cavitation measured at various HIFU intensities in samples of PRP. Graph a) shows RCD results of HIFU exposure of PRP containing 1 $\mu$L UCA per mL PRP at 1 atm, with RCD increasing significantly with intensity. Graph b) shows RCD results of HIFU exposure of PRP samples at 1 atm. Graph c) depicts RCD results of HIFU exposure of PRP samples at 7 atm overpressure. RCD does not increase significantly with intensity for cases b) and c). Error bars indicate standard error for n $\geq$ 3.

a)



b)



c)
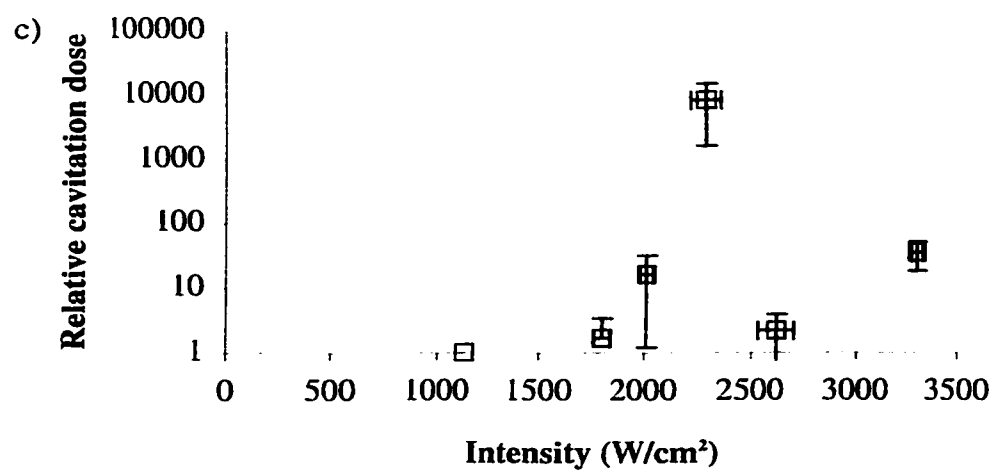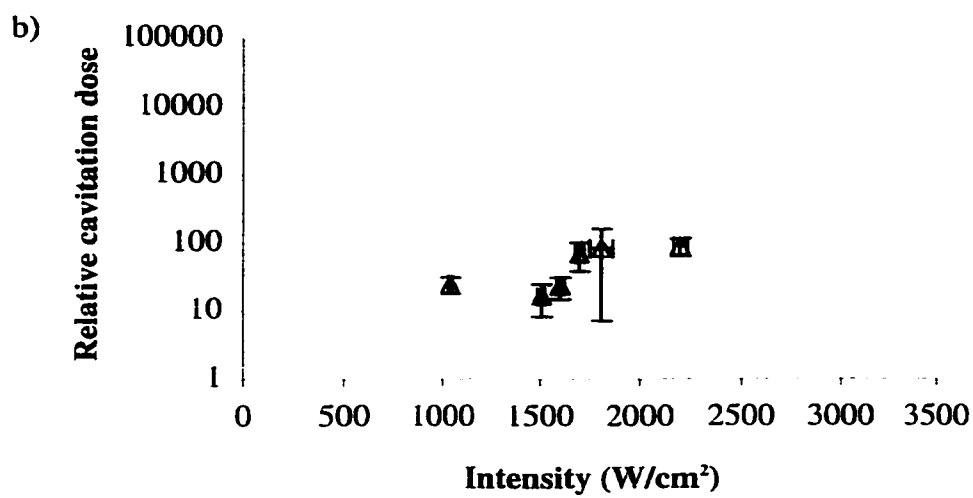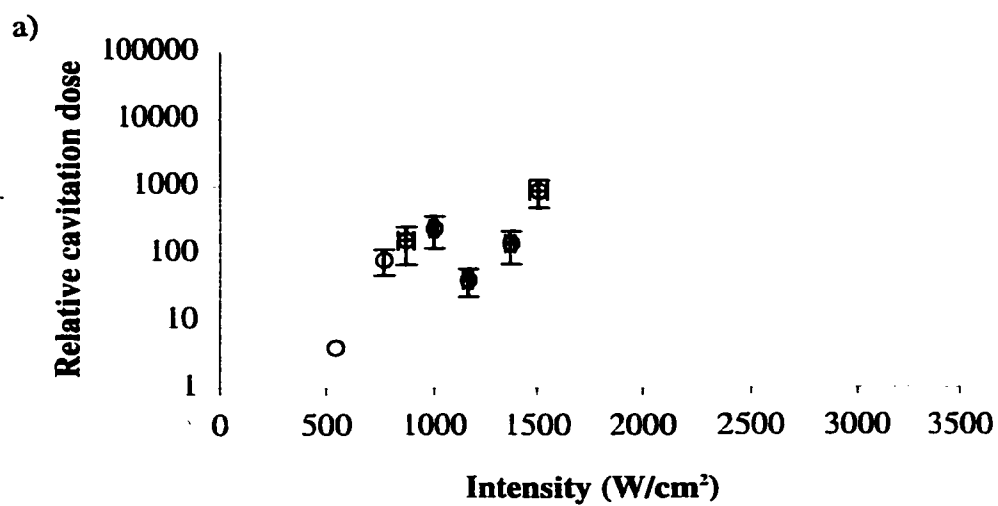
Figure 23: Platelet aggregation response to HIFU intensity. These data demonstrate the amount of platelet aggregation measured at various HIFU intensities in samples of PRP. Graph a) shows platelet aggregation results for HIFU exposure of PRP containing 1 $\mu$L UCA per mL PRP at 1 atm, showing a significant increase in aggregation with intensity. Graph b) shows platelet aggregation results for HIFU exposure of PRP samples at 1 atm. Graph c) depicts platelet aggregation results for HIFU exposure of PRP samples at 7 atm overpressure. Platelet aggregation does not increase significantly with intensity for cases b) and c). Error bars indicate standard error for n $\geq$ 3.

a)

b)

c)
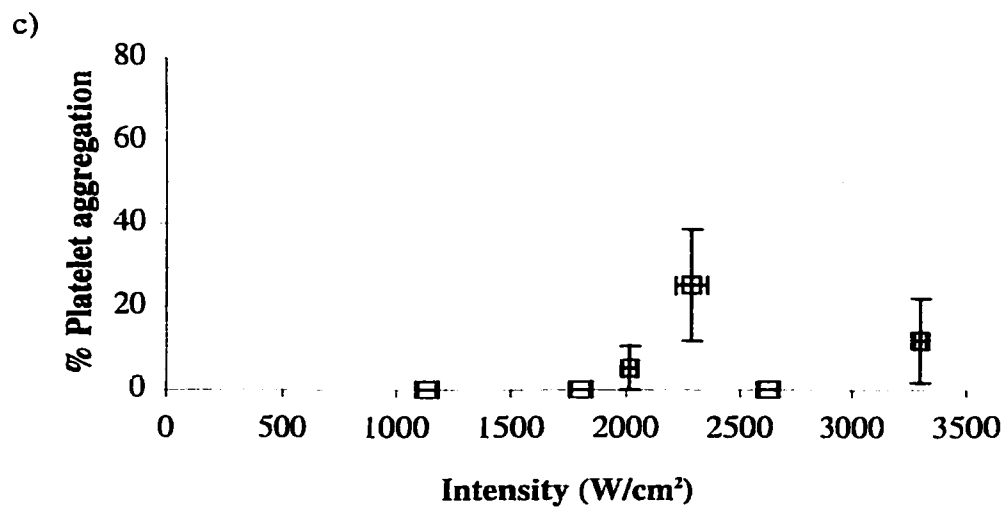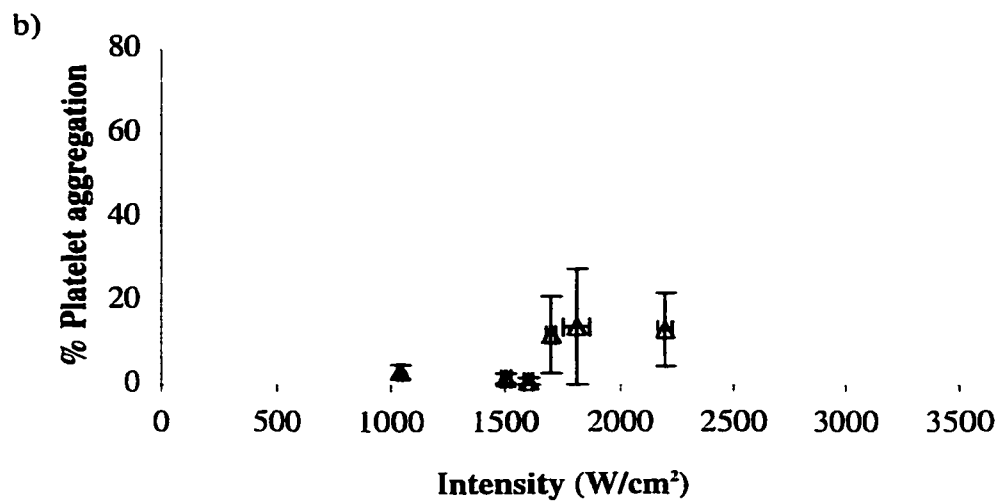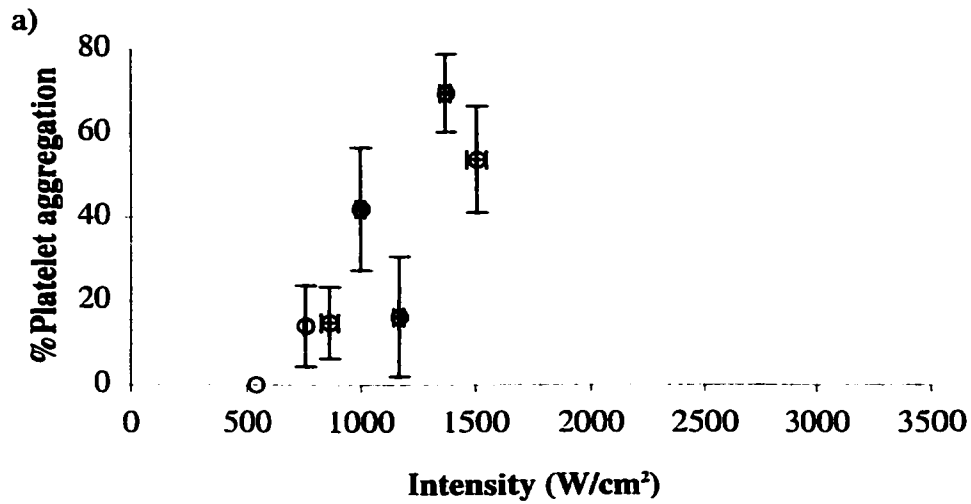
Figure 24: Platelet aggregation response to cavitation dose. These data demonstrate the relationship between acoustic cavitation and platelet aggregation in three different types of PRP samples. In a) platelet aggregation related to RCD for HIFU exposure of PRP samples with 1 $\mu$L UCA/mL PRP at 1 atm, showing no significant increase in platelet aggregation with RCD increase. In b) samples of PRP at 1 atm, and in c) samples are PRP under an overpressure of 7 atm, showing significant increases in platelet aggregation with RCD increase. These data seem to indicate that platelet aggregation does not occur without cavitation. Error bars indicate standard error for n $\geq$ 3.

a)

b)

c)
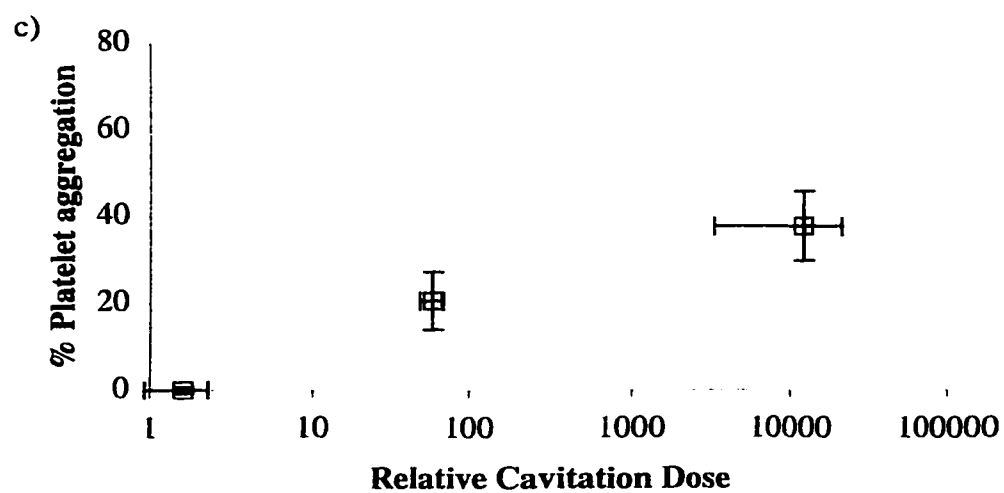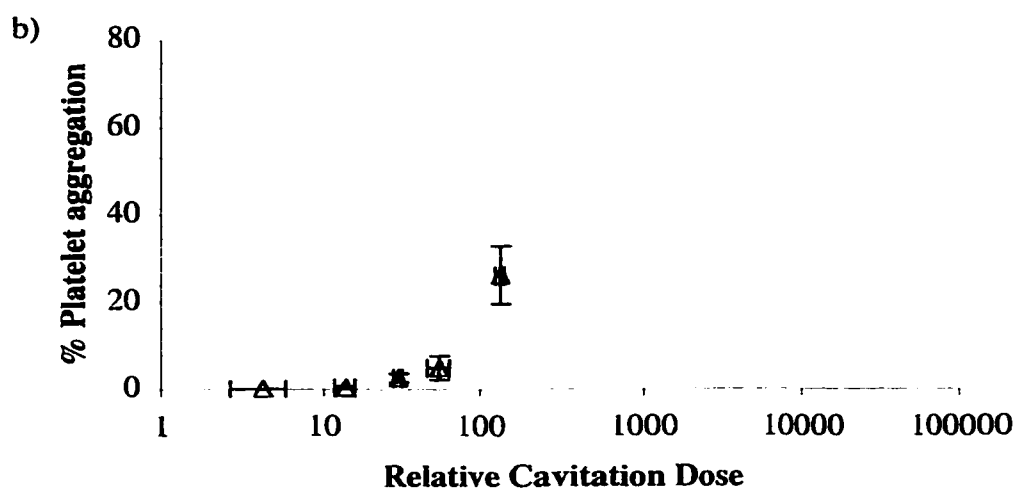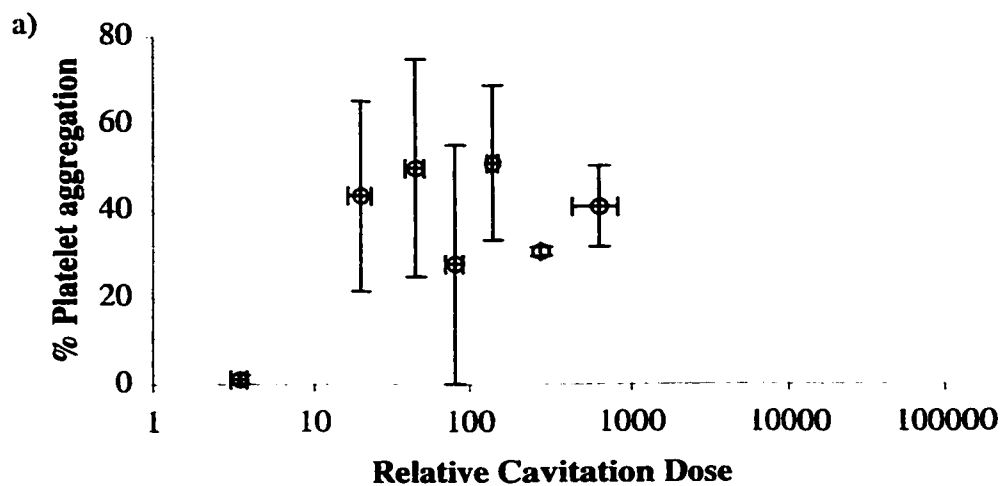
samples without UCA. This is easily understood because in samples without microbubbles cavitation is somewhat of a stochastic process, related to the number and composition of nucleation sites available in each sample.

To investigate the possibility that HIFU induced cavitation initially rips a few platelets apart, thus releasing their contents such that other platelets may be activated, short and intense 10 s HIFU exposures of PRP samples followed by stirring with a magnetic stirbar for 490 s were conducted at various intensities. Control samples that are not exposed to HIFU are stirred for 500 s and result in no detectable aggregation. Figure 25 shows examples of results from a 10 s exposure followed by stirring. In Figure 25a, an intensity of 3630 W/cm$^2$ results in an RCD of 7 with no detectable aggregation. In Figure 25b, an intensity of 4055 W/cm$^2$ produces an RCD of 182 with an aggregation of 12.6% after 490s of stirring. In Figure 25c, an intensity of 4860 W/cm$^2$ produces an RCD of 2845 and an aggregation of 25.2% after stirring. Thus, sufficient cavitation during brief HIFU exposure leads to measurable aggregation in samples of PRP.

### 7.4.2 Platelet Aggregation and Cavitation in Whole Blood

Impedance aggregometry was used to measure platelet aggregation in samples of whole blood, with and without UCA. Calibration of the impedance aggregometer was accomplished by simultaneously measuring aggregation in PRP using laser and impedance aggregometry. A comparison of aggregation data from laser and impedance aggregometry is presented in Figure 26. During the comparison trials, platelet aggregation on the impedance sensor wires was clearly visible.
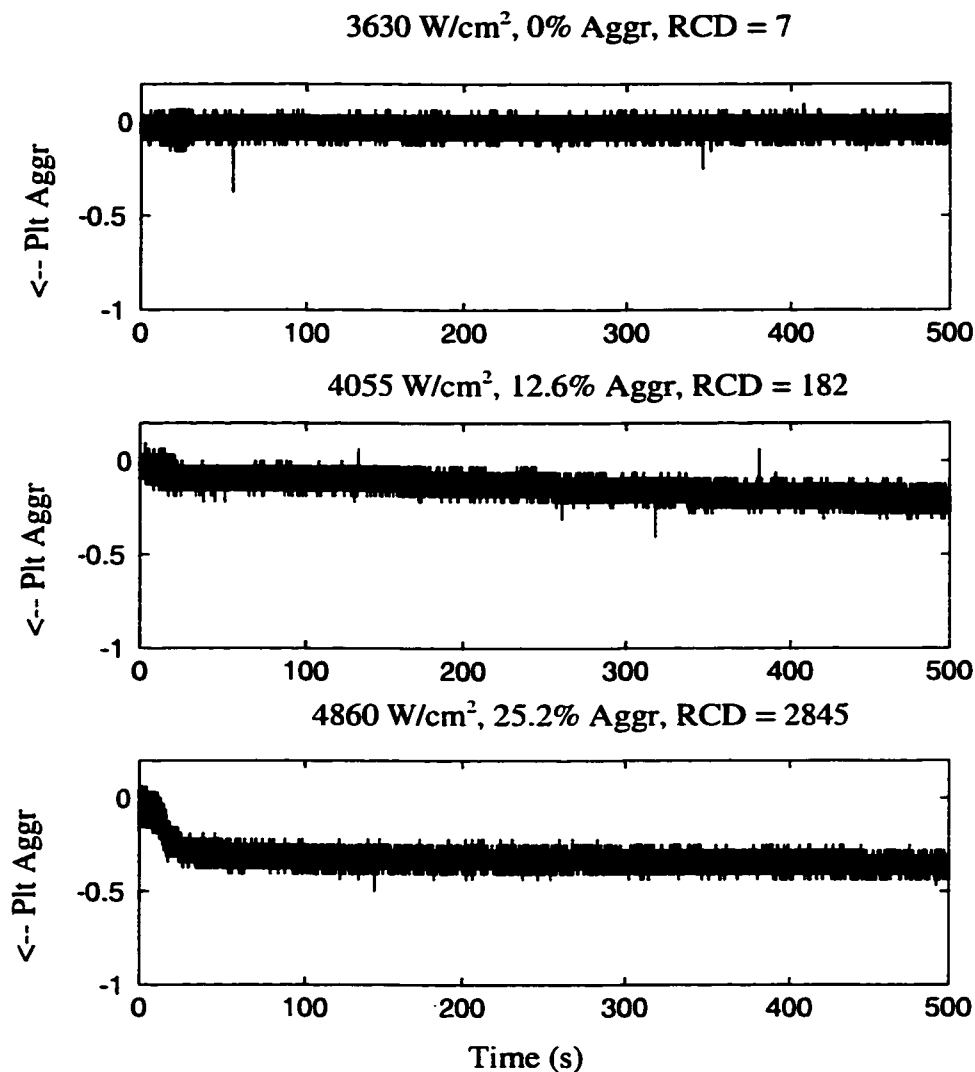
Figure 25: Samples of PRP were exposed to 10 s of HIFU followed by stirring with a stir bar for 490 s to determine if initial HIFU-induced cavitation was sufficient to disrupt a few platelets whose contents are then released enabling activation of other platelets. In trace a), very little cavitation occurred (RCD = 7) and no measurable aggregation occurred. In trace b), an RCD of 182 indicates greater cavitation activity and a resulting aggregation of 12.6%. Trace c) displays data from a trial with extensive cavitation (RCD = 2845), and a resulting aggregation of 25.2%, thereby suggesting that an initial burst of cavitation is sufficient to release platelet contents which can then activate other platelets.
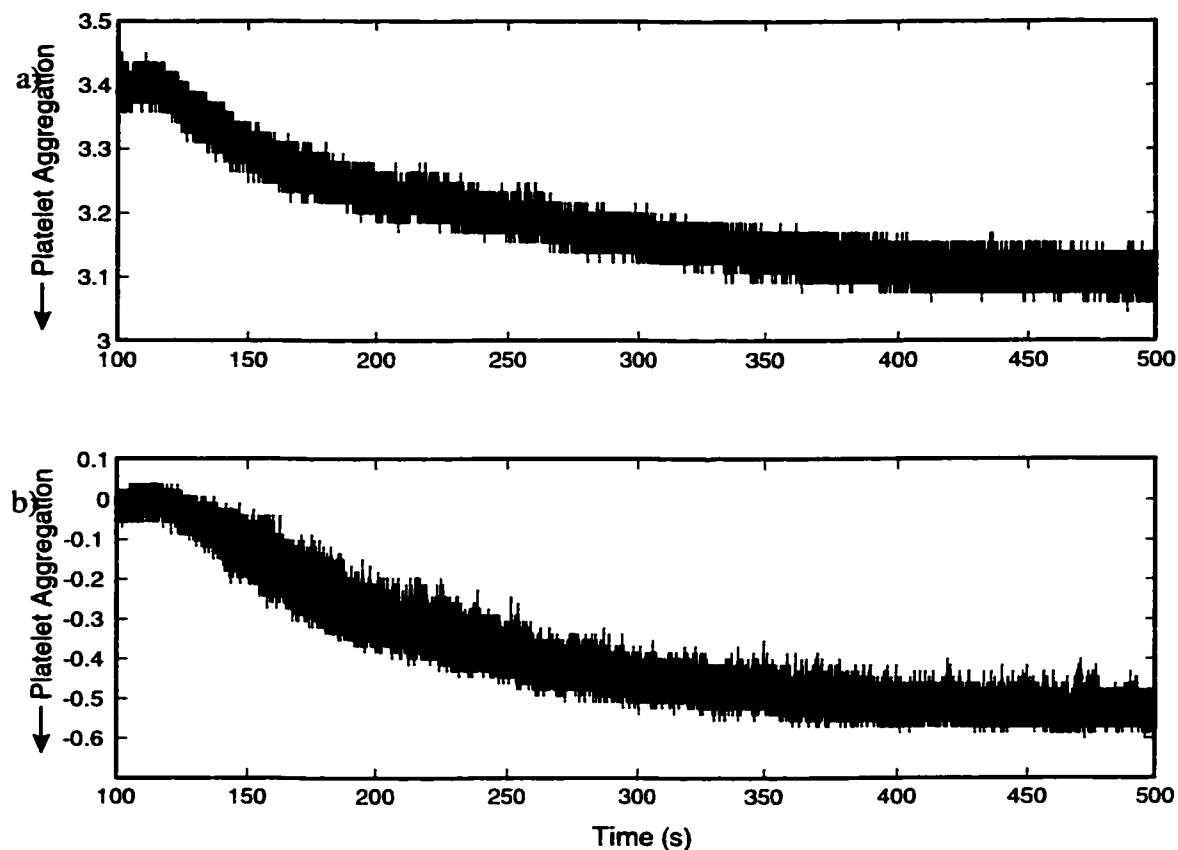
Figure 26: Comparison of data from impedance aggregometry and laser aggregometry, collected in sample of PRP stimulated with 7 $\mu$L of 10 $\mu$M ADP. In a) data from the impedance aggregometer are presented, while b) shows data from the laser aggregometer.

Whole blood samples exposed to HIFU were analyzed and the cavitation occurring for various intensities is presented in Figure 27. Cavitation in samples of whole blood with UCA started to occur at intensities of 1150 W/cm$^2$, and in whole blood without UCA, cavitation activity occurs at the lowest exposure level and increases with intensity. For both types of whole blood samples, no significant increase occurs in the amount of cavitation activity detected between any intensity levels. Platelet aggregation in whole blood with and without UCA is presented in Figure 28 as a function of intensity. Aggregation occurs in whole blood samples with

UCA at intensities as low as 1150 W/cm$^2$, increases with intensity, and then drops off as intensities increase beyond 1600 W/cm$^2$. No significant increase occurs in platelet aggregation with intensity for samples of whole blood with UCA. For whole blood alone, platelet aggregation starts at intensities of 1920 W/cm$^2$ and then drops off after 2500 W/cm$^2$, with no significant increase in platelet aggregation with intensity.

Platelet aggregation was also plotted as a function of cavitation, in Figure 29. For both whole blood with and without UCA, platelet aggregation occurred at relatively low RCD, but as RCD increased beyond 250, platelet aggregation decreased. Samples with RCD above 250 tended to produce cavitation strong enough to rip cells apart. Hemolysis measurements of some of the whole blood samples showed hemolysis of 50% or greater for RCD values above 100. Statistical analysis resulted in no significant increases of platelet aggregation with RCD for either whole blood or whole blood with UCA.

Although statistically significant intensity thresholds were not found in samples of PRP at overpressure, Table 3 presents apparent intensity thresholds below which aggregation did not occur.

## 7.5 Error Analysis

Some calibration measurements completed with known dilutions of PRP were used to check the linearity of the laser aggregometer. Results are presented in Figure 30. The data are non-linear, yet in keeping with clinical practice, the data are interpreted linearly, leading to errors as large as 50% for platelet aggregation in the
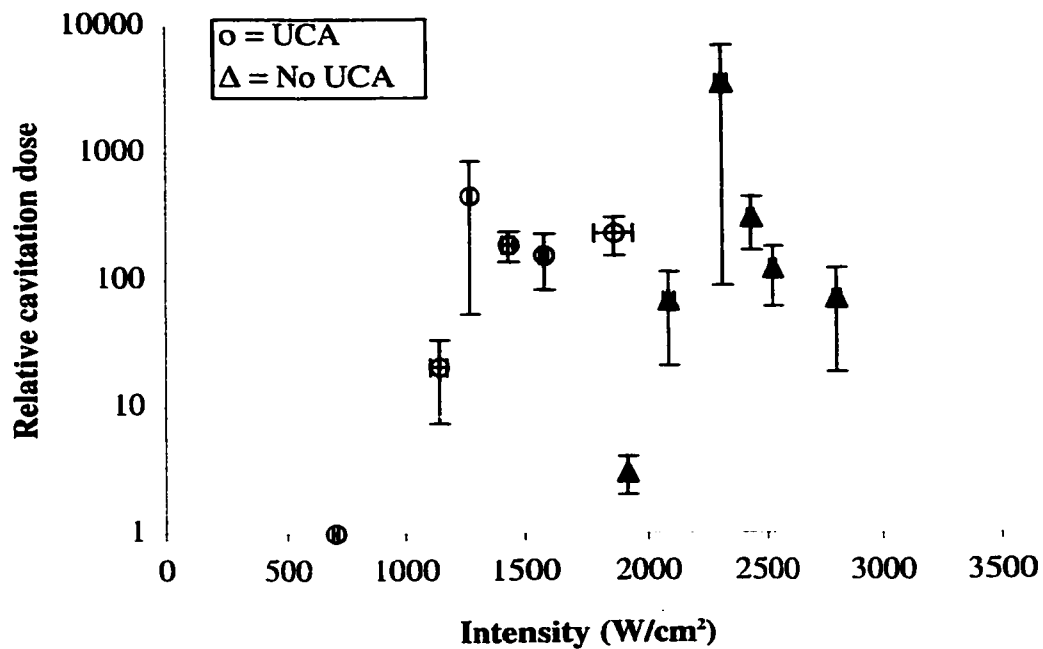
Figure 27: Cavitation data and HIFU intensity in whole blood. These data demonstrate the amount of cavitation measured at various HIFU intensities in samples of whole blood and whole blood with UCA. Cavitation tends to increase with intensity.

range of 50 - 80% aggregation, resulting in a calculated aggregation that is less than

actual aggregation. Since whole blood impedance measurements of aggregation are

Table 4: Apparent intensity thresholds for HIFU induced platelet aggregation

| Condition | Apparent Intensity Threshold ($W/cm^2$) |
|---|---|
| PRP | 1750 |
| PRP + UCA | 750 |
| PRP at 7 atm | 2000 |
| whole blood | 1920 |
| whole blood + UCA | 1150 |
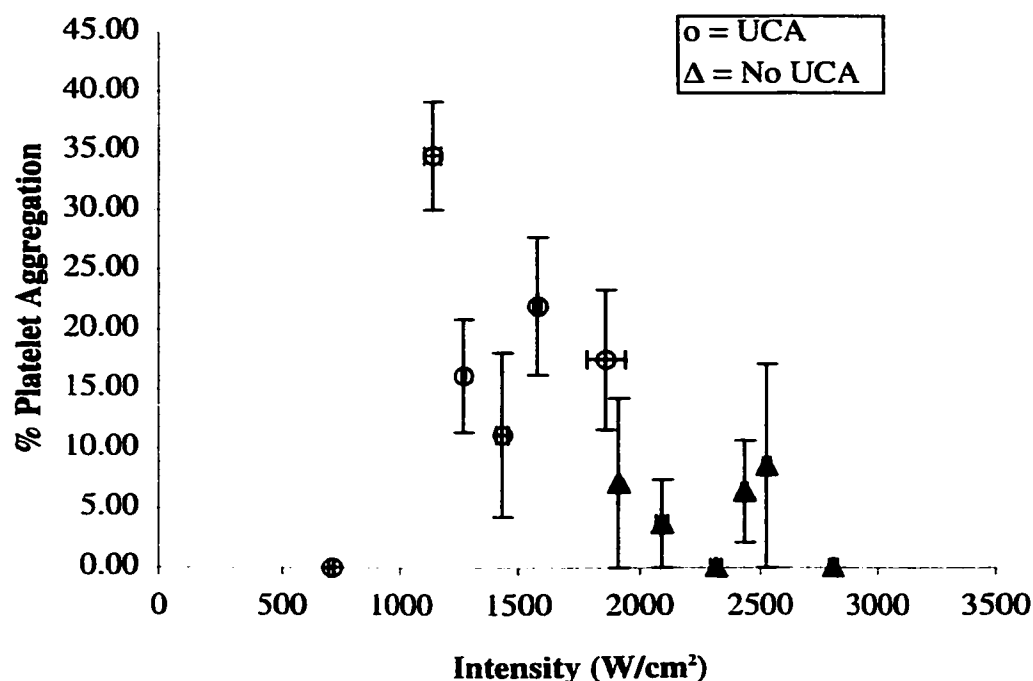
Figure 28: Platelet aggregation response to HIFU intensity in whole blood. These data demonstrate the amount of platelet aggregation measured at various HIFU intensities in samples of whole blood and whole blood with UCA. Platelet aggregation does not increase regularly with an increase in intensity.

based on a calibration with the laser aggregometer, the amount of platelet aggregation using the impedance method is not linear either, yet in keeping with clinical practice, both types of aggregometers assume a linear response of the system.

In the overpressure trials, the PETE bottle used as the pressure chamber caused a 15% attenuation of the HIFU signal. Ideally, the HIFU transducer would be placed within the pressure chamber with the sample, but because it is air-backed, the HIFU transducer is too fragile to withstand the application of overpressure. The PETE bottle also may have caused some reflections of the HIFU signal, which may

have resulted in the matching network output voltage fluctuation. This would result in an inaccurate calculation of the HIFU intensity seen by the sample.

A source of error for aggregation studies is the cleanliness of the HIFU tank and overpressure bottle. If items were not cleaned prior to the experiment, the range of the detected voltage is limited, thereby limiting the resolution of the system.

Two issues arise with the use of the impedance aggregometer. The first is the temperature effect on the impedance sensor. In clinical use, the samples to be tested
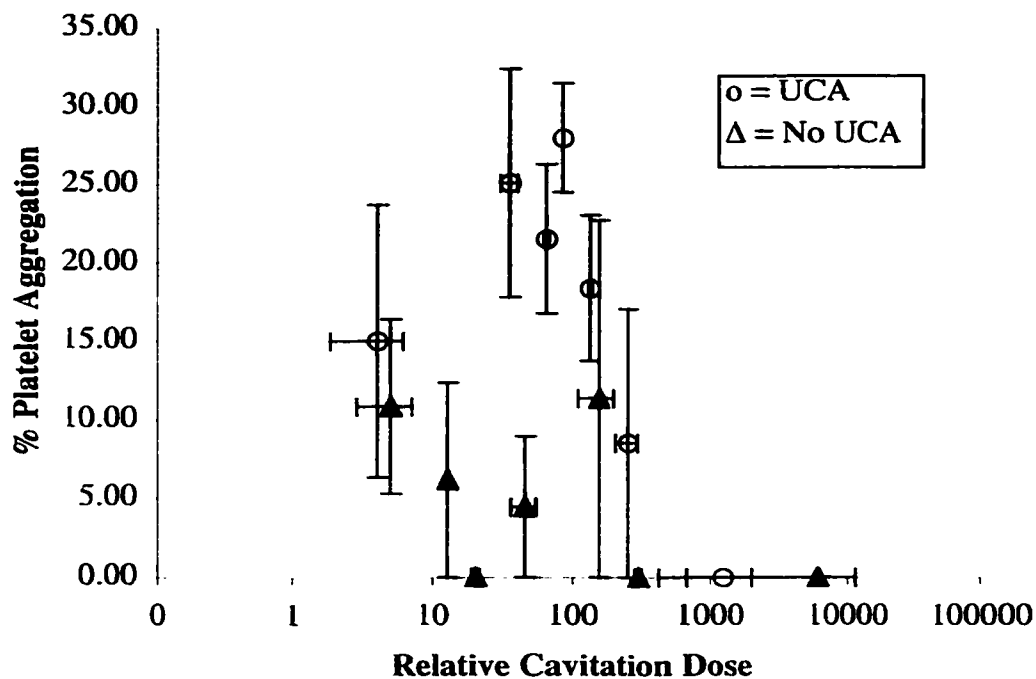


Figure 29: Platelet aggregation response to cavitation dose. These data demonstrate the relationship between acoustic cavitation and platelet aggregation in whole blood and whole blood with UCA samples. As in PRP samples, these data seem to indicate that platelet aggregation does not occur without cavitation and at higher RCD values more cavitation seems to decrease the amount of aggregation due to destruction of platelets that occur during high cavitation exposure.

with the impedance sensor are held at a constant temperature (± 0.1%) while the sample is stirred with a magnetic stirbar and aggregating agents are added. The electrodes are sensitive to temperature, with rapid cycling of temperature giving rise to an unstable baseline. Under HIFU exposure, the temperature in the sample chamber tends to rise several degrees within the first 50 s of exposure, then stabilize. This temperature change is linearly related to the response of the impedance sensor and can be characterized such that the data can be compensated. Figure 11 shows calibration data generated by increasing sample temperature at different rates, all
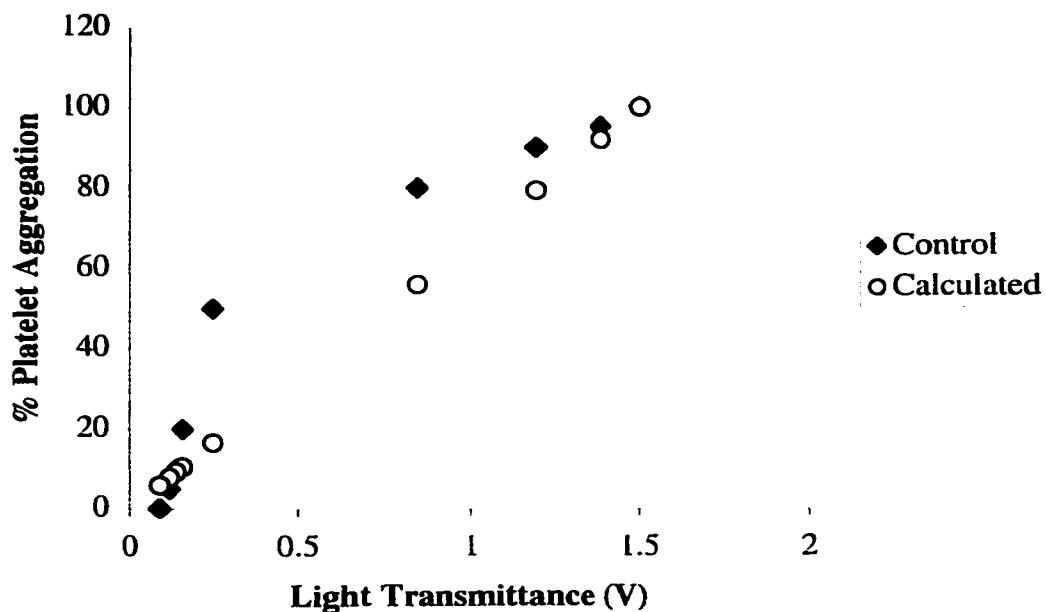


Figure 30: Calibration of laser aggregometry. Various known concentrations of platelets were measured using laser aggregometry. Platelet aggregation corresponding to the known platelet concentrations are plotted above (solid diamonds). Light transmission for control platelet aggregations are compared to calculated platelet aggregations (open circles) as used in clinical practice and HIFU-induced platelet aggregation trials.

resulting in similar correction factors for temperature compensation, as discussed in the temperature section. Because the impedance sensor used in whole blood aggregometry is sensitive to temperature, the sensor responded to HIFU induced heating as well as platelet aggregation. The calibration of the impedance sensor with temperature gives a linear response within 8%, and was used to compensate data from HIFU exposure trials.

The second issue is the quality of the stirring system. Inconsistent stirring can lead to erratic data that is not suitable for quantifying. During the HIFU exposures, inconsistent stirring is not a problem because the acoustic streaming and radiation pressure produced by the ultrasound provide complete and consistent stirring within the sample chamber.

The impedance of the electrodes in whole blood aggregation is related to the number of platelets that accrete on the sensor wires. It is assumed that only platelets will adhere to the wires, but it is possible that erythrocytes or lymphocytes could also be trapped on the wires (Cardinal et al. 1980).

## 7.6 Summary and Discussion

In aggregation studies, when cavitation nuclei (UCA) are added to PRP samples, HIFU intensity is significantly related to aggregation and cavitation dose. Without exogenous cavitation nuclei, aggregation is significantly related to cavitation dose, while intensity is not significantly related to aggregation or cavitation. In whole blood samples, no significant relationships between aggregation, intensity and cavitation were discovered, yet trends are obvious. Apparent intensity thresholds below which aggregation and cavitation do not occur exist for whole blood and whole

blood containing UCA. Aggregation does not occur without cavitation, yet excessive cavitation causes too much cell damage to allow aggregation to occur.

PRP studies do not reveal a significant intensity threshold for aggregation in samples without UCA, although aggregation did increase with intensity. In samples containing UCA, a significant difference in aggregation occurs between intensities of 1160 and 1375 W/cm$^2$. From the aggregation results presented in Figure 21 and aggregation traces of Figure 18, exposures at comparable intensities show that the amount of aggregation is greater, and occurs more rapidly, in PRP samples containing UCA than in those without UCA. Whole blood samples exposed to HIFU also do not have a significant intensity threshold. Whole blood containing UCA shows most aggregation at mid-level intensities, which then drops off for higher intensities. HIFU exposure of whole blood alone produced small amounts of aggregation that varied slightly with intensity. An intensity threshold exists below which platelet aggregation does not occur. This threshold is highest in the overpressure system, and lowest in samples containing UCA.

In the overpressure system, even at intensities as high as 2200 W/cm$^2$, cavitation does not occur unless some cavitation nuclei are present in the sample. Overpressure is only 7 atm, and per dosimetry the maximum rarefactional pressure is 7 times more than 7 atm. Mild overpressure serves to decrease cavitation, but does not eradicate it. A pressure of approximately 5 MPa would be required to eliminate bubble growth due to HIFU exposures at the intensities used in these studies. Once cavitation does occur, it appears to be much more extreme than cavitation in samples of PRP or PRP + UCA. This result is similar to findings by Sapozhnikov et al. (2001), where increased pulse repetition frequency of lithotripsy pulses in an

overpressure system led to more extensive cavitation than in samples without overpressure.

In PRP samples containing UCA, the extent of aggregation is greater than in any other type of sample, and lower doses of cavitation lead to the greater aggregation. This effect may be a result of radiation force attracting platelets to the microbubbles, where they are effectively sheared and activated without causing extensive platelet damage. PRP alone did not reach aggregation values as high as PRP with UCA, possibly due to excessive platelet fragmentation occurring in PRP alone, which created fragments that were unable to aggregate and thus clouded the chamber. In this case, it appears as if slight stimulation of cavitation by addition of UCA leads to large amounts of aggregation at lower intensities, whereas the higher intensities required to aggregate platelets without UCA also lead to more cavitation and greater damage to the platelets. These differences may be a result of different mechanisms at work in UCA samples compared to samples without UCA. The quicker aggregation response may be due to microstreaming induced shear, in which activated platelets adhere readily to one another, while in non-UCA samples the longer aggregation times seem more typical of a chemical stimulus -- released platelet contents from cavitation-damaged platelets causing aggregation.

In whole blood, HIFU exposed samples with UCA aggregated more than samples without UCA, yet neither aggregated as much as PRP samples. In both whole blood cases, a higher cavitation dose produced a higher degree of platelet aggregation, until cavitation reached levels greater than 250, after which aggregation decreased presumably due to enhanced platelet destruction. When very high cavitation doses were produced, the platelets and platelet aggregates were apparently

torn apart by the cavitation resulting in low levels of aggregation. This suggests that an optimal range of relative cavitation dose exists for platelet aggregation -- enough to activate platelets and stimulate aggregation, but not so high as to destroy the majority of the platelets and aggregates.

The type of cavitation which activates the platelet may play a role in the aggregation process. Stable cavitation produces microstreaming which may shear platelets, leaving more intact to form aggregates, whereas inertial cavitation may rip platelets apart, releasing activating agents but reducing the amount of aggregation that can occur. In whole blood, cells may be attracted to bubbles by radiation forces. Because of the greater density of cells in the whole blood samples, violent cavitation may destroy more cells (erythrocytes and platelets) due to their proximity to the bubbles, thus resulting in less aggregation.

In the 10 s HIFU exposures, HIFU-induced streaming occurred for only 10 s, followed by stirring with a magnetic stir bar. In these trials, cavitation seems to be the dominant mechanism because aggregation occurred only in those samples which produced cavitation at RCD greater than 180. HIFU-induced streaming without cavitation, followed by stirring, did not induce platelet aggregation. In these trials, inertial cavitation seems to be ripping apart a few platelets and releasing activating factors when cavitation levels are large enough. In some of the 10 s HIFU exposures, microaggregates appeared and then reverted back to individual platelets (disaggregation), displaying a response similar to the "sub-threshold" activation of platelet aggregation observed by Chater et al. (1977) and Williams et al. (1978). These sub-threshold trials produced cavitation at RCD between 100 and 150, which

may have been sufficient to disrupt some platelets but not enough to provide activating agents to produce proper aggregation.

Except for PRP samples containing UCA, cavitation is not statistically related to intensity. In samples without UCA, cavitation only occurs if sufficient cavitation nuclei exist. These nuclei may be introduced during sample handling or because of imperfections in sample chambers, but are unrelated to HIFU intensities once the intensity threshold is surpassed. In whole blood samples, cavitation dose rises with intensity and then reaches a plateau. This cavitation limit may be a result of blood cells damping cavitation bubbles, as suggested by Miller (1988b), Miller (1985), and Ellwart et al. (1988).

Whole blood studies were pursued because the characteristics of whole blood vary from PRP in that more cells are present ($5 \times 10^6$ red blood cells in addition to $2 \times 10^5$ platelets). Absorption of sound is different in whole blood, thereby changing the amount of heating and acoustic streaming. Distribution of cells is also different and the released contents of platelets interact with red blood cells and white blood cells as well as platelets. The higher cell count in the sample may prevent platelets from encountering the released platelet contents and activating as much as they do in PRP samples. Because of the great number of cells present, aggregation using laser light transmission cannot be performed on whole blood samples.

HIFU exposures of PRP above 1750 W/cm$^2$ (3.7 MPa rarefactional) generally caused cavitation and platelet aggregation. Studies by Deng et al. (1996) found they could not cause cavitation in whole blood at up to 5.2 MPa peak negative pressure for 2.5-MHz pulsed ultrasound (0.81% duty cycle), or up to 6.2 MPa peak negative pressure for 4.3-MHz pulsed exposures. 1.1-MHz HIFU exposures were used in this

study, and thus a lower cavitation threshold is expected. However, cavitation threshold differences may also be attributed to differences between the cell density in whole blood and PRP. The concentration of platelets per UCA microbubble in PRP is 1000, and in whole blood is 10,000. Higher cell densities may serve to damp bubbles as suggested by Brayman and Miller (1993), or the distance and number of cells between cavitation nuclei and platelets may change the effectiveness of cavitation in producing platelet activity.

Many studies have attributed hemolytic effects to cavitation (Azadniv et al. 1996; Brayman et al. 1995, 1996, 1999b; Brayman and Miller 1997a, 1999b; Dalecki et al. 1995; Everbach et al. 1997; Miller et al. 1997; Miller and Gies 1998; Poliachik et al. 1999). In order for cavitation to occur, samples must contain cavitation nuclei, which may include bubbles on the order of $10^{-9}$ to $10^{-6}$ m that are protected from dissolution by organic molecules in the sample, or dirt in which air is trapped (Leighton 1994). Whole blood samples containing UCA are seeded with cavitation nuclei and thus the production of cavitation is expected. Whole blood without UCA, however, would seem to be devoid of cavitation nuclei, unless the samples harbor cavitation nuclei. The lower aggregation and higher intensity threshold in whole blood without UCA demonstrate that cavitation is less likely to occur without exogenous cavitation nuclei.

# 8.0 QUANTIFICATION OF ACOUSTIC STREAMING RESULTING FROM HIFU EXPOSURE

Acoustic streaming and radiation pressure produce bulk fluid motion in PRP and whole blood samples exposed to HIFU. Doppler ultrasound and high speed camera observations were used to estimate the velocity of particles in cylindrical sample chambers exposed to a range of HIFU intensities. From the velocity estimates, maximum probable shear stresses were calculated.

## 8.1 Materials and Methods

The bulk acoustic streaming and radiation pressure imparted on PRP and whole blood samples by HIFU causes vigorous stirring in the sample chambers. Since platelets may be activated by adequate shear forces, measuring the velocity in the sample chamber allows an estimate of the shear stresses resulting from the bulk streaming during HIFU exposures. Two methods were used to determine the velocity of particles within the cylindrical sample chamber: Doppler ultrasound and high speed camera video analysis.

Doppler ultrasound works on the principle of frequency shift of a reflected sound wave (see Appendix G). Because the HIFU signal is of a much higher intensity than the reflected Doppler pulse, a series of long HIFU pulses was used -- sufficient to vigorously stir the sample, but with a duty cycle adequate for Doppler investigation in between HIFU pulses. An HDI 1000 diagnostic ultrasound machine (ATL, Bothell WA) with a curvilinear CL10-5 transducer, center frequency 6.13-MHz, was used to measure the velocity of 1 - 35 $\mu$m diameter polystyrene particles (Duke Scientific Corp., Palo Alto CA) within the cylindrical sample chambers at intensities up to 2635 W/cm$^2$. The CL10-5 transducer was aligned to investigate the

focal zone within the sample chamber. Samples containing polystyrene spheres with 0.03% UCA (Optison®) by volume were also used in velocity measurements.

The second method of velocity measurement used a Kodak Ektapro 4540 high speed digital camera (Eastman Kodak Company, Rochester NY) at a rate of 500 frames per second to record the movement of platelet aggregates in the sample chamber exposed to HIFU at intensities up to 2040 W/cm$^2$. The sample chamber was backlit with a 1000W floodlight and the platelet aggregate velocity was filmed through the acrylic wall of the HIFU tank. The video was then analyzed by tracing the movement of the platelet aggregates as they moved through the sample volume on different video frames. With a known frame rate, the platelet aggregate velocity was calculated as distance moved over 20 - 25 frames.

The results of the two velocity measuring methods were compared and a maximum particle velocity was determined for each HIFU intensity. With this velocity, the shear in the sample chamber due to bulk streaming was calculated.

## 8.2 Shear Calculations

Using a plasma viscosity of 1.35 cP and a whole blood viscosity of 5.5 cP for a shear rate of 1 - 1000 s$^{-1}$ (Nageswari et al. 2000), the shear stress on a cell can be calculated using:

$$\sigma = \eta \ (u/y)$$

where $\sigma$ is the shear stress (dyne/cm$^2$), $\eta$ is dynamic viscosity (cP), u is velocity (cm/s) and y is distance across fluid layers (cm), the HIFU focus in this case. For the cylindrical sample chamber in which velocities were measured, Figure X depicts the flow pattern and the HIFU focus with velocity profile as shown in the enlargement of the focus. An assumption of zero velocity at the edge of the focus was used, although

the focus is located completely within the fluid, resulting in an overestimate of the calculated shear.
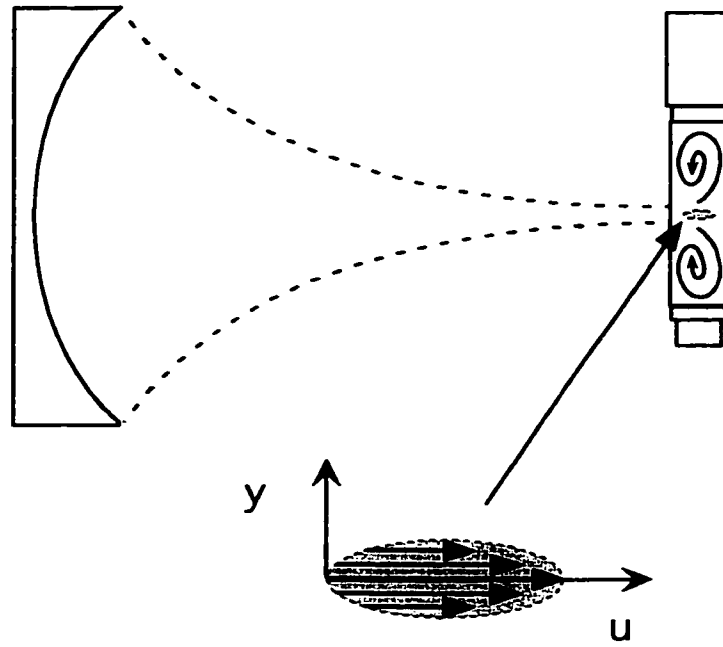


Figure 31: Enlarged view of the HIFU focus in which particle velocities were measured. The velocity u was measured and used in calculations along with the distance across fluid layers (y) and viscosity ($\eta$) to estimate the amount of shear occurring in a sample due to bulk fluid motion.

## 8.3 Results

Velocity measurements made with Doppler ultrasound and high speed camera are presented in Figure 31. Doppler ultrasound measurements indicate the maximum values measured in samples of degassed PBS containing polymer microspheres, or degassed PBS containing polymer microspheres and UCA. The high speed camera data indicate the maximum speed measured in samples of PRP, which had been induced to aggregate by (addition of 7 $\mu$L of 10$\mu$M ADP plus stirring) prior to velocity measurements.
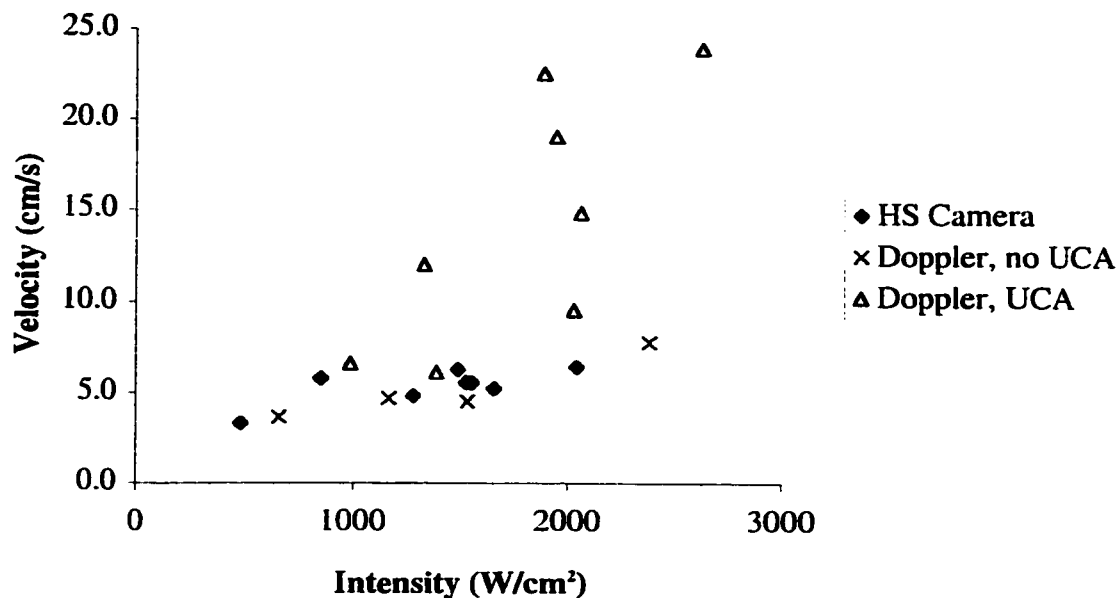
Figure 32: Measured velocities of HIFU exposed particles and platelet aggregates in cylindrical sample chambers. Doppler ultrasound measured velocities of polymer spheres in PBS with and without UCA. Platelet aggregate velocities were measured using high speed camera observations. Variations in velocity in samples containing UCA is due to different amounts of cavitation occurring in each trial.

Assuming the maximum velocity occurs in the center of the focus, the shear was calculated using the values velocity = 8 cm/s (no UCA), velocity = 25 cm/s (UCA), $\eta$ = 1.35 cP for plasma, $\eta$ = 5.5 cP for whole blood, and y = 0.05cm (equal to 1/2 the focal spot diameter). Shear stress was then calculated as presented in Table 4.

According to data from Anderson (1978), for 5 minute exposures, a shear stress of 160 dyne/cm$^2$ is required to lyse platelets, with platelet aggregation occurring at 75 dyne/cm$^2$. Even though the duration of sample exposure to HIFU was on the order of 5 minutes, because of the bulk flow in the sample chamber individual platelets were only exposed to the velocity gradient in the HIFU focus for approximately 50 ms. According to Sakariassen et al. (1998), for exposures of 75 ms a shear rate of 10,500 s$^{-1}$ corresponding to shear stress of 315 dyne/cm$^2$ is necessary to

stimulate platelet activation. Thus, the HIFU exposed platelets in PRP and whole blood samples in these experiments are unlikely to be affected by bulk flow shear.

Table 5: HIFU induced shear stress based on Doppler velocity measurements

|  | No UCA | UCA |
| --- | --- | --- |
| plasma | 2.2 dyne/cm$^2$ | 6.8 dyne/cm$^2$ |
| whole blood | 8.8 dyne/cm$^2$ | 27.5 dyne/cm$^2$ |

## 8.4 Error Analysis

Measurements of particle velocity using the high speed camera may be subject to errors due to the three dimensional nature of flow in the sample chamber. The video images were analyzed tracking platelet clumps as they moved across the screen. The clumps were assumed to move in a plane parallel to the camera across the screen, though in reality they may have moved towards or away from the camera as they moved horizontally. This movement in the depth field of the camera was on the order of 1 mm and thus would have an effect of 2% error for a velocity measured over a 5 mm distance.

Doppler measurements of velocity were completed by capturing the maximum velocity detected during 5 minute exposures of particles. Transducer alignment was shifted during exposures in an attempt to locate the volume with the maximum velocity. This shifting may have caused some velocity data to be missed.

## 8.5 Summary and Discussion

Results of the Doppler investigation of acoustic streaming velocity allow us to estimate the amount of bulk (due to bulk flow) versus microscopic (near bubbles)

shear stress within a sample. Acoustic streaming and radiation pressure produce flow in the sample chamber, as seen in Figure 12, but velocities of less than 25 cm/s are insufficient to produce shear adequate to activate platelets. Based on the velocity estimates and duration of exposure to the velocity gradient, shear stress is not a factor during exposure of PRP samples, and although addition of UCA tends to increase the likelihood of sufficient bulk shear to activate platelets by increasing the radiation force within the chamber, the shear is still insufficient to cause platelet activity. The small size of the platelets (2-4 $\mu$m) require large shear gradients which cannot be achieved by acoustic streaming alone in our experimental setup.

# 9.0 CONCLUSIONS

## 9.1 Summary

In these studies, the ability of HIFU to stimulate the natural coagulation system -- specifically primary hemostasis, was investigated. Samples of PRP and whole blood were exposed to HIFU and the amount of cavitation and platelet activation and aggregation was determined, and platelet adhesion to a collagen-coated surface was observed.

Previous studies have shown that ultrasound can produce bioeffects in blood. The primary hypothesis guiding our proposed research is that application of HIFU to PRP causes cavitation that will shear and/or rip the platelets, thus causing platelet activation factors to be released. HIFU induced bulk fluid flow will then mix samples to allow activation of other platelets. Activated platelets will bind together, or aggregate, and will adhere to exposed collagen. Bulk fluid flow alone is insufficient to shear platelets enough to cause activation, but the mixing provided by the flow is essential to allow platelet-platelet and platelet-collagen interactions. Conditions within a sample of whole blood (number of cells, ability to absorb energy) are sufficiently different from PRP that the cavitation and shearing effects generated by HIFU, with and without UCA, will be less effective at producing platelet aggregation.

## 9.2 Discussion

The occurrence of HIFU induced cavitation is necessary to produce platelet aggregation. HIFU exposures of PRP show the relationship between cavitation and platelet aggregation. When cavitation nuclei in the form of UCA are added to PRP, aggregation occurs to a greater extent, more quickly and at lower intensities than in samples of PRP without UCA. HIFU exposures of PRP subjected to 7 atm

overpressure will not produce platelet aggregation unless cavitation occurs, despite continual bulk fluid flow caused by HIFU. Short HIFU exposures of PRP samples also do not produce platelet aggregation unless cavitation is detected.

For HIFU exposures of whole blood, platelets do not aggregate as much as in samples of PRP and higher HIFU intensities are required to produce aggregation. As in PRP, cavitation occurs in all trials where platelet aggregation is measured. Extensive cavitation in whole blood, however, leads to excessive cell damage that precludes platelet aggregation.

In considering acoustic mechanisms, our main hypothesis is that HIFU causes cavitation, which can lead to ripping or shearing of a small number of platelets whose contents are then released serving to activate other platelets. Ripping of platelets may occur due to inertial cavitation, the violent collapse of a bubble, which can be generated as a result of HIFU exposure. If platelets are being destroyed and contents released, the longer aggregation times in samples without UCA seem more typical of a chemical stimulus, where released platelet contents from cavitation-damaged platelets cause aggregation.

The cavitation measured in these experiments is most likely inertial cavitation. Stable cavitation is more difficult to identify because it does not efficiently produce large amounts of broadband noise, although spectral analysis of cavitation data can provide information on generation of harmonics that may allow distinction between stable and inertial cavitation. Higher resolution of cavitation data is required in order to extract information of the generation of harmonics during HIFU exposures. With long CW HIFU exposures, storing and analyzing the amount of data required to evaluate cavitation data for the generation of harmonics is a challenge. A higher

sampling rate than was available for these experiments would be necessary to evaluate data for indications of stable cavitation.

Microstreaming that occurs close to oscillating bubbles may produce shear stresses capable of shearing or ripping apart platelets that are in the vicinity of the bubble. Microstreaming produced by an oscillating wire, simulating a cavitating bubble, has been shown to produce sufficient hydrodynamic shear stress to disrupt platelets (Williams et al. 1974), while 2.1-MHz diagnostic ultrasound exposure caused microstreaming which led to platelet aggregation formation around gas-filled pores *in vitro* (Miller et al. 1979). *In vivo* studies have also shown that acoustic microstreaming produced by a wire oscillating at 20-kHz can create platelet aggregates in murine blood vessels (Williams 1977), and vigorous streaming from 1-MHz ultrasound applied to a micropipette can cause thrombi to form in mouse mesenteric vessels (Frizzel et al. 1986). However, the former studies used simulated cavitation (oscillating wire) or fixed bubbles. Platelets in the current study would have to be in very close proximity to a moving bubble to be activated by bubble oscillation that produces microstreaming. Microstreaming may be more likely in samples containing UCA, where the faster aggregation times seem to indicate that the shearing mechanism promotes platelet aggregation.

It is important to distinguish between acoustic streaming, radiation pressure and microstreaming to understand the forces at work in a sample during HIFU exposure. Acoustic streaming results from momentum transfer to an absorbing homogeneous fluid. Radiation pressure occurs due to momentum transfer of acoustic energy due to scattering at some impedance discontinuity in an inhomogeneous fluid. Microstreaming is the fluid flow within a boundary layer (approximately 2 $\mu$m;

Nyborg 1968) that surrounds bubbles undergoing stable cavitation. Shear stress sufficient to activate platelets depends on the duration of exposure. As the duration of exposure increases, the shear necessary to activate platelets decreases. Because of the small focal volume and bulk streaming that moves the platelets in and out of the focus within milliseconds, a large shear stress is necessary to produce platelet activity in these HIFU exposures. The shear forces that occur due to bulk streaming in HIFU samples herein are on the order of 10 dyne/cm$^2$ and thus are not a likely mechanism of platelet activity.

The amount of HIFU induced platelet aggregation in samples of whole blood is less than in samples of PRP. Some researchers have suggested that blood cells tend to damp the oscillation of cavitation bubbles, thereby reducing the amount of damage caused by cavitation (Nyborg and Miller 1982, Brayman and Miller 1993, Ellwart 1988). This theory has been refuted in studies by Brayman et al. (1996), where findings indicate that the amount of hemolysis increases with hematocrit, yet the relative fraction of lysed cells decreases. The reduced effect of HIFU in whole blood aggregation samples may be due to the proximity of platelets to cavitation bubbles. At the higher cell concentrations in whole blood (25 erythrocytes to each platelet), cavitation effects may depend on the distance and number of cells between cavitation nuclei and platelets.

One issue to consider when discussing cavitation is that most biological samples tend to contain very few cavitation nuclei unless they are excessively handled (lung and bowel being exceptions). Samples which are free of dirt and contamination have a higher cavitation threshold than those which are not (Greenspan and Tschiegg 1967; Apfel 1970). Centrifuging, washing and diluting, as well as

pipetting, can all add air bubbles and thus potential cavitation nuclei to a sample. Samples in these studies were handled as little as possible in an effort to decrease the amount of impurities present in samples. Randomly trapped impurities in the sample may contribute to the variation in the cavitation threshold from sample to sample and result in the lack of consistent cavitation generation with intensity. Application of overpressure to PRP samples helped to eliminate some of this effect.

Use of UCA allows partial control of the number of cavitation nuclei available in a sample. Although handling of samples may or may not add cavitation nuclei, addition of UCA definitely will. Optison® and Albunex® were used in studies, and Optison® provides cavitation nuclei that do not dissolve as readily in samples. This is because Optison® contains perfluorocarbon gas while Albunex® contains air, and perfluorocarbon based UCA has been shown to last longer than air based UCA (Miller and Gies 1998). Lower doses of Optison® were used because Optison®-treated samples show more damage than samples with Albunex®.

The thermal mechanism for cell damage results from exposure to temperatures which tend to denature proteins, that is, to alter the properties of proteins such that they lose their biological activity. The temperature required to cause damage is dose-dependent. The time required to kill 90% of Chinese hamster lung fibroblasts is 58 minutes at 43°C and 27 minutes at 44 °C (ter Haar 1986). The highest temperature reached in any of the preliminary study trials was 42.7 °C, while most trials did not rise above 40 °C. The maximum duration of exposure was 500 s, so thermal effects are not a likely mechanism in causing platelet activity in these HIFU trials. Because temperature measurements at the focus of the HIFU transducer may lead to artifacts due to absorption by the thermocouple wires in the acoustic field (Waterman and

Leeper 1990), the temperature measurements in preliminary studies were taken within the HIFU tank, but not within the sample. During aggregation trials, temperature was measured in the sample chamber above the HIFU focus. Temperature tended to rise within the first 50 s of exposure and then stabilize. The maximum temperature rise was from 30°C to 37.4°C at 2825 W/cm$^2$. Because the maximum temperature is below the threshold to cause platelet membrane disorganization, the thermal mechanism can be eliminated.

## 9.3 Conclusions

We conclude that HIFU induced cavitation is responsible for platelet rupture that leads to platelet activation, adhesion to a collagen-coated surface and aggregation. HIFU induced bulk fluid flow, while insufficient to activate platelets alone, is necessary to mix platelet activating factors and allow platelet-platelet and platelet-collagen interactions. An optimal range of cavitation dose exists for achieving platelet activation and aggregation without causing extensive platelet and erythrocyte damage. These results suggest that use of HIFU and UCA may provide a means to supplement the natural hemostatic system.

## 10.0 FUTURE DIRECTIONS

Further studies on the effect of HIFU on supplementing the natural hemostatic system include evaluating and quantifying cavitation to better control its effects, investigating the effect of HIFU on steps in the coagulation cascade, and studies in a flow system. The results from future work will be helpful in developing an optimized protocol for HIFU application.

To investigate cavitation in more detail, a higher sampling rate and greater data capacity is required. With sufficient resolution, FFTs may be performed on cavitation data permitting analysis of harmonics that may allow distinction between stable and inertial cavitation. Another benefit of the higher sampling rate is that a standard method of quantifying cavitation can be developed. Some combination of cavitation dose and FFT analysis that can be used in both CW and pulsed systems is an appropriate method. With more specific information on the type and amount of cavitation occurring in a system, better control of cavitation bioeffects may be possible.

The research presented here investigated the effect of HIFU on primary hemostasis. This platelet-related hemostasis is just the first step in the coagulation process. Further studies that investigate the effect of HIFU-induced cavitation on elements of the coagulation cascade are needed to determine if HIFU exposure produces any bioeffects on components necessary for clot formation.

Results in a flow system may vary from those measured in a static system. Platelets will not undergo exposure for a long duration in a flow system. Cavitation may cause some platelets to disrupt and release contents immediately, yet released contents of disrupted platelets may not interact as readily with resting platelets in a

flow system. However, if HIFU can create a "mini arterial environment" (i.e. a local region of high flow and shear), flow at the application point may differ from the remainder of the system, and activation and adherence may occur at a specific site. Acoustic streaming effects necessary to create the "mini arterial environment" may allow effects of HIFU application to be localized. Depending on the outcome of the flow studies, eventual application to *in vivo* studies will allow a more comprehensive evaluation of HIFU exposure as a method of stimulating hemostasis.

# 11.0 BIBLIOGRAPHY

Anderson, GH, Hellums, JD, Moake, JL, Alfrey, CP. Platelet lysis and aggregation in shear fields. Blood Cells 1978;4:499-507.

Apfel, RE. The role of impurities in cavitation -threshold determination. J Acoust Soc Am 1970;48(5):1179-1186.

Azadniv, M, Doida, Y, Miller, MW, et al. Temporality in ultrasound-induced cell lysis in vitro. Echocardiography 1996;13:45-55.

Bailey, MR, Couret, LN, Sapozhnikov, OA, et al. Use of overpressure to assess the role of bubbles in focused ultrasound lesion shape *in vitro*. Ultrasound Med Biol 2001;27:695-708.

Brayman, AA, Miller, MW. Cell density dependence of the ultrasonic degassing of fixed erythrocyte suspensions. Ultrasound Med Biol 1993;19:243-252.

Brayman, AA, Azadniv, M, Makin, IRS, et al. Effect of a stabilized microbubble echo contrast agent on hemolysis of human erythrocytes exposed to high intensity pulsed ultrasound. Echocardiography 1995;12:13-21.

Brayman, AA, Azadniv, M, Cox, C, Miller, MW. Hemolysis of Albunex-supplemented, 40% hematocrit human erythrocytes *in vitro* by 1 MHz pulsed ultrasound: acoustic pressure and pulse length dependence. Ultrasound Med Biol 1996;22:927-938.

Brayman, AA, Miller, MW. Acoustic cavitation nuclei survive the apparent ultrasonic destruction of Albunex® microspheres. Ultrasound Med Biol 1997a;23:793-796.

Brayman, AA, Strickler, PL, Luan, H et al. Hemolysis of 40% hematocrit Albunex®-supplemented human erythrocytes by pulsed ultrasound: frequency, acoustic pressure and pulse length dependence. Ultrasound Med Biol 1997b;23:1237-1250.

Brayman, AA, Coppage, ML, Vaidya, S, Miller, MW. Transient poration and cell surface receptor removal from human lymphocytes *in vitro* by 1 MHz ultrasound. Ultrasound Med Biol 1999a;25:999-1008.

Brayman, AA, Miller, MW. Sonolysis of Albunex®-supplemented, 40% hematocrit human erythrocytes by pulsed 1 MHz ultrasound: pulse number, pulse duration and exposure vessel rotation dependence. Ultrasound Med Biol 1999b;25:307-314.

Calabrese, AM. Threshold measurements and production rates for inertial cavitation due to pulsed, megahertz-frequency ultrasound. Dissertation, The University of Mississippi, May 1996.

Cardinal, DC, Flower, RJ. The electronic aggregometer: a novel device for assessing platelet behavior in blood. J Pharm Meth 1980;3:135-158.

Chater, BV, Williams, AR. Platelet aggregation induced *in vitro* by therapeutic ultrasound. Thromb Haemost 1977;38:640-651.

Christensen, DA. Ultrasonic bioinstrumentation. New York, NY: John Wiley & Sons, 1988:176-179.

Colman, RW, Hirsh, J, Marder, VJ, Salzman, EW, ed. Hemostasis and thrombosis. Philadelphia: J.B. Lippincott Company, 1994, p. 818; pp. 524-544.

Dalecki, D, Raeman, CH, Child, SZ, et al. Hemolysis *in vivo* from exposure to pulsed ultrasound. Ultrasound Med Biol 1997;23:307-313.

Damianou, CA, Sanghvi, NT, Fry, FJ, Maass-Moreno, R. Dependence of ultrasonic attenuation and absorption in dog soft tissues on temperature and thermal dose. J Acoust Soc Am 1997, 102(1): 628-634.

Delius, M. Minimal static excess pressure minimises the effect of extracorporeal shock waves on cells and reduces it on gallstones. Ultrasound Med Biol 1997;23:611-617.

Delon-Martin, C, Vogt, C, Chignier, E, et al. Venous thrombosis generation by means of high-intensity focused ultrasound. Ultrasound Med Biol 1995;21:113-119.

Deng, CX, Xu, Q, Apfel, RE, Holland, CK. *In vitro* measurements of inertial cavitation thresholds in human blood. Ultrasound Med Biol 1996;22:939-948.

Elder, SA. Cavitation Microstreaming. J Acoust Soc Am 1959;31:54-64.

Ellwart, JW, Brettel, H, Kober, LO. Cell membrane damage by ultrasound at different cell concentrations. Ultrasound Med Biol 1988;14:43-50.

Everbach, EC, Makin, IRS, Azadniv, M, Meltzer, RS. Correlation of ultrasound-induced hemolysis with cavitation detector output *in vitro*. Ultrasound Med Biol 1997;23:619-624.

Everbach, EC, Makin, IRS, Francis, CW, Meltzer, RS. Effect of acoustic cavitation on platelets in the presence of an echo-contrast agent. Ultrasound Med Biol 1998;24:129-136.

Flynn HG. Cavitation II Free pulsations and models for cavitation bubbles. J Acoust Soc Am 1975, 58(6): 1160-1170.

Frizzell, LA, Miller, DL, Nyborg, WL. Ultrasonically induced intravascular streaming and thrombus formation adjacent to a micropipette. Ultrasound Med Biol 1986;3:217-221.

Goss, SA, Johnston, RL, Dunn, F. Comprehensive compilation of empirical ultrasonic properties of mammalian tissues. J Acoust Soc Am 1978, 64(2): 423-457.

Greenspan, M, Tschiegg, CE. Radiation-induced acoustic cavitation; apparatus and some results. J Res Natl Bur Stand Sect C 1967, 71:299-311.

Hynynen, K, Chung, AH, Colucci, V, Jolesz, FA. Potential adverse effects of high-intensity focused ultrasound exposure on blood vessels *in vivo*. Ultrasound Med Biol 1996a;22:193-201.

Hynynen, K, Colucci, V, Chung, A, Jolesz, F. Noninvasive arterial occlusion using MRI-guided focused ultrasound. Ultrasound Med Biol 1996b;22:1071-1077.

IEEE Std 790-1989, IEEE Guide for Medical Ultrasound Field Parameter Measurements (ANSI), 1989.

Ivey, JA, Gardner, EA, Fowlkes, JB, Rubin, JM, Carson, PL. Acoustic generation of intra-arterial contrast boluses. Ultrasound Med Biol 1995;21:757-767.

Leighton, TG. The Acoustic Bubble. London: Academic Press, 1994.

Lokhandwalla, M, McAteer, JA, Williams, JC, Sturtevant, B. Mechanical haemolysis in shock wave lithotripsy (SWL): II. *In vitro* cell lysis due to shear. Phys Med Biol 2001; 46:1245-1264.

Martin RW, Vaezy S, Kaczkowski P, et al. Hemostasis of punctured vessels using Doppler-guided high-intensity ultrasound. Ultrasound Med Biol 1999; 25:985-90.

Miller, DL, Nyborg, WL, Whitcomb, CC. Platelet aggregation induced by ultrasound under specialized conditions *in vitro*. Science 1979;205:505-507.

Miller, DL. The influence of hematocrit on hemolysis by ultrasonically activated gas-filled micropores. Ultrasound Med Biol 1988a;14:293-297.

Miller, DL. Particle gathering and microstreaming near ultrasonically activated gas-filled micropores. J Acoust Soc Am 1988b; 84:1378-1387.

Miller DL, Thomas RM. The influence of variations in biophysical conditions on hemolysis near ultrasonically activated gas-filled micropores. J Acoust Soc Am 1990;87:2225-30.

Miller, DL, Thomas, RM. A comparison of hemolytic and sonochemical activity of ultrasonic cavitation in a rotating tube. Ultrasound Med Biol 1993;19:83-90.

Miller, DL, Gies, RA, Chrisler, WB. Ultrasonically induced hemolysis at high cell and gas body concentrations in a thin-disc exposure chamber. Ultrasound Med Biol 1997;23:625-633.

Miller, DL, Gies, RA. Enhancement of ultrasonically-induced hemolysis by perfluorocarbon-based compared to air-based echo-contrast agents. Ultrasound Med Biol 1998;24:285-292.

Miller, MW. *In vitro* studies: single cell and multi cell spheroids. In Biological Effects of Ultrasound. ed. Nyborg, WL and Ziskin,MC. Chap 4 pp 34-48, Vol 16, Clinics in Diagnostic Ultrasound. Churchill Livingstone Inc., New York, 1985.

Miller, MW, Miller, DL, Brayman, AA. A review of *in vitro* bioeffects of inertial ultrasonic cavitation from a mechanistic perspective. Ultrasound Med Biol 1996;22:1131-1154.

Nageswari, K, Banerjee, R, Gupte, RV, Puniyani RR. Effects of exercise on rheological and microcirculatory parameters. Clin Hemorheology Microcirc 2000; 23: 243-247.

Nyborg, WL. Mechanisms for nonthermal effets of sound. J Acoust Soc Am 1968;44:1302-1309.

Nyborg, WL, Miller, DL. Biophysical implications of bubble dynamics. Appl Sci Res 1982; 38:17-24.

Poliachik, SL, Chandler, WL, Mourad, PD, et al. Effect of high-intensity focused ultrasound on whole blood with and without microbubble contrast agent. Ultrasound Med Biol 1999; 25: 991-998.

Rooney, JA. Hemolysis near an ultrasonically pulsating gas bubble. Science 1970;169:869-871.

Rooney, JA. Shear as a mechanism for sonically induced biological effects. J Acoust Soc Am 1972;52:1718-1724.

Sakariassen, KS, Holme, PA, Orvim, U, Barstad, RM, Solum, NO, Brosstad, FR. Shear-induced platelet activation and platelet microparticle formation in native human blood. Thrombosis Res 1998, 92: S33-S41.

Samal, AB, Adzerikho, ID, Mrochek, AG, Loiko, EN. Platelet aggregation and change in intracellular $Ca^{2+}$ induced by low frequency ultrasound *in vitro*. Eur J Ultrasound 2000; 11:53-59.

Sapozhnikov, OA, Khokhlova, VA, Bailey, MR et al. Effect of overpressure and pulse repetition frequency on cavitation in shock wave lithotripsy. submitted to J Acoust Soc Am 2001.

Schmiedl UP, Carter S, Martin RW, Eubank W, Winter T, Chang PP, Bauer A, Crum LA. Sonographic detection of acute parenchymal injury in an experimental porcine model of renal hemorrhage: gray-scale imaging using a sonographic contrast agent. AJR Am J Roentgenol 1999 Nov;173(5):1289-94.

Steen, HB. Characteristics of flow cytometers. In: Melamed, MR, Lindmo, T, Mendelsohn,ML ed. Flow cytometry and sorting. New York, NY, 1990:11-19.

Tait, JF, Smith, C, Wood, BL. Measurement of phosphatidylserine exposure in leukocytes and platelets by whole-blood flow cytometry with annexin V. Blood Cells Mol Dis 1999, 25:271-278.

ter Haar, G. Effects of increased temperature on cells, on membranes and on tissues. In: Watmough, DJ, Ross WM ed. Hyperthermia. London: Blackie & Son Limited, 1986:14-40.

Thomas, CL ed. Taber's Cyclopedic Medical Dictionary, Philadelphia: F A Davis Company, 1978:P-92.

Vaezy, S, Martin, R, Schmiedl, U, et al. Liver hemostasis using high-intensity focused ultrasound. Ultrasound Med Biol 1997;23:1413-1420.

Vaezy, S, Martin, R, Yaziji, H, et al. Hemostasis of punctured blood vessels using high-intensity focused ultrasound. Ultrasound Med Biol 1998;24:903-910.

Vaezy S, Martin R, Keilman G, et al. Control of splenic bleeding by using high intensity ultrasound. J Trauma 1999a; 47:521-525.

Vaezy S, Martin R, Kaczkowski P, et al. Use of high-intensity focused ultrasound to control bleeding. J Vasc Surg 1999b; 29:533-542.

Waterman FM, Leeper JB. Temperature artifacts produced by thermocouples used in conjunction with 1 and 3 MHz ultrasound. Int J. Hyperthermia, 1990, Mar-Apr; 6(2): 383-399.

Williams, AR. Release of serotonin from human platelets by acoustic streaming. J Acoust Soc Am 1974;56:1640-1643.

Williams, AR, O'Brien, WD Jr, Coller, BS. Exposure to ultrasound decreases the recalcification time of platelet rich plasma. Ultrasound Med Biol 1976a;2:113-118.

Williams, AR, Sykes, SM, O'Brien, WD Jr. Ultrasonic exposure modifies platelet morphology and function *in vitro*. Ultrasound Med Biol 1976b;2:311-317

Williams, AR. Intravascular mural thrombi produced by acoustic microstreaming. Ultrasound Med Biol 1977;3:191-203.

Williams, AR, Chater, BV, Allen, KA, Sherwood, MR, Sanderson, JH. Release of β-thromboglobulin from human platelets by therapeutic intensities of ultrasound. Br J Haematol 1978;40:133-142.

Williams, JC, Woodward, JF, Stonehill, MA et al. Cell damage by lithotripter shock waves at high pressure to preclude cavitation. Ultrasound Med Biol 1999;25:1445-1449.

Williams, MJ, Morris, MW, Nelson, DA, "Examination of Blood" in *Williams Hematology* edited by E. Beutler, MD (McGraw Hill, New York, 1995), pp. 8-14.

Wood, BL, Gibson, DF, Tait JF. Increased erythrocyte phosphatidylserine exposure in sickle cell disease: flow-cytometric measurement and clinical associations. Blood 1996; 88:1873-1880.

Zarod, AP, Williams, AR. Platelet aggregation *in vivo* by therapeutic ultrasound. Lancet 1977;1:1266.

## 12.0 APPENDICES

### A. MatLab Programs

MatLab file "convert.m":

```
% 20 May 2001
% This program converts whole blood aggregometry raw data files from
% temperature (3 x 502 array) and impedance voltage files (from 5002 to
% 250002 values) to 1 x 500 (or so) arrays


% load data


T = input ('Temperature file = ');


I = input ('Impedance file = ');


% Determine size of temp and imp arrays
tsize = length (T);
isize = length (I);


% Determine which temperature probe was in sample
disp('Which thermocouple was in the sample? Enter "1" for one and "2" for two.')
ch = input ('Thermocouple channel = ')


% Format temperature array


wbtemp1 = T(tsize +1:tsize*2);


wbtemp2 = T (tsize *2 +1 : tsize * 3);


if ch == 1
        wbtemp = wbtemp1;
else wbtemp = wbtemp2;
end


% Format impedance array (average values in array to create a ~500 member array)
j = round (isize/500);
```

```
for i = 1:500
        midimp (i) = mean ( I ( ( (i -1) * j) +1: i * j) );
end
```

```
% Remove any "Inf" values from wbimp
nuke = isfinite (midimp);
key = find (nuke);
klen = length (key);
```

```
for i = 1:klen-1
        wbimp(i) = midimp (key(i));
end
implen = length (wbimp);
```

```
% Set axis limits for plots
ttop = max(wbtemp) + 0.2;
tbot = min(wbtemp) - 0.2;
itop = max(wbimp) + 0.05;
ibot = min(wbimp) - 0.05;
```

```
% Plot arrays
subplot (4,1,1), plot (0:tsize -1, wbtemp), ylabel ('Temp (C)'), axis ([0 tsize tbot ttop])
subplot (4,1,2), plot (0:implen-1, wbimp), axis ([ 0 implen ibot itop]), title ('Raw'),
ylabel (' Imp (V)')
```

---

MatLab file "wbimpadj.m"

```
% Impedance voltage adjustment for temperature
% 2 May 2001
% Whole blood aggregometry
```

```
% Run the program "convert.m" prior to this program for proper loading of files.
% Temperature and impredance arrays should exist from the "convert.m" program:
% Temperature = wbtemp; Impedance = wbimp.
```

```
% Set baseline values
bt = wbtemp(1);
bi = max (wbimp);


% Determine length of arrays
tempsize = length (wbtemp);
impsize = length (wbimp);


if tempsize < impsize
        index = tempsize;
        else index = impsize;
end



% Calculate new voltages for impedance values, based on temperature variation.
% For every degree C increase in temperature, the output voltage of the impedance
% circuit drops 0.099V.
for i = 1:index
        comp = wbtemp(i) -bt;
        adjimp (i) = wbimp(i) + (0.099 * comp);
end


% Set axis limits for plots
aitop = max(adjimp) + 0.05;
aibot = min(adjimp) - 0.05;


% Find index for wbtemp and adjimp
tlen = length (wbtemp);
ilen = length (adjimp);


% Plot results

subplot (4,1,3), plot (0:ilen-1, adjimp), title ('Adjusted'), ylabel (' Imp (V)'), axis ([ 0
implen aibot aitop])
```

—————————————————

MatLab file "invert.m":

```
% 22 May 2001
% This file is designed to invert impedance voltage measurements from whole blood
% aggregometry experiments such that they are simliar in appearance to laser aggregometry
% results.

% This program should be run after the series: convert.m and wbimpadj.m

% Invert data

len = length (adjimp);

for i = 1: len
        invimp(i) = adjimp(i) * -1;
end

% Find limits to set axis for plotting
invbot = min (invimp) - 0.05;
invtop = max (invimp) + 0.05;

% Plot inverted data

subplot (4,1,4), plot (0:len-1, invimp), title ('Inverted'), ylabel (' Imp (V)'), axis ([ 0
len invbot invtop]), xlabel ('Time (s)')
```
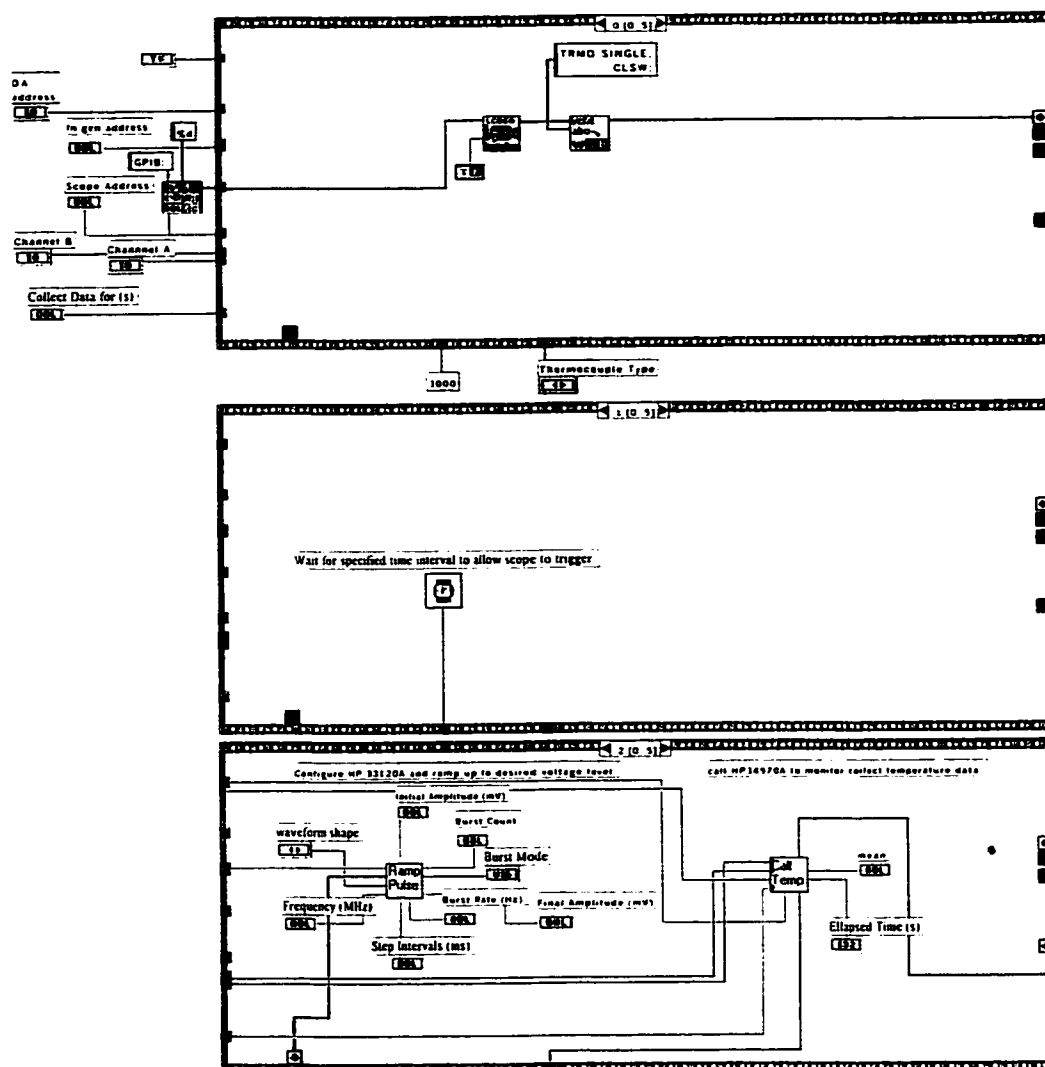
## B: LabVIEW Programs

Block diagrams for LabVIEW programs are included below. The main cavitation data collection program (no_mistakes2.vi) triggers the oscilloscope and function generator and then saves data collected by the oscilloscope (cavitation as well as aggregometry data) once the trial has ended. A simple data collection program (Displaydata.vi) can be used to save oscilloscope data to disk without triggering any other components during the experiment. To review previously saved data, the laserview.vi program will display data from saved files. The DataIntegral.vi program calculates the integral of the cavitation data above a noise level determined by the program, leading to determination of the relative cavitation dose. The RampPulse1.vi program increases the function generator output through a range controlled by the user. For trials in which temperature data as well as cavitation data was collected, the 2temp_nomistakes.vi program was used to trigger the oscilloscope, function generator, data acquisition unit and to collect and store data after the trial ended.

no_mistakes2.vi
C:\Users\Ryan\no_mistakes2.vi
Last modified on 7/22/01 at 12:35 AM
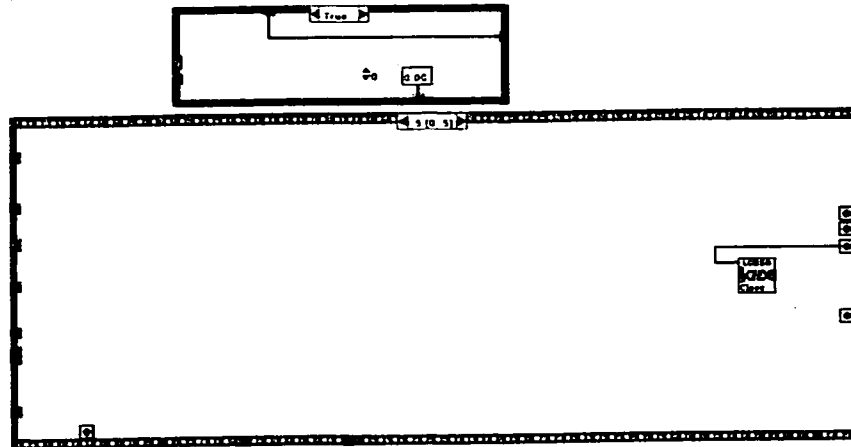Printed on 7/22/01 at 12:58 AM

Block Diagram



**B.1 Main data collection program (no_mistakes2.vi)**

no_mistakes2.vi
C:\Users\Ryan\no_mistakes2.vi
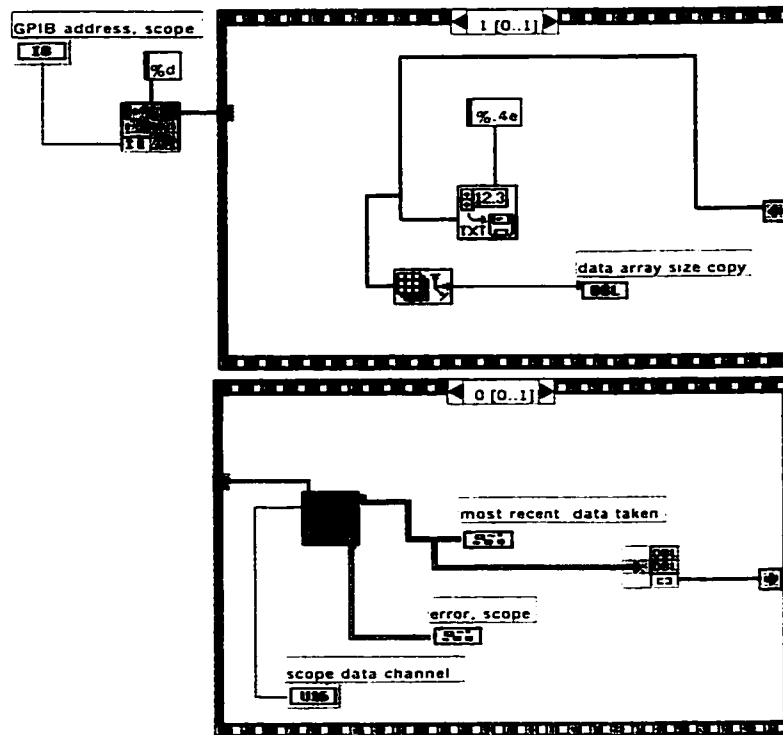Last modified on 7/22/01 at 12:35 AM
Printed on 7/22/01 at 12:58 AM
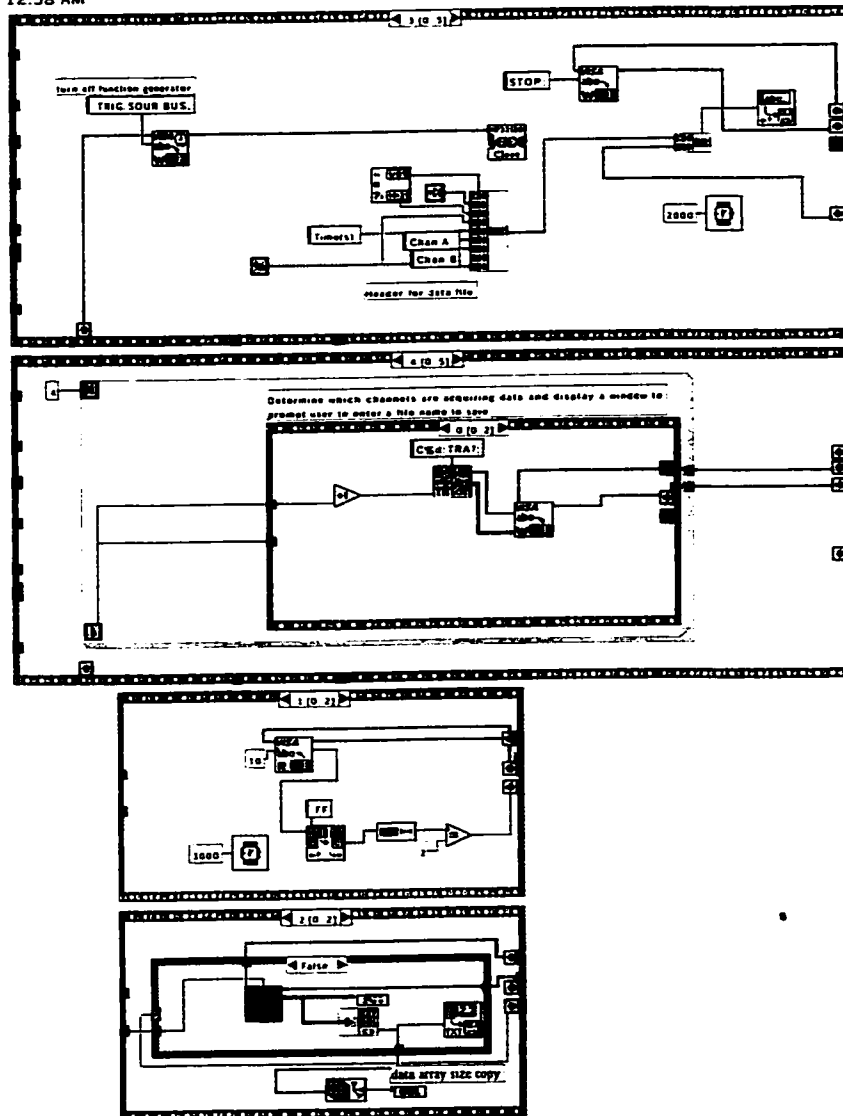
no_mistakes2.vi
C:\Users\Ryan\no_mistakes2.vi
Last modified on 7/22/01 at 12:35 AM
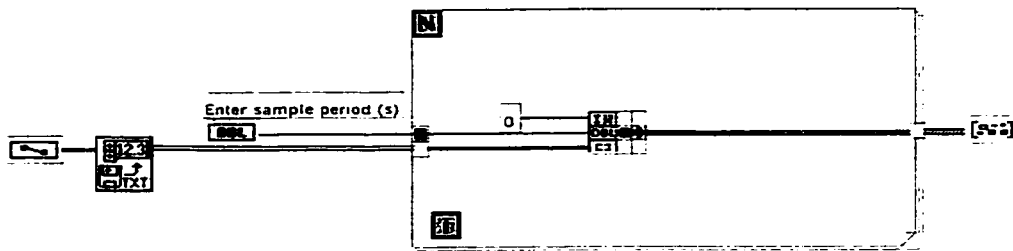Printed on 7/22/01 at 12:59 AM

displaydata.vi
C:\Users\Ryan\displaydata.vi
Last modified on 4/20/01 at 3:31 PM
Printed on 7/22/01 at 1:08 AM

Block Diagram



B.2  Data collection program (Displaydata.vi)

laserview.vi
C:\Users\Ryan\laserview.vi
Last modified on 7/22/01 at 1:11 AM
Printed on 7/22/01 at 1:11 AM

Block Diagram



Enter sample period (s)

B.3  Data review program (laserview.vi)

Page 1

Block Diagram



Enter sample period (s)

500

500

max of baseline

Override baseline?

Baseline override

clipped data

numerical integration result

num int error
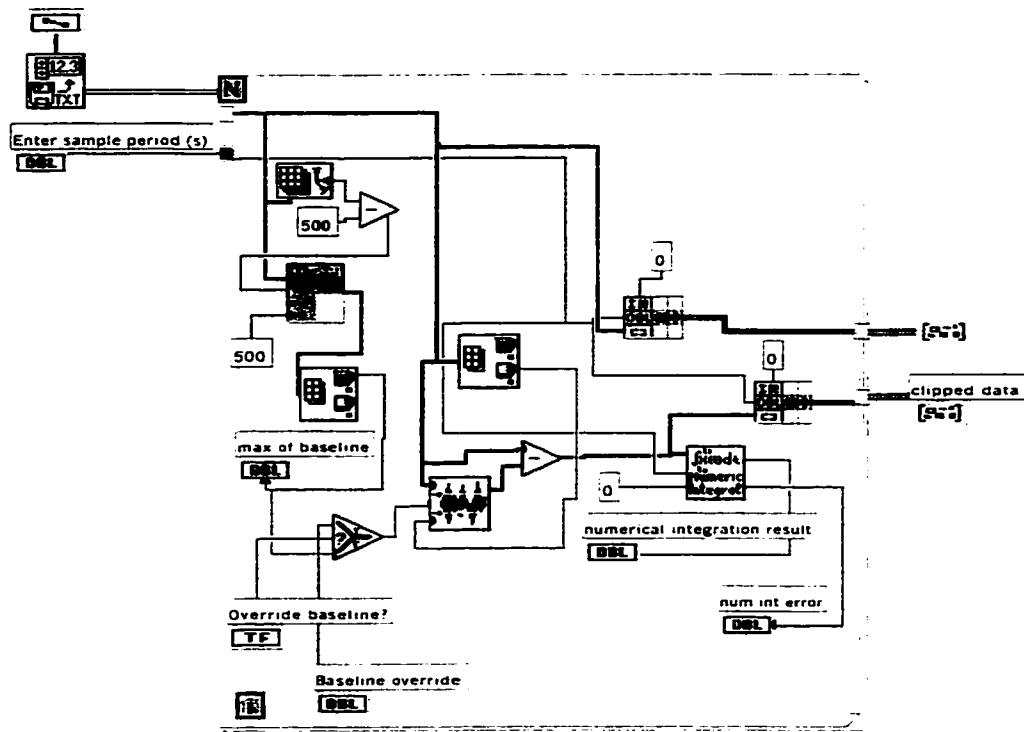
**B.4  Cavitation dose calculator (DataIntegral.vi)**

RampPulse1.vi
C:\Users\Ryan\9304 VI's & others\RampPulse1.vi
Last modified on 7/22/01 at 12:41 AM
Printed on 7/22/01 at 12:58 AM
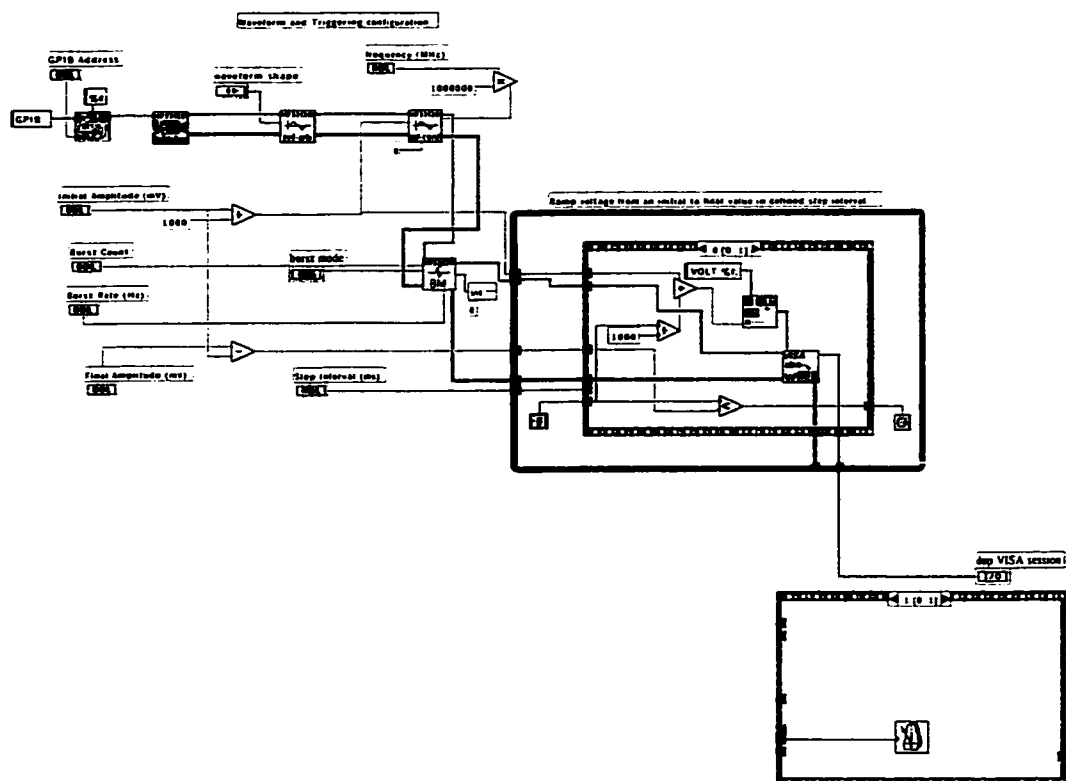
**Block Diagram**



B.5  Function generator ramp program (RampPulse1.vi)

Call
Temp

2temp_nomistakes.vi
C:\Users\Ryan\9304 VI's & others\2temp_nomistakes.vi
Last modified on 7/22/01 at 12:57 AM
Printed on 7/22/01 at 12:57 AM

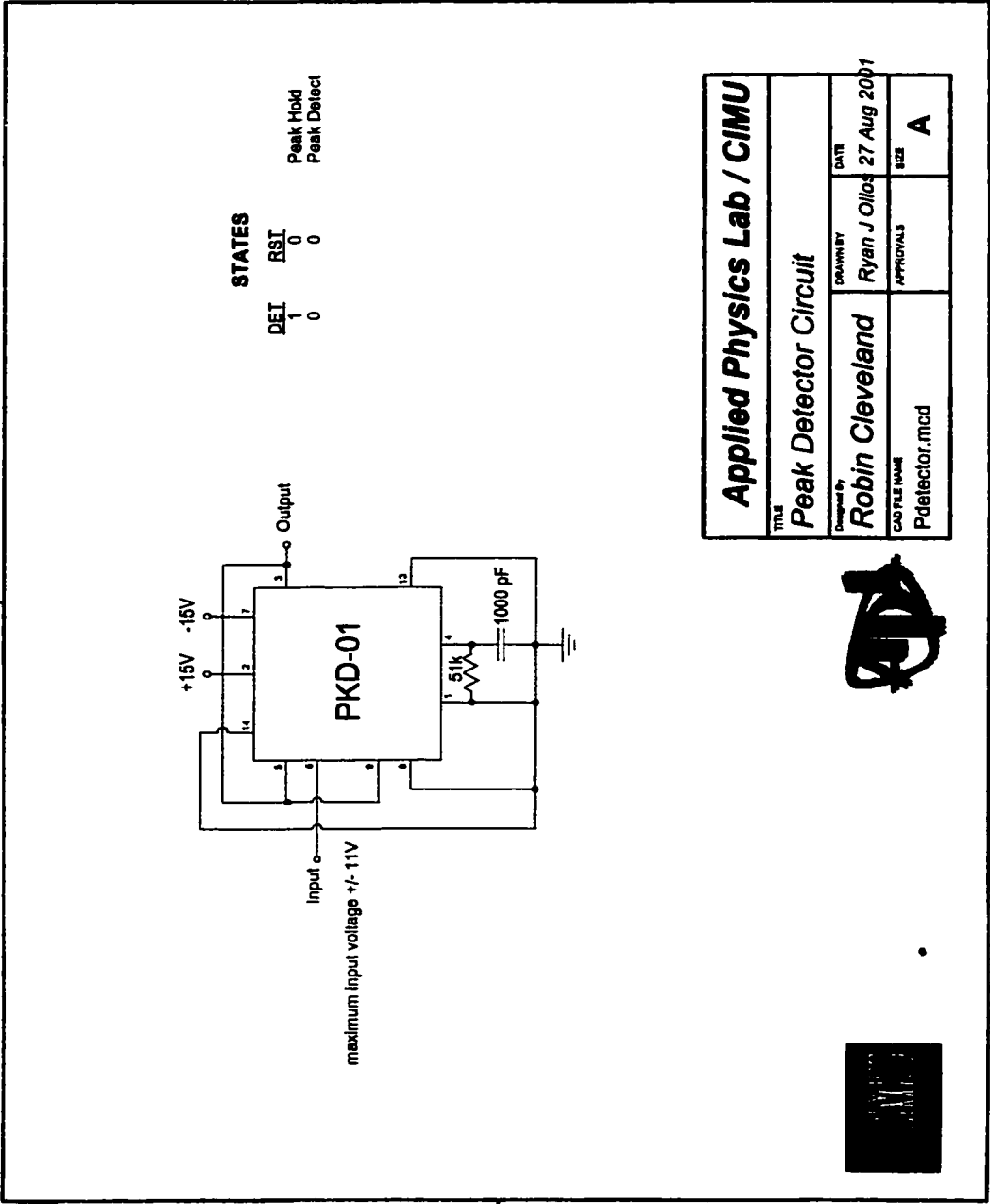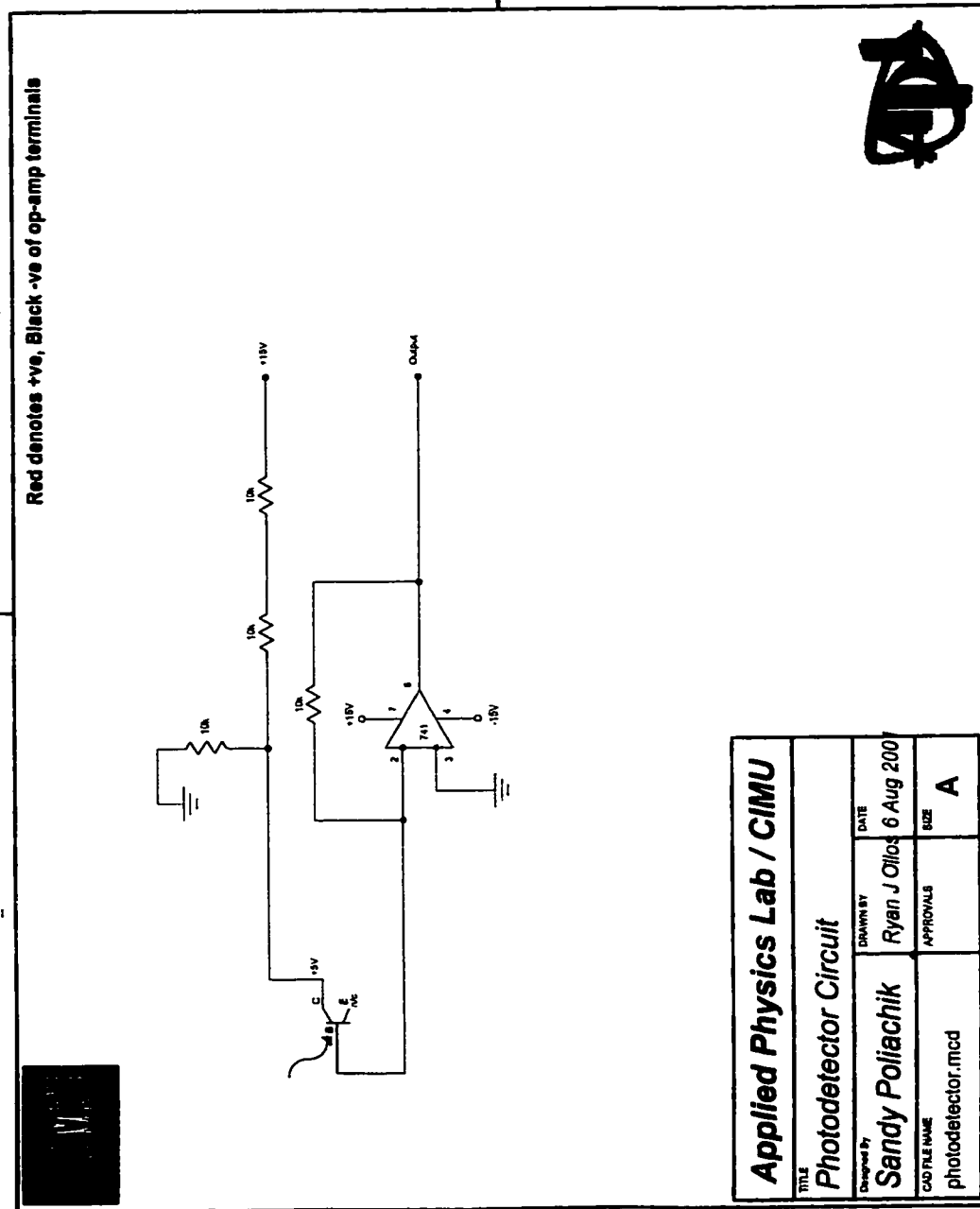Block Diagram
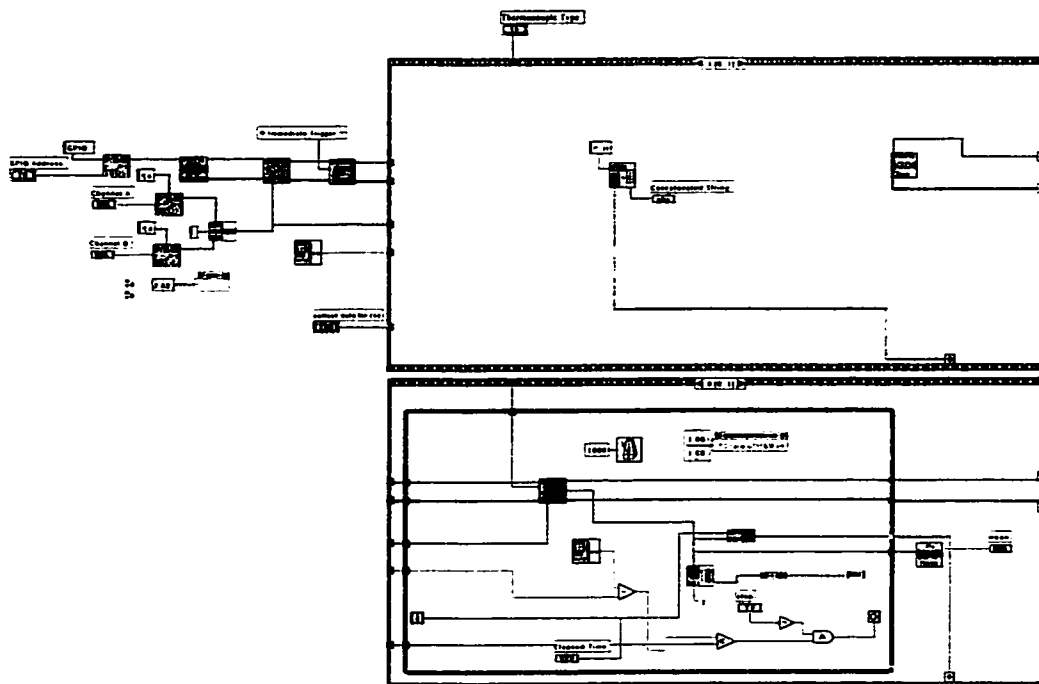


B.6  Cavitation and temperature data collection    (2temp_nomistakes.vi)
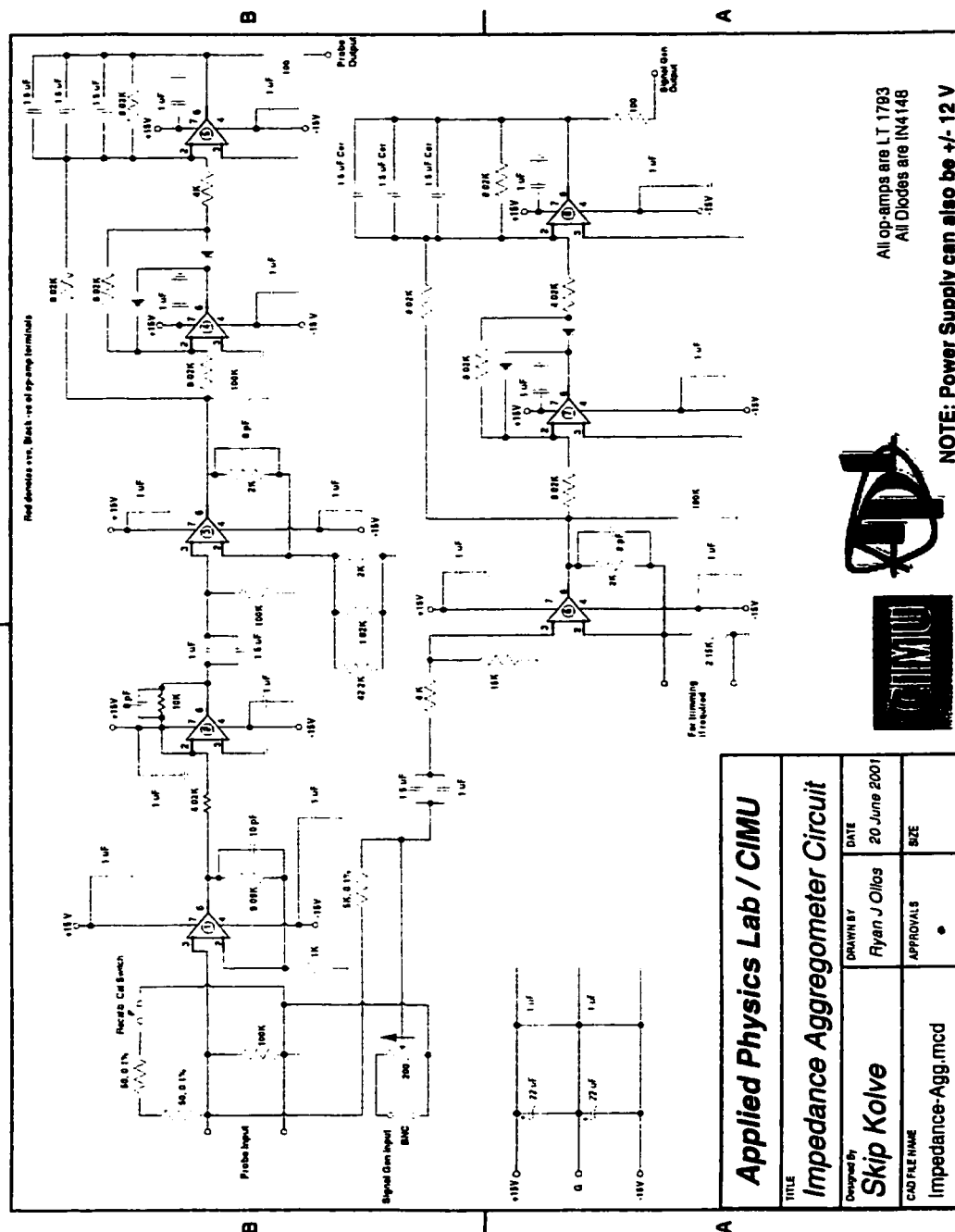
## C: Electrical Circuit Diagrams

Electrical circuits used in collecting data during experiments are shown below. The Peak Detector Circuit was used in conjunction with the 5-MHz PCD to collect cavitation data for the entire HIFU exposure time. The Photodetector Circuit was used to collect laser aggregometry data. The Impedance Aggregometry Circuit was used to convert impedance difference resulting from platelet aggregation into a voltage.

STATES

| DET | RST | |
|---|---|---|
| 1 | 0 | Peak Hold |
| 0 | 0 | Peak Detect |

Output

+15V  -15V

PKD-01

1000 pF

51k

Input

maximum input voltage +/- 11V

**Applied Physics Lab / CIMU**

TITLE
**Peak Detector Circuit**

| Designed By | DRAWN BY | DATE |
|---|---|---|
| *Robin Cleveland* | *Ryan J Ollos* | 27 Aug 2001 |
| CAD FILE NAME | APPROVALS | SIZE |
| Pdetector.mcd | | A |

C.1 Peak Detector Circuit

C.2 Photodetector Circuit

C.3  Impedance Aggregometer Circuit

## D: Flow Cytometry Overview

In analyzing platelets, flow cytometry may be used to determine the expression of certain proteins, activation of receptors, or inversion of the phospholipid bilayer. Specific assays used to determine platelet activity are listed in Table D.1.

Table D.1: Fluorescently labeled antibodies used to detect platelet activity

| Antibody | Detects |
|----------|---------|
| CD62 | P-selectin protein expression |
| PAC-1 | GPIIb/IIIa receptor activation |
| Annexin V | Exposure of negative phospholipids |

P-selectin granules are released upon activation, thus making their release a marker for platelet activation. Upon activation, the fibrinogen receptor GPIIb/IIIa allows platelets to stick to each other through a fibrinogen or vWf bridge. Upon sufficient activation, the platelet membrane will invert, exposing a negative charge to which Annexin V may attach. These anionic phospholipids are necessary components of the coagulation cascade, the next step in hemostasis after platelet aggregation.

Figure D.1 shows a schematic of a flow cytometer used to detect fluorescence and light scattering. Cell samples are carried through the laser in the measuring area of the flow cytometer by a microscopic jet of water. If the cell has a fluorescently labeled antibody attached to it, a flash of fluorescence is produced with an intensity proportional to the amount of antibody bound. This signal travels through an optics

system where the signal is sensed by a light sensitive detector. The detector converts the flashes into electrical pulses that may be recorded and saved in a computer.

The flow chamber that creates the microscopic jet of water contains a nozzle that generates hydrodynamic focusing by producing a narrow flow path through the measuring region of the flow cytometer. The sheath flow, or surrounding liquid, is supplied from a pressurized source, while the sample flows into the center of the sheath flow through a thin tube. This hydrodynamic focusing confines the sample to the central core of laminar flow leaving the nozzle. Sheath flow is generally 5 mL/min and sample flow is 100 $\mu$L/min.

Laser light is commonly focused on the sample by one or two lenses, creating a flat focus. The short axis of the light is oriented in the direction of sample flow. A lens orthogonal to the laser and the stream focuses the light from the sample at the analysis point into a pinhole, which eliminates light from other sources. Light scattered by cells may also be detected. This scattered light will be the same wavelength as the laser, whereas fluorescence is always shifted to higher wavelengths. Dichroic mirrors may be used to reflect some wavelengths into detectors and pass longer wavelengths through to other detectors. Wavelengths sensed by the detectors are converted to electrical signals. The data is analyzed by a computer and are commonly presented in scatter plots.
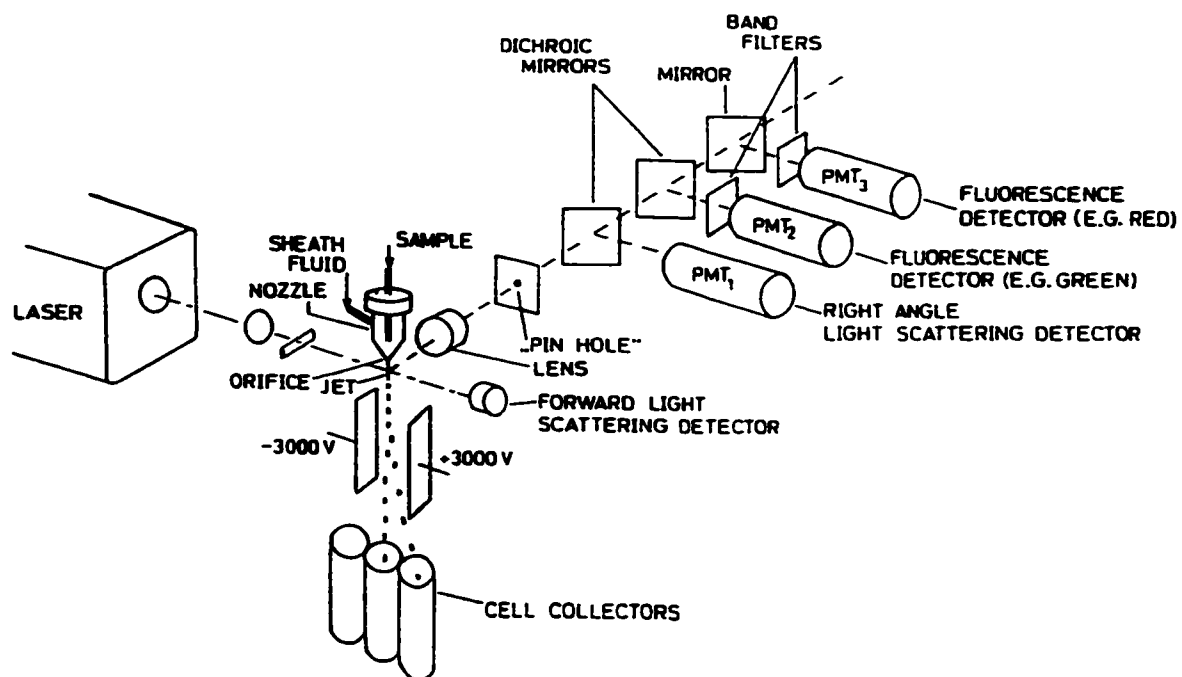
from Steen, 1990

Figure D1: Schematic of a flow cytometer. The sample is introduced to the measurement area through the sheath fluid nozzle. Laser interrogation provides information used to count particle (backscatter), and identify particles to which fluorescently labeled antibodies are attached.

## E: Environmental Scanning Electron Microscope Overview

Scanning electron microscopy (SEM) uses electrons and magnetic lenses to bend the electrons and create a magnified image, much in the same way that conventional microscopes bend light with glass lenses. Scanning coils are used to move the focused beam of electrons back and forth across a sample. As the electron beam encounters each portion of the sample, secondary electrons are knocked free of the surface. A detector counts the secondary electrons and sends a corresponding signal to an amplifier. This information is processed and the SEM image is constructed from the number of electrons emitted from each portion of the sample.
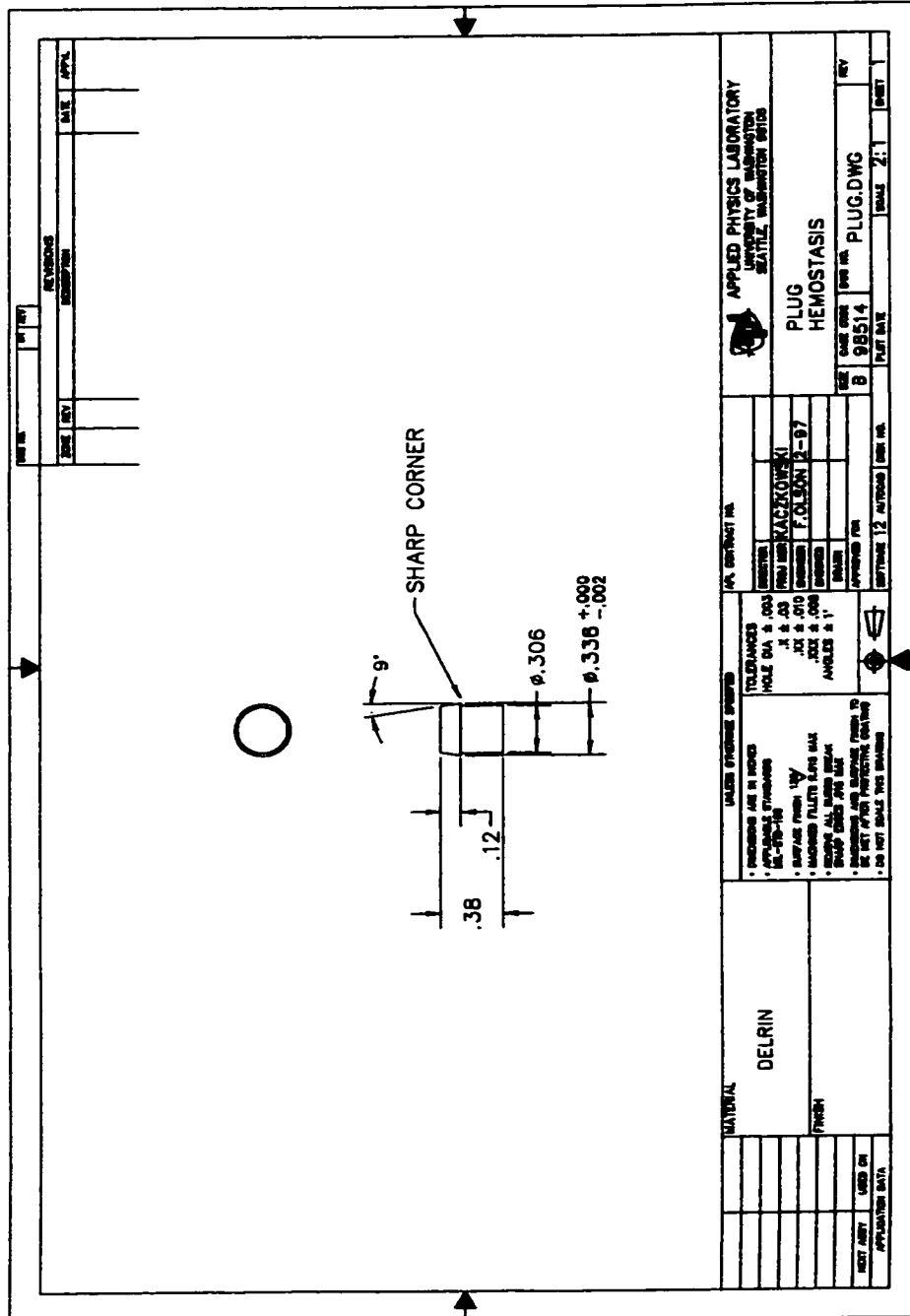
In SEM, samples must be clean, dry and electrically conductive necessitating gold plating for some samples. The preparation of a sample can introduce artifacts. The sample must be placed under high vacuum to produce the proper environment for shooting electrons and achieving high resolution. Environmental SEM (ESEM) allows samples to be investigated at near atmospheric pressures. Two closely spaced pressure limiting apertures protect the high vacuum optical regions of the ESEM. The resolution of ESEM may be lower than SEM, depending on the sample.

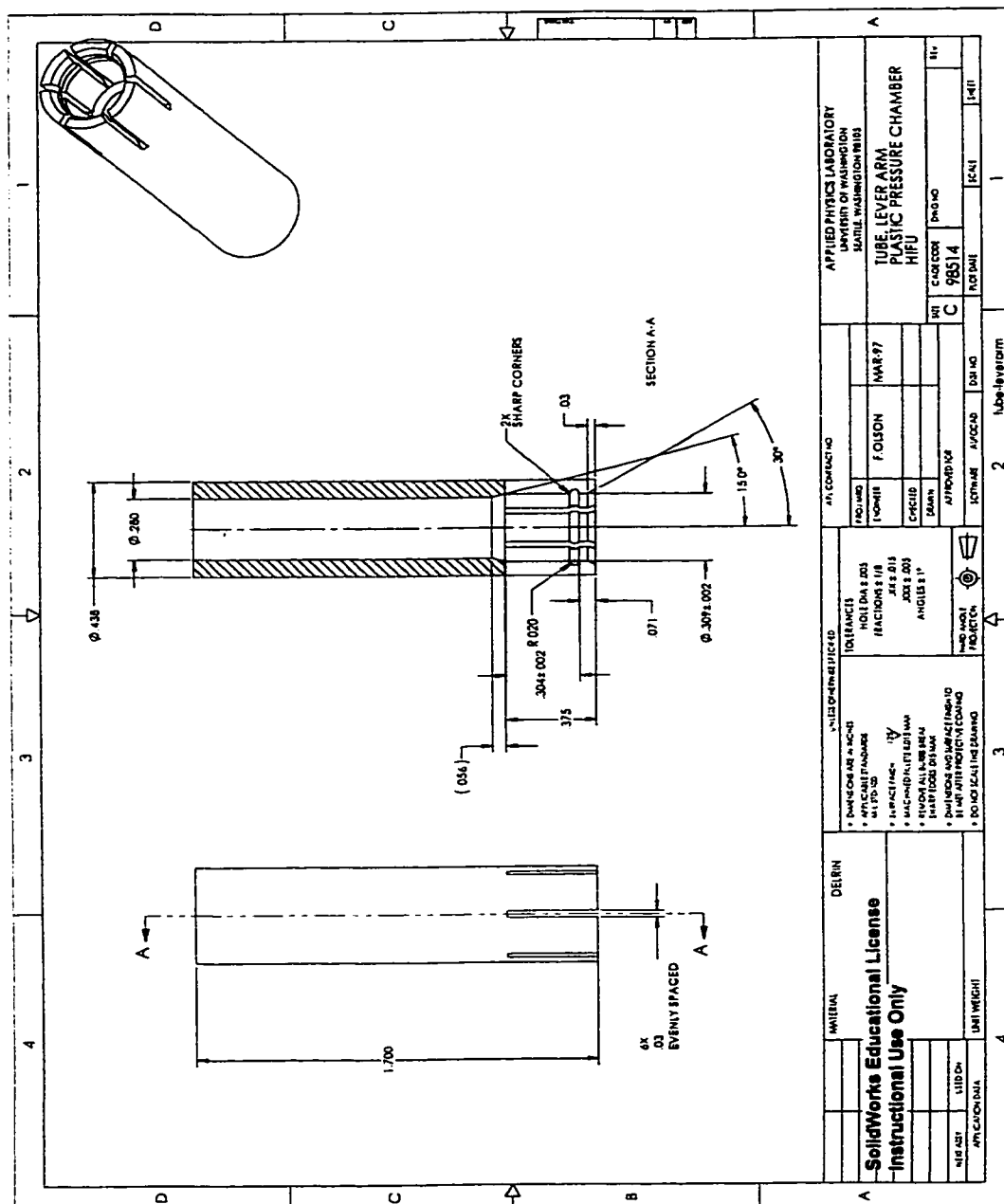## F: Part Drawings and Information

Engineering drawings with material information are included for sample chamber parts, overpressure tube adapters and overpressure chamber parts.
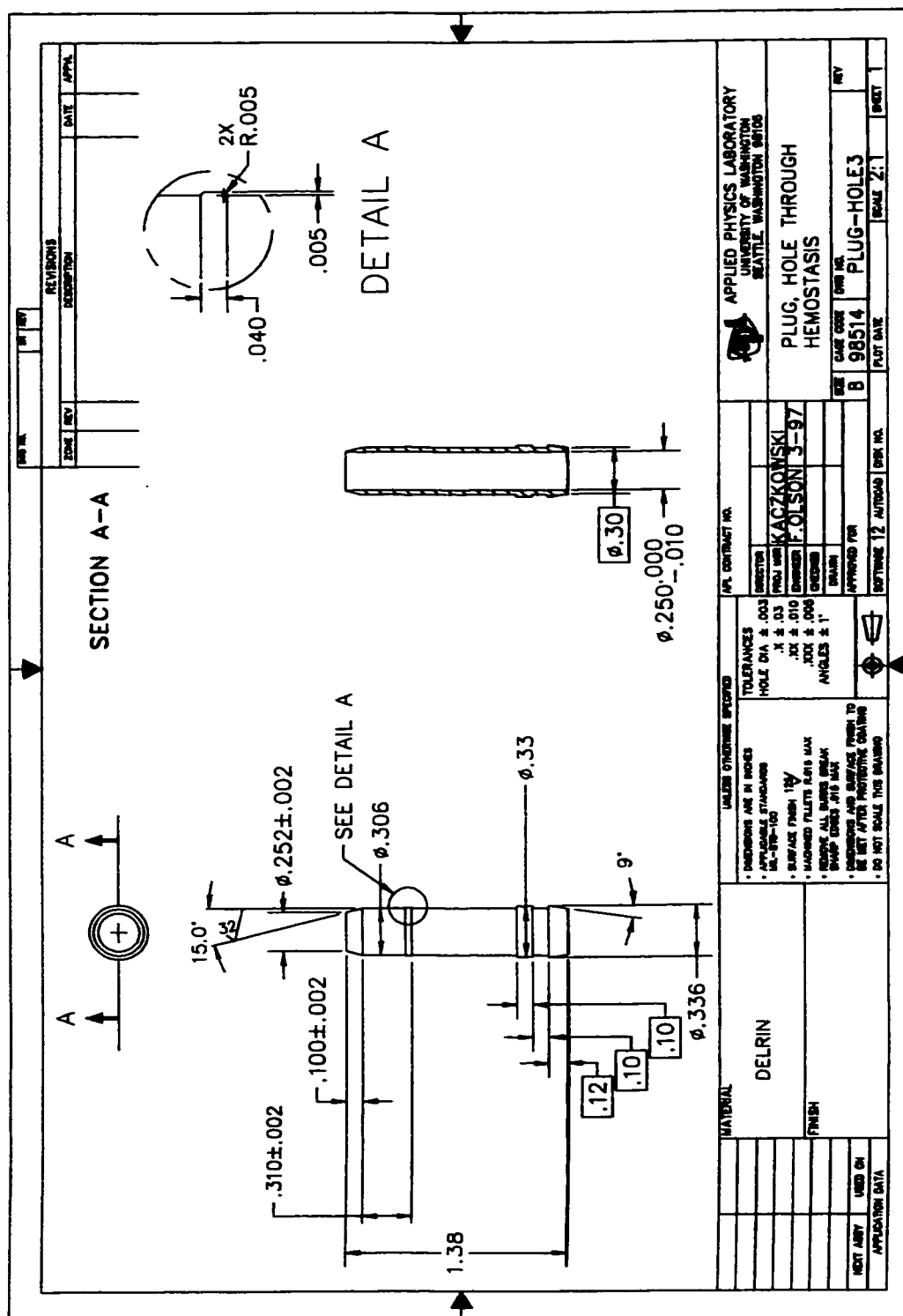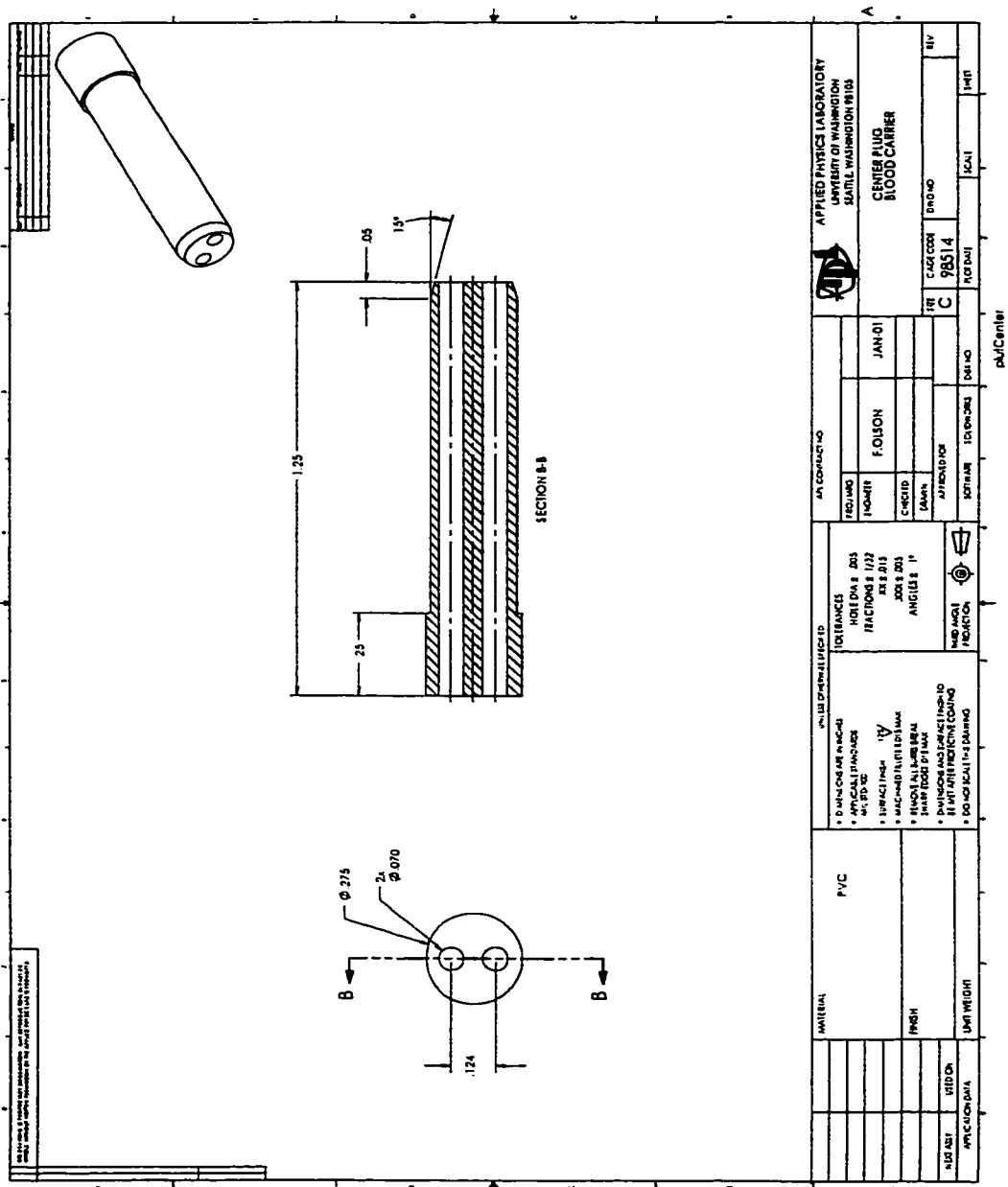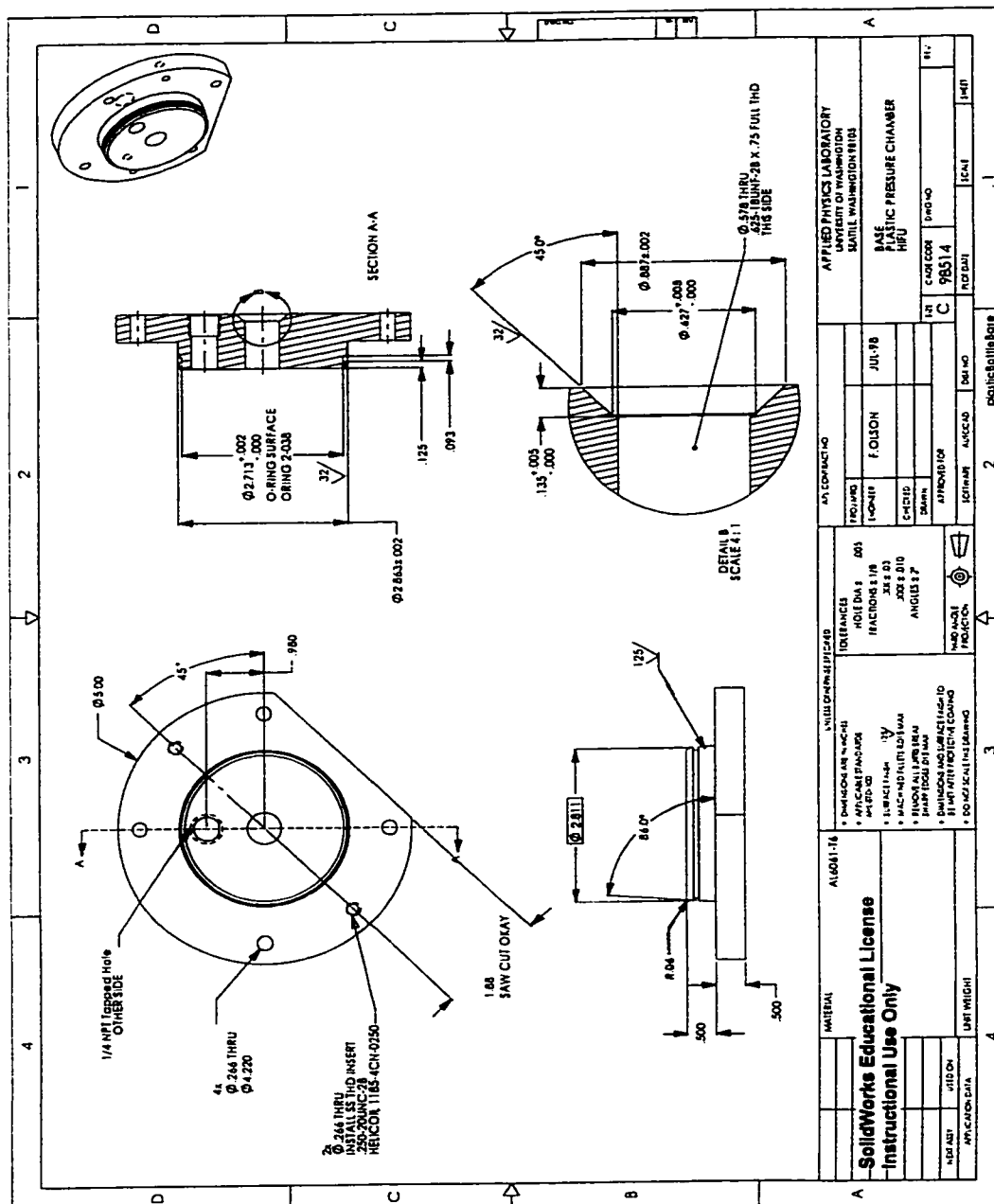
F.1 Plug, Hole Through Hemostasis
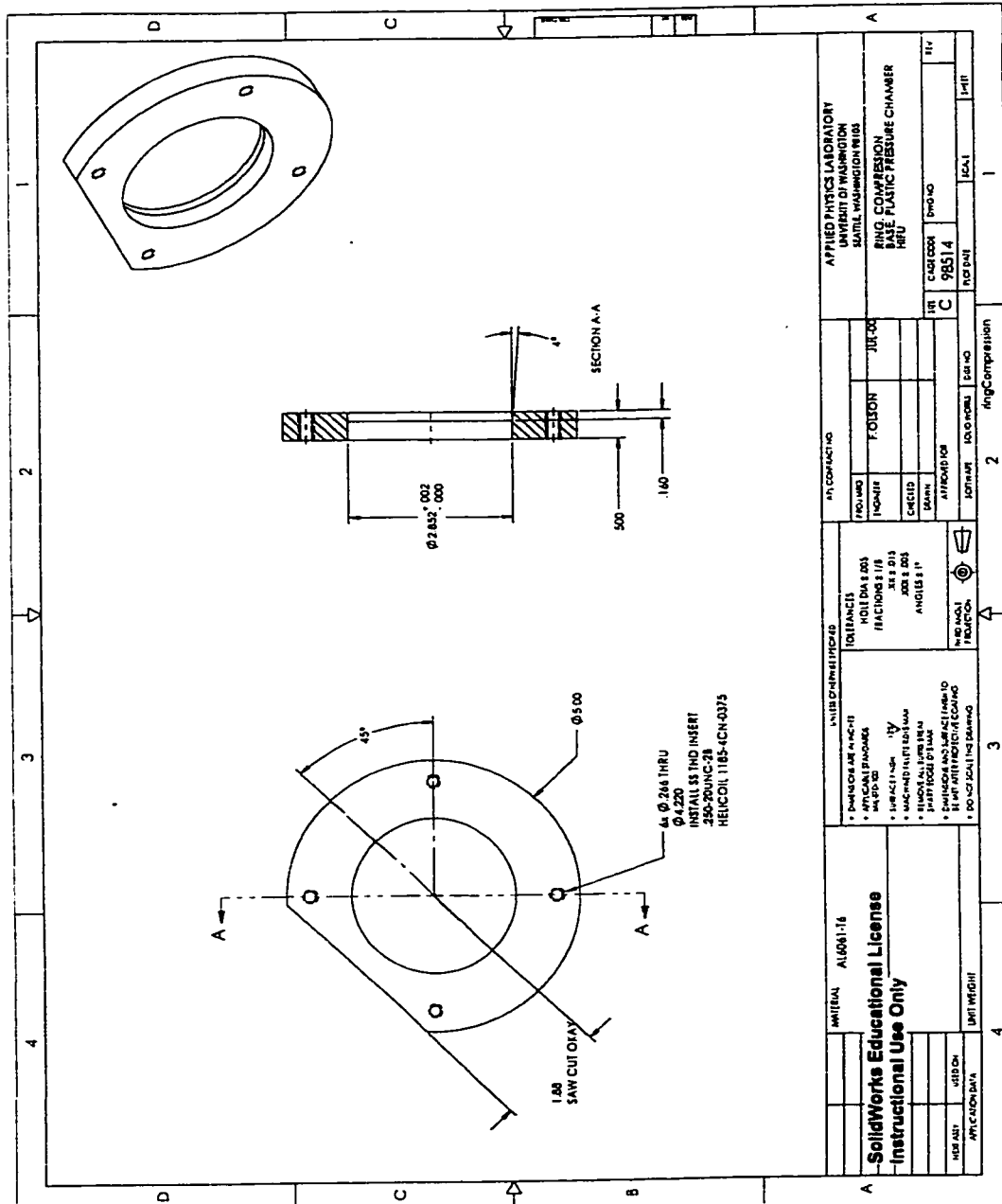
124

125



F.2 Plug, Hemostasis

F.3 Tube, Lever Arm, HIFU

F.4 Center Plug, Blood Carrier

SECTION B-B

1.25

.25

.05

15°

Ø.275

2x Ø.070

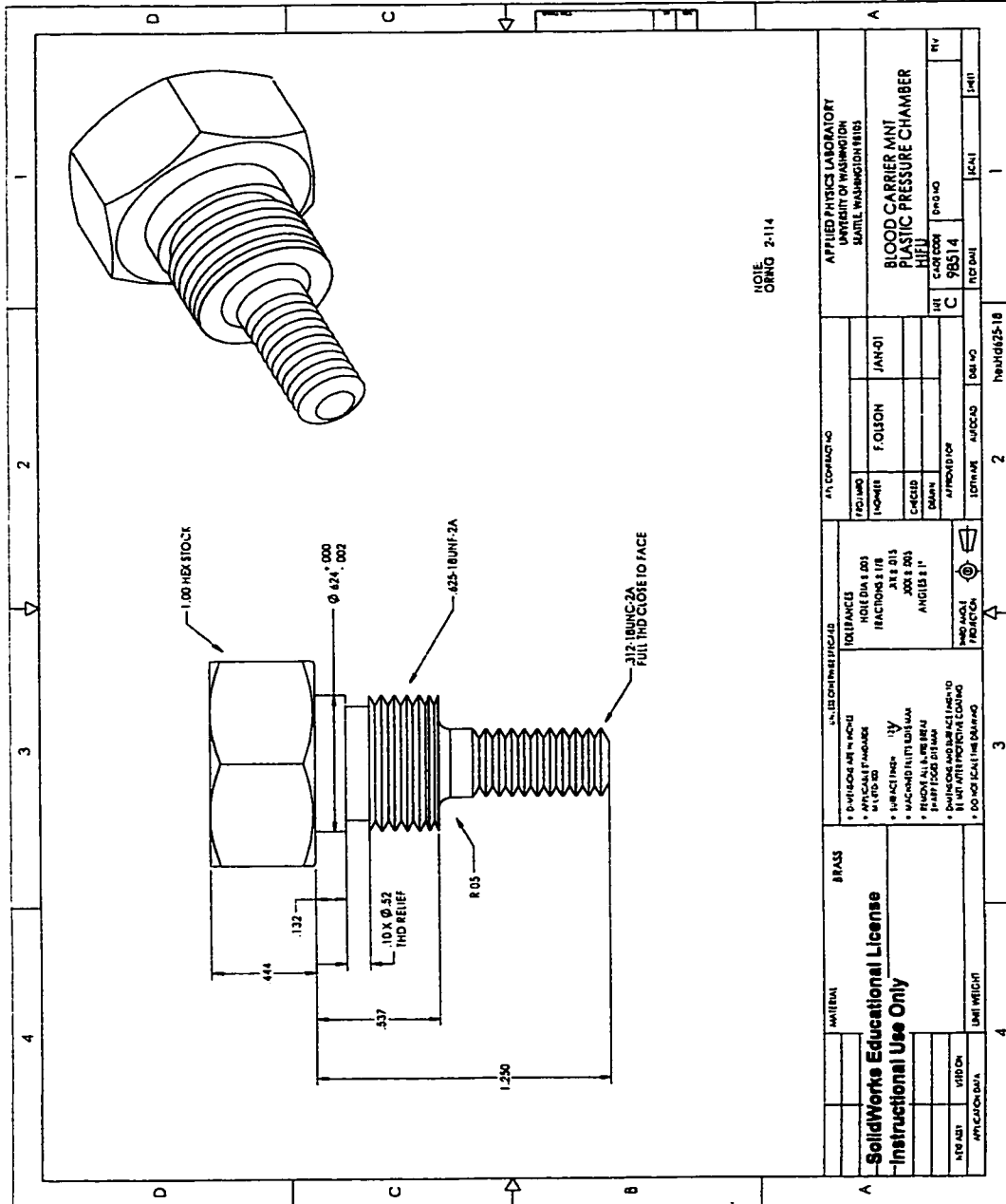.124

B

B

PVC

MATERIAL

FINISH

UNIT WEIGHT

pl/Center

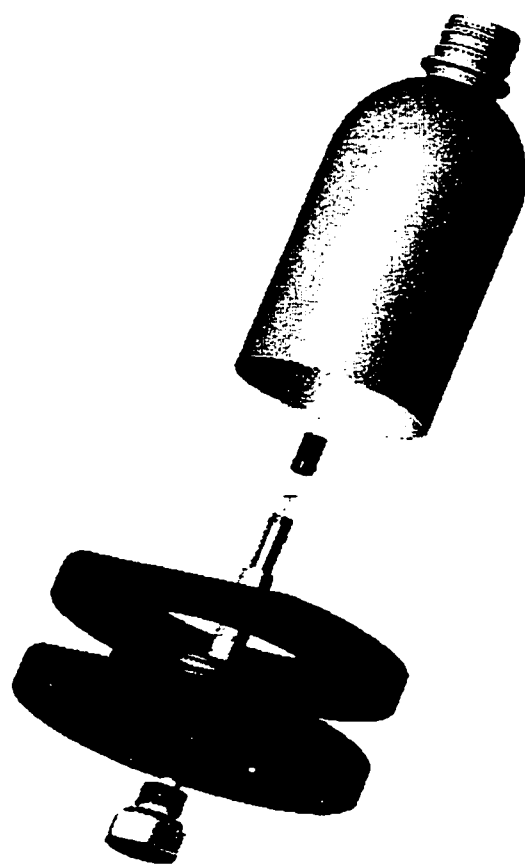F.5 Tube Plug, Blood Carrier

F.6 Base, Plastic Pressure Chamber, HIFU
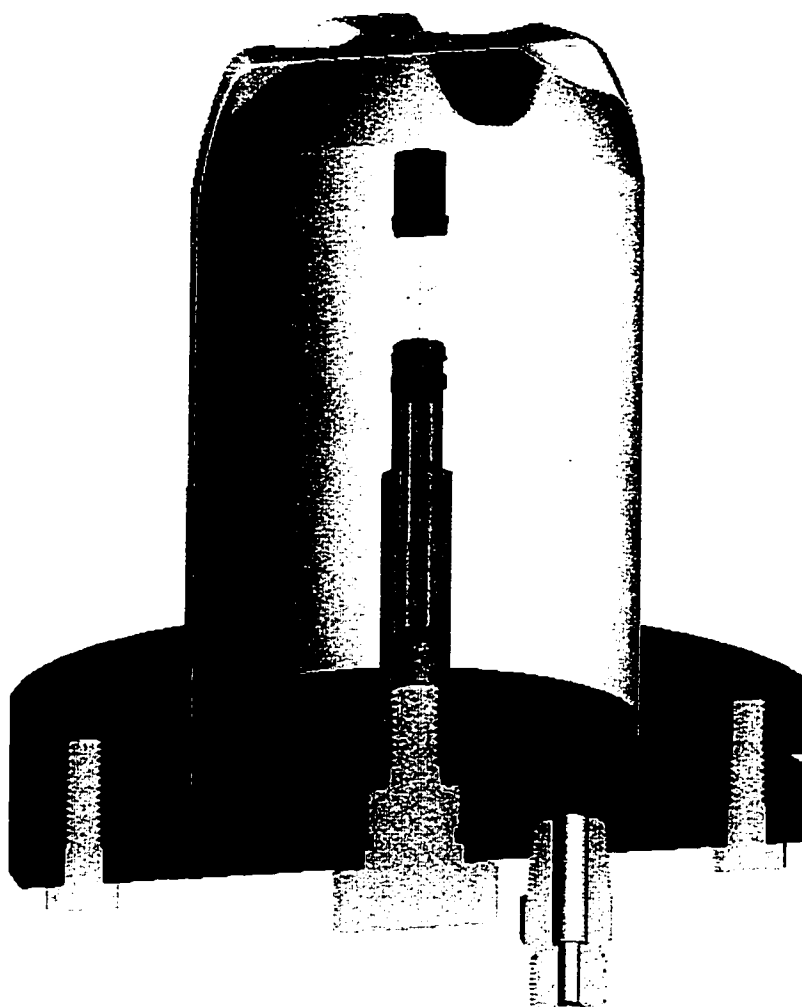
F.7 Ring, Compression Base, Plastic Pressure Chamber, HIFU

F.8 Blood Carrier Mnt, Plastic Pressure Chamber, HIFU

F.9 Overpressure Chamber, Exploded View

F.10 Overpressure Chamber, Cutaway View

## G:  Doppler Method

Ultrasound waves that reflect off of a moving boundary shift in frequency and can give information on the velocity of the moving object.  The Doppler shift frequency is defined as the difference between the frequency of the incident wave and the frequency of the reflected wave.  The Doppler shift frequency ($f_d$) may be calculated by:

$$f_d = - (V/c)(\cos \theta_i + \cos \theta_r)f_i ,$$

where V is the velocity of the object, c is the phase velocity of the fluid in which the object is moving, $\theta_i$ is the incident angle of the ultrasound, $\theta_r$ is the reflected angle of the ultrasound, and $f_i$ is the frequency of the incident wave.  For experiments using known conditions, the Doppler shift may be used to calculate the velocity of the reflecting object.

If the reflecting object is moving away from the ultrasound source/receiver, the reflected wave will be down-shifted in frequency.  If the object is moving towards the ultrasound source/receiver, the reflected frequency will be larger than the incident frequency (Christensen, DA 1988).

# VITA

## SANDRA L. POLIACHIK

University of Washington

2001

---

**EDUCATION**     **Ph.D. in Bioengineering**              **2001**
University of Washington                            Seattle WA
project: Bioeffects in platelets from high intensity focused ultrasound
          exposure

**MS in Mechanical Engineering**             **1991**
Virginia Polytechnic Institute and State University      Blacksburg VA
project: Transplant Organ Transport Cooler - Designed and built pump,
          powered by compressed oxygen, to cool and circulate fluid
          through transplant organ.

**BS in Mechanical Engineering**             **1987**
Virginia Polytechnic Institute and State University   Blacksburg VA

---

## PUBLICATIONS

Sandra L. Poliachik, Wayne L. Chandler, Pierre D. Mourad, Michael R. Bailey, Susannah Bloch, Robin O. Cleveland, Peter Kaczkowski, George Keilman, Tyrone Porter, Lawrence A. Crum. Effect of High-Intensity Focused Ultrasound on Whole Blood with and without Microbubble Contrast Agent, Ultrasound Med Biol 1999; 25: 991-998.

Vaezy, S, Martin, R, Keilman, G, Kaczkowski, P, Chi, E, Yazaji, E, Caps, M, Poliachik, S, Carter, S, Sharar, S, Cornejo, C, Crum, L. Control of splenic bleeding using high intensity ultrasound. J Trauma 1999; V.47, No.3:521-525.

Chang, PP, Chen, WS, Mourad, PD, Poliachik, SL, Crum, LA. Thresholds for inertial cavitation in Albunex suspensions under pulsed ultrasound conditions. IEEE Trans Ultrason, Ferroelect, Freq Contr 2001, 48, No. 1: 161-170.

Mourad, PD, Murthy, N, Porter, TM, Poliachik, SL, Crum, LA, Hoffman, AS, Stayton, PS. Focused ultrasound and Poly(2-ethylacrylic acid) act synergistically to disrupt lipid bilayers in vitro. Macromolecules 2001; 34: 2400-2401.

Poliachik, SL, Chandler, WL, Mourad, PD, Ollos, RJ, Crum. LA. Activation, Aggregation and Adhesion of Platelets Exposed to High Intensity Focused Ultrasound. Ultrasound Med Biol 2001 in press.

## PROCEEDINGS AND POSTERS

Poliachik, S, Mourad, P, Chandler, W. Effect of high intensity focused ultrasound on whole blood with and without Albunex®. 1998 IEEE Ultrasonics Symposium, Sendai, Miyagi, Japan, 5-8 October, 1998. (poster)

Chang, P, Mourad, PD, Poliachik, SL. Ultrasound contrast agents: present but not seen. 1998 IEEE Ultrasonics Symposium Proceedings, IEEE, Piscataway, NJ, USA; 1998;Vol. 2 pp. 1795-1798.

Poliachik, SL, Chandler, WL, Mourad, PD, Ollos, RJ, Crum, LA. Effect of high-intensity focused ultrasound on platelet aggregation, activation and adhesion. 9th Congress of the World Federation for Ultrasound in Medicine and Biology, Florence, Italy, 6-10 May 2000. (poster)

Poliachik, SL, Chandler, WL, Mourad, PD, Ollos, RJ, Crum. LA. Activation, Aggregation and Adhesion of Platelets Exposed to High Intensity Focused Ultrasound. 2000 IEEE Ultrasonics Symposium Proceedings, IEEE, Piscataway, NJ, USA; 2000; Vol. 2 pp. 1433-1436.

## PRESENTATIONS

Poliachik, S, Chandler, W, Mourad, PD, Bloch, S, Bailey, M, Cleveland, R, Crum, LA, Kaczkowski, P, Keilman, G, Porter, T. Ex-vivo studies of the effects of high-intensity focused ultrasound on whole blood. Proceedings of the 16th International Congress on Acoustics/ 135th Meeting Acoustical Society of America, Seattle, Washington, pp. 727-728, 23 June 1998.

Poliachik, SL, Chandler, WL, Mourad, PD, Bloch, S, Bailey, M, Cleveland, RO, Kaczkowski, P, Keilman, G, Porter, T, Crum, LA. Effect of high-intensity focused ultrasound on whole blood, whole blood containing contrast agents, and platelets. Moscow State University, 7 September 1998.

Poliachik, SL, Chandler, WL, Mourad, PD, Ollos, RJ, Crum, LA. Effect of high-intensity focused ultrasound on platelet aggregation, activation and adhesion. Institute of Cancer Research, Joint Department of Physics, Royal Marsden Hospital, Surrey England, 26 April 2000.

Poliachik, SL, Chandler, WL, Mourad, PD, Ollos, RJ, Crum, LA. Effect of high-intensity focused ultrasound on platelet aggregation, activation and adhesion. 139th Meeting Acoustical Society of America, Atlanta, GA, 31 May 2000.

Poliachik, SL, Chandler, WL, Mourad, PD, Ollos, RJ, Crum, LA. Effect of high-intensity focused ultrasound on platelet activation, aggregation and adhesion. 2000 IEEE International Ultrasonics Symposium, San Juan, Puerto Rico, 22-25 October 2000.

Poliachik, SL, Chandler, WL, Mourad, PD, Ollos, RJ, Crum, LA. Platelet activity as a result of exposure to high intensity focused ultrasound. 140th Meeting Acoustical Society of America, Newport Beach, CA, 6 December 2000

Poliachik, SL, Chandler, WL, Ollos, RJ, Crum, LA. Role of high intensity focused ultrasound induced cavitation on platelet aggregation. 141st Meeting Acoustical Society of America, Chicago IL, 7 June 2001.

Poliachik, SL, Chandler, WL, Ollos, RJ, Crum, LS. Role of high intensity focused ultrasound induced cavitation on platelet aggregation. 17th International Congress on Acoustics, Rome Italy, 6 September 2001.

## EXPERIENCE

| | | |
|---|---|---|
| **Research Assistant** | University of Washington | 1996- 2001 |
| **Instructor** | Seattle University, Physics 350 | Autumn 1998 & 1999 |
| **Senior Engineer** | The Boeing Commercial Airplane Group, Seattle WA | 1991- 1996 |
| **Teaching Assistant** | Virginia Polytechnic Institute and State University | 1989-1991 |
| **Engineer I** | Newport News Shipbuilding, Newport News VA | 1987-1989 |

## PROFESSIONAL AFFILIATIONS

Acoustical Society of America

Biomedical Engineering Society

Technical Committee on Biomedical Ultrasound/Bioresponse to Vibration, Student Council, Women in Acoustics Committee, Acoustical Society of America